Title
Analysis of Real-Time Tracking over a Multiple-Access Channel and its Application to Vehicular Safety Communications

Author
Huang, Ching-Ling

Publication Date
2011

Peer reviewed|Thesis/dissertation

Analysis of Real-Time Tracking over a Multiple-Access Channel and its Application to Vehicular Safety Communications

by

Ching-Ling Huang

A dissertation submitted in partial satisfaction
of the requirements for the degree of

Doctor of Philosophy

in

Engineering - Civil and Environmental Engineering

in the

GRADUATE DIVISION

of the

UNIVERSITY OF CALIFORNIA, BERKELEY

Committee in charge:

Professor Raja Sengupta, Chair
Professor Kannan Ramchandran
Professor Alexander Skabardonis

Fall 2011

Analysis of Real-Time Tracking over a Multiple-Access Channel and its Application to Vehicular Safety Communications

by

Ching-Ling Huang

Abstract

Analysis of Real-Time Tracking over a Multiple-Access Channel and its Application to Vehicular Safety Communications

by

Ching-Ling Huang

Doctor of Philosophy in Engineering - Civil and Environmental Engineering

University of California, Berkeley

Professor Raja Sengupta, Chair

We address the interesting question of how multiple dynamical systems should track each other in real-time over a shared channel. This dissertation covers a wide spectrum of results on this topic: our theories, engineering designs, computer simulations, prototype implementation and real-world evaluations. This research is motivated by the V2V (vehicle-to-vehicle) communications for active roadway safety, which is an important application in Intelligent Transportation Systems.

Our theoretical work is presented in Chapter 2. Two formulations of real-time tracking are analyzed. In the first formulation, we assume a scalar continuous-time continuous-state source and an AWGN (additive white Gaussian noise) channel without feedback. The analysis shows the MMSE (minimum mean-squared error) optimality of the innovation encoder and its tracking performance. In the second formulation, we assume a discrete-time continuous-state LTI (linear time-invariant) source and a G/G/1-∞ queueing network to deliver the information flow of the source from the encoder to the decoder. We derived a necessary and sufficient condition for real-time tracking stability in the form of a bound on the entropy rate of the LTI source. This bound is a function of the queueing server capability and other performance parameters. In both formulations, we extend the analysis to a multiple-access channel to understand the basic principle of designing encoders for real-time tracking multiple dynamical systems over a shared channel.

Our engineering designs for multiple dynamical systems to track each other over a shared channel are presented in Chapter 3. To model packet-switched networks, we assume that the source process state, e.g., a real scalar or a real vector, can be delivered in a message with negligible distortion. This assumption is valid since practical applications usually do not require infinite precision of the source state. In the analysis, we further assume a slotted ALOHA channel for tracking multiple scalar LTI systems. First, non-adaptive channel access schemes are analyzed for tracking stability and MSE (mean squared-error) performance. Adaptive transmission control schemes are then proposed for each node to adjust its message rate based on the tracking error of its own state at other nodes. With preliminary Matlab simulations, a comparison is made and a transmission rate control is proposed for vehicles

to broadcast state information and track each other in real-time. This rate control has an on-demand nature and considers both tracking error and channel congestion. A microscopic traffic simulator and a network simulator are used to show that tracking performance of the proposed design is robust to variations in different traffic conditions.

We start Chapter 4 by stating our understanding of the V2V safety communications problem and our design approach. The error-dependent message generation control from Chapter 3 is then enhanced with a transmission power allocation for each out-going safety message. This power control uses sensed channel utilization as side-information used by each vehicle to infer the condition of the shared channel. Our proposed rate/power control responds to channel congestion by maintaining the same information intensity, i.e., the same message rate, to as many neighboring vehicles as possible while temporarily stopping communication to farther vehicles by reducing transmission power. The robustness of the proposed design is verified by large-scale network simulations. Its real-time tracking accuracy is shown to outperform the currently proposed 100-millisecond beaconing of messages with 20-dBm transmission power.

In Chapter 5, we present implementation and real-world evaluations of the V2V transmission rate and power control proposed in Chapter 4. The implementation details are described as message generation and power assignment functional blocks. We also summarize results from outdoor vehicle mobility and scalability evaluations conducted at the General Motors Technical Center. In addition, updated performance measures and simulation results are provided for challenging highway and intersection scenarios. Overall, the prototype evaluations and simulation results show the superior tracking performance of our design over the currently proposed 100-millisecond beaconing with 20-dBm power. Our design has been adopted by General Motors R&D and serves as a candidate for a national standard defining how vehicles should track each other for active roadway safety.

Professor Raja Sengupta
Dissertation Committee Chair

Acknowledgements

First of all, I want to thank my advisor, Professor Raja Sengupta, for his guidance of my research work and his dedication to enlightening students. It was because his patience and encouragement I could grow professionally and intellectually over such a short time. It was through him I could understand what science means and how rigorous a true researcher should be. Secondly, I want to thank Dr. Hariharan Krishnan, a staff researcher in General Motor R&D, for supporting and funding our research over the years. He constantly inspired us to push the boundary of design and engineering. Dr. Krishnan was very kind, generous, and willing to spend a lot of time instructing and taking care of young researchers like myself. It was my privilege to have the opportunity to work closely with Dr. Yaser Fallah and to publish many interesting papers together. I also want to express my gratitude to my committee members, Professor Kannan Ramchandran and Professor Alexander Skabardonis, for providing numerous suggestions to improve this dissertation. I cannot finish this dissertation without the help from everyone. In additional, I have to say that I really enjoyed the cozy life style in Berkeley and the companionship of fellow graduate students. Last but not least, I want to thank my parents, my brother, and my lovely wife for their supports along the way.

Contents

List of Figures

List of Tables

Chapter 1

Introduction

This dissertation addresses the interesting question of how multiple dynamical systems should track each other in real-time over a shared and potentially unreliable channel. This research is motivated by the inter-vehicle communications for active roadway safety applications in the ITS (intelligent transportation system) research domain. In this active safety concept, vehicles track each other over a shared channel and monitor the states (e.g., position, speed, heading) of all the other vehicles in proximity to avoid hazardous situations. This dissertation provides original contributions in advancing the theoretical understanding of real-time tracking over a shared channel and the practical design for intelligent vehicles to broadcast state information and to track each other in real-time.

Our theoretical work on this topic is presented in Chapter 2. Our engineering design and analysis for multiple dynamical systems to track each other over a shared channel are presented in Chapter 3 along with a message generation control for V2V (Vehicle-to-Vehicle) safety communications so that vehicles can track each other in real-time with robust performance in different traffic scenarios. In Chapter 4, this message rate control is extended with a transmission power control for each message. We state our design approach and theoretical understanding of vehicular real-time tracking and propose a joint transmission rate/power control for V2V safety communications. Simulation results are used to show the effectiveness and robustness of the proposed transmission control under different traffic scenarios. In Chapter 5, the prototype implementation, evaluations, and enhancements to the design are presented. Our design has been implemented by General Motors R&D and is considered for the national standard defining how vehicles should communicate with each other for active safety applications. Our citations and literature reviews can be found in each chapter. More specifically, the structure and content of this dissertation are summarized in the following paragraphs.

In Chapter 2, two formulations of real-time tracking are analyzed to gain more theoretical understanding of the problem. In the first formulation (in Section 2.1), we assume continuous-time continuous-state sources and a AWGN (Additive White Gaussian Noise)

channel without feedback. Our analysis shows that MMSE (minimum mean-squared error) optimality of the innovation encoder and the associated optimal tracking performance. In the second formulation (in Section 2.2), we assume a discrete-time continuous-state source and a queueing network to deliver information from the encoder to the decoder. A necessary and sufficient condition is derived on the entropy rate of the source as a function of the queueing server capability and other performance parameters to ensure the real-time tracking stability (i.e., the finite moment of the tracking error). In both formulations, we extend the analysis to a multiple access channel to understand how to design the encoders for tracking multiple dynamical systems over a shared channel.

In Section 2.1, we first analyze the real-time tracking MMSE of a scalar linear continuous-time source over a scalar AGWN channel *without* channel feedback. With a Gaussian distributed source innovation, the optimality of the linear innovation encoder and associated optimal tracking performance are shown for the one-to-one channel case. We then extend the one-to-one channel formulation to the case of tracking multiple sources over a shared AWGN channel and study a simple case of tracking two identical linear sources. As a corollary, we show that it is impossible to achieve finite asymptotic MSE for real-time tracking of an unstable process *without* feedback.

In Section 2.2, we derive a condition for stable real-time tracking of an unstable, scalar, LTI (linear time-invariant) dynamical system. In particular, we use a G/G/1-∞ queue to model a broad class of unreliable networks. The communication server re-transmits lost information bits until they are received by the estimator. The stability condition is shown to be a bound on the entropy rate of the unstable process. This bound is a function of the moment to be stabilized, encoder efficiency, quantization accuracy, and network parameters. Finally, we apply this bound to the stable real-time tracking of multiple dynamical systems over a slotted wireless medium using three channel access protocols.

In Chapter 3, we address the question of how multiple dynamical systems should track each other in real-time over a shared channel with the assumption that a real scalar or a real vector can be delivered in a message with a negligible distortion (since practical applications usually do not require infinite precision of the source state). This assumption is dramatically different from that in Chapter 2 and used mainly to model the packet-switched nature of modern communication networks. We start by assuming a slotted ALOHA channel and multiple scalar LTI dynamical systems. First, non-adaptive channel access schemes are analyzed (in Section 3.1) for tracking stability and MSE (mean squared-error) tracking performance. Adaptive transmission control schemes are then proposed and analyzed (in Section 3.2). With preliminary Matlab simulations, a comparison is made and a transmission rate control is proposed (in Section 3.3) for intelligent vehicles to broadcast state information and track each other in real-time. A microscopic traffic simulator and a network simulator are used to show that the tracking performance of the proposed design outperforms the currently proposed 100-millisecond beaconing design for V2V safety communications.

In Section 3.1, model-based real-time tracking of multiple scalar LTI dynamical systems over a multi-access slotted ALOHA network is studied with non-adaptive channel access policies. A mathematical framework is proposed and the tracking MSE of three non-adaptive channel access schemes is analyzed. Asymptotic behavior and stability condition are also

derived. Our results suggest that, while designing real-time tracking systems, the channel access parameters should be chosen based on the amplification factor $|a|$ of the LTI dynamical process. If $|a| \geq 1$, the deterministic design (round-robin scheduling) can achieve strictly lower estimation MSE. Otherwise, for $0 < |a| < 1$, three methods have roughly the same range of MSE asymptotically.

In Section 3.2, we explore the Error-Dependent communication design for real-time tracking in a multi-access channel setting and the tracking MSE of error-dependent communication policy is analyzed. Its performance is compared with uncontrolled policies analyzed in Section 3.1. Based on analysis, an *Error-Collision-Dependent* policy is proposed that considers both tracking error and channel congestion to achieve robust real-time tracking performance. This result suggests that, while designing communication logic for vehicular safety applications, joint consideration of source system dynamics and channel congestion status can lead to better real-time tracking performance.

Our study in Section 3.1 and Section 3.2 is motivated by the inter-vehicle safety communications for active roadway safety applications. In this V2V framework, each vehicle is essentially equipped with on-board sensors and a 802.11p wireless radio as the *ad hoc* information exchange platform among vehicles. Based on the analysis, we propose a transmission rate control algorithm in Section 3.3 for each vehicle to disseminate its own state information. The proposed algorithm has an on-demand nature and adapts the V2V message transmission intensity for each vehicle in a decentralized fashion. This message rate control helps each vehicle decide when it should broadcast a safety message and avoids channel congestion. Performance evaluations, both in preliminary Matlab simulations and in large-scale traffic/network simulations, confirm that the proposed algorithm achieves better tracking accuracy than the currently proposed 100-millisecond beaconing design and is more robust to variations in traffic conditions.

In Chapter 4, we describe our real-time tracking formulation, assumptions, and proposed design for V2V safety communications. First, we state our theoretical understanding of the V2V safety communications problem and our design approach to it (in Section 4.1). A transmission rate and power control is then proposed for V2V safety communications (in Section 4.2) and its performance is verified by a network simulator integrated with a microscopic traffic simulator. In our design, the Error-Dependent rate control of Chapter 3 is enhanced with an adaptive transmission power control for each out-going safety message. The power control on each vehicle is done based on the sensed channel utilization (i.e., channel busy ratio) which serves as the side-information used by each vehicle to infer the channel congestion. The tracking accuracy of proposed V2V transmission control is again shown to outperform the 100-millisecond beaconing of messages.

In Section 4.1, we propose to first control the message rate based on host vehicle dynamics and the tracking errors based on safety considerations. For each message, we propose to control the transmission range to maximize the information broadcast throughput. What is implied in this two step design is that our design assumes that accurate tracking at nearby vehicles is more desirable than poor tracking over a large neighborhood. Therefore, our design responds to channel congestion by maintaining the same information flow (i.e., keeping the

same message rate) to the nearest neighbors and temporarily stopping communication to farther vehicles by reducing transmission range to relieve channel congestion.

The 10 Hz uncontrolled transmission of state information by each vehicle (i.e., beaconing with 100-millisecond interval) has been shown to produce excessive and redundant data traffics that could choke the vehicular wireless network. In Section 4.2, we propose a joint transmission rate/power control for inter-vehicle safety communications. This joint rate/power control helps each vehicle decide when it should broadcast a safety message (i.e., when a vehicle should talk) and how to allocate the transmission power for each safety message (i.e., how load a vehicle should talk). Simulation results confirm that the proposed design is robust in different traffic conditions and can considerably reduce the tracking error compared to that of the 100-millisecond beaconing solution.

In Chapter 5, we describe our implementation, real-world evaluations, and enhancements of the V2V communications design proposed in Chapter 4. The implementation details are presented as message generation and power assignment functional blocks (in Section 5.1). We ran the real-world evaluations for vehicle mobility and scalability tests at the General Motors Technical Center (in Section 5.2). The evaluations show that the behavior and performance of our V2V design match the computer simulations. Updated performance metrics and challenging traffic scenarios are also provided along with our updated simulation results for these scenarios (in Section 5.3).

The prototype evaluations presented in Section 5.2 show that our design works well in practice and is a promising scalable solution for V2V safety communications. In Section 5.3, we present updated performance metrics, challenging highway and intersection scenarios, and updated simulation results for these challenging scenarios. The performance of our proposed design is again compared with the 100-millisecond, 20-dBm beaconing. Overall, our design provides 1) better tracking accuracy when a new remote vehicle has been tracked by a host vehicle; and 2) a longer time or distance before a host vehicle detects a new remote vehicle approaching.

From Chapter 2 to Chapter 5, this dissertation covers a wide spectrum of theories for real-time tracking, our engineering design for V2V safety communications, computer simulations, and an implementation at the General Motors Technical Center and real-world evaluations. Chapter 6 provides the concluding remarks of this dissertation.

Chapter 2

Real-Time Tracking over an Unreliable Channel

In this chapter, two formulations of real-time tracking are analyzed to gain more theoretical understanding of the problem. In Section 2.1, our first formulation assumes continuous-time continuous-state sources and a scalar AWGN (Additive White Gaussian Noise) channel without feedback. Our analysis shows the MMSE (minimum mean-squared error) optimality of the innovation encoder and the associated optimal tracking performance. In Section 2.2, our second formulation assumes a discrete-time continuous-state source and a queueing network to deliver the information flow from the encoder to the decoder. A necessary and sufficient condition is derived on the entropy rate of the source as a function of the queueing server capability and required parameters to ensure the real-time tracking stability. In both formulations, we extend the analysis to a multiple access channel to understand the basic principle of designing the encoder for real-time tracking multiple dynamical systems over a shared channel.

2.1 Real-Time Tracking over an Unreliable Channel: A Continuous-Time Continuous-State Approach

In this section, we formulate the problem of tracking a diffusion in real-time without channel feedback and derive several MMSE optimality results. It has been noted (e.g., by [2,4]) that Shannon's classical information theorems [1] cannot be applied directly to real-time control or tracking problems. For example, many channels that have the same Shannon's capacity do not behave the same way when the encoded sequence is short; they only *function*

similarly when the encoded sequence is long enough to achieve decoding typicality and thus channel capacity [1,27]. Since real-time tracking cannot tolerate such a long encoding delay, other formulations have been examined in the literature, e.g., see [2-9], on how to track a source process in real-time over an unreliable channel. The literature on real-time tracking can be roughly categorized into that pertaining to stability, and another pertaining to optimality. Our analysis in Section 2.1 focuses on the optimality of real-time tracking.

Real-time tracking stability: This line of research, e.g., see [3-7], focuses on the necessary and sufficient conditions to achieve asymptotically stable real-time tracking. Tatikonda [3], Sahai [4], and Mitter treat the case of the unstable Linear Time-Invariant (LTI) source and derive real-time information measures for controlling this specific type of source processes over an unreliable channel, namely 1) the *sequential rate distortion* [3] for the bit rate at the source encoder required to achieve stable tracking; and 2) the *anytime capacity* [4] which the channel input bit rate cannot exceed so that the channel bit errors can be corrected exponentially fast thus enabling uses of the channel for stable real-time tracking. Note that their results in [3,4] focus on the tracking stability instead of tracking optimality and their formulation assumes a discrete-time channel with perfect (or noisy) channel feedback.

For real-time tracking *without* channel feedback, there is also a literature on a packet transmission formulation (e.g., see [5-7]). These papers assume that the source state information (a real number) can be transferred by the packet without distortion. The lossy channel usually drops packets according to a known distribution, e.g., a sequence of Bernoulli trials. Once the latest state measurement arrives at the decoder, any past tracking error is reset by a renewal process. In [5], Seiler and Sengupta assume a discrete-time, continuous-state Markovian Jump Linear Process (MJLP) source, a discrete-time Markovian lossy channel to deliver state observation in packets, and derive a necessary and sufficient condition as a linear matrix inequality (LMI) for stable tracking. Sinopoli *et. al.* [6] use a time-varying Kalman filter as the decoder and derive a bound on the channel error probability limiting stable tracking. Xu and Hespanha [7] derive the minimum required packet rate to achieve a stable mean-squared error (MSE) when tracking an unstable LTI source using the error-dependent transmission. This packet formulation [5-7] has gained wide acceptance in control theory as evidenced by the literature survey on Networked Control Systems [49].

Real-time tracking optimality: This line of research, e.g., see [2,8,9], focuses on finding the optimal encoder-decoder pair for real-time tracking. For real-time tracking *with* perfect channel feedback, Walrand and Varaiya [2] derive an optimal information structure of the encoder. A discrete-time discrete-state Markov source is tracked over an unreliable discrete-time channel with perfect feedback, i.e., the encoder knows exactly what has been received by the decoder. Their cost function is defined as a measure over the true state and estimated state. The measurability of the encoder in the current source state is shown to be sufficient for optimal real-time tracking. This formulation is extended by Teneketzis [9] with the channel feedback removed. The optimal encoder in [9] turns out to be a function of current source state and the probability measure over the decoder memory (as a sufficient statistic at the encoder for the decoder's knowledge of the source). Our work in Section 2.1 adds to this literature on optimal real-time tracking [2,9] by analyzing the continuous-time, continuous-state counterpart of the formulation in [9]. We assume a continuous-time

scalar AWGN channel. This channel has been used extensively in information theory, e.g., see [1,27]. We also extend this one-to-one channel formulation to a multiple-access AWGN channel.

Like us, Gupta and Murray [8] derive an optimal MMSE encoder for a discrete time lossy channel similar to [5-7]. Their work is based on the packet formulation. A packet contains a real number and carries the accumulated source state innovation. The arrival of the latest packet gives all the past source innovation and *washes away* all previous channel errors. This packet channel assumption makes the lossy channel an on-off switch delivering the source information. Their optimal encoder [8] relies heavily on this assumption. We study the same performance measure for the continuous time continuous state AWGN channel of information theory. Since a real-number bearing packet carries infinite information in an information-theoretic formulation, our encoder has a structure different from [8]. Finally, we extend our results to a multiple-access channel while references [2,8,9] do not treat multiple access channels.

In Section 2.1, we focus on finding the optimal encoder-decoder design for real-time tracking. We start with a continuous-time, continuous-state source and formulate the MMSE real-time tracking problem. Like [9], we study the formulation with no channel feedback. We only study the case of a scalar AWGN channel. We show that an MMSE encoding of the innovation of the source process at each time epoch gives the MMSE state estimates for all time. For the case of tracking one source, we derive an optimal encoder-decoder pair and the achievable MMSE. We obtain our results by borrowing from non-linear filtering theory [11,12,17], an approach different from [2-9]. We then extend the one-to-one channel results (shown in Figure 2.1) to a multiple-access AWGN channel (shown in Figure 2.2) with multiple source processes being tracked in real-time. Again, the optimality of innovation encoders is proven for the multiple-access channel. We establish stronger results for the multiple-access channel with two identical linear sources to get more understanding of the formulated problem. The optimal encoders are derived when the Signal-to-Noise Ratio (SNR) of the channel is within a range decided by the correlation of two sources. Optimal tracking performance is given when this SNR condition is satisfied. When this channel SNR condition is not satisfied, upper and lower bounds of the optimal tracking performance are given.

This section is organized as follows: The formulation of tracking one source over an AWGN channel is presented in Subsection 2.1.1 along with our main results: the MMSE optimal encoder-decoder pair and its tracking performance. The multiple-access AWGN channel formulation is presented Subsection 2.1.2 along with a case study of tracking two identical linear sources. Subsection 2.1.3 summarizes this section.

2.1.1 One-to-One Channel Formulation

Figure 2.1 shows the analyzed framework. We consider a finite time horizon problem with time $t \in [0,1]$. Let C be the Banach space of all continuous functions $z : [0,1] \to \mathbf{R}$ with norm $\|z\| = \max\{|z(t)| : 0 \le t \le 1\}$, where $|r|$ is the Euclidean norm of $r \in \mathbf{R}$. Let Γ_t be the smallest σ-field of subsets of C which contains all sets of the form $\{z|z(\tau) \in \beta\}$

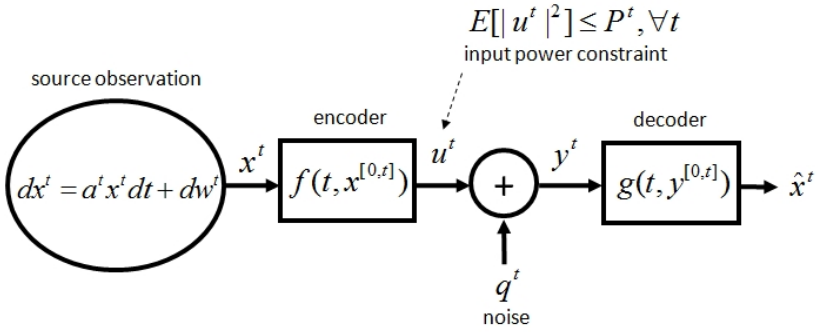

Figure 2.1. Analyzed one-to-one channel formulation: the real-time tracking of a scalar linear process over an AWGN channel *without* feedback

where $\tau \in [0,t]$ and β is a Borel subset of $\mathbf{R}$. Let $\Gamma = \Gamma_1$. Let B be the set of the Borel measurable subsets of $[0,1]$.

The source is a specific type of *Itô process* (e.g., see [12,16,21]) with the differential structure in eq. (2.1). More specifically, the source process x^t is a scalar linear continuous-time process described by the stochastic differential equation:

$$dx^t = a^t x^t dt + dw^t, x^0 \sim \mathbf{N}(0, \Lambda^0) \tag{2.1}$$

where $t \in [0,1]$ is the time, $x^t \in \mathbf{R}$ is the process state, $a^t \in \mathbf{R}, a^t > 0$ is the amplification factor, and $w^0 = 0, w^t \in \mathbf{R}$ is a Wiener process [19,21] that steers the source process. For $0 \le s < t \le 1$, $w^t - w^s \sim \mathbf{N}(0, V(t-s))$ for $V > 0$. The dw^t in eq. (2.1) is defined as $dw^t \equiv w^{t+dt} - w^t$ and thus $dw^t \sim \mathbf{N}(0, Vdt)$. The trajectory of a Wiener process is known to be continuous but not differentiable *almost everywhere* [19,21]. However, a generalized sense of derivative (defined with the integration by parts) for Wiener process can be shown to be a white Gaussian noise [21]. In other words, a Wiener process can be viewed as the limiting behavior of a random walk consisting of small independent increments. In our formulation, this Wiener process w^t is equipped with a generalized sense of derivative $\frac{d}{dt}w^t$, denoted as $v^t \equiv \frac{d}{dt}w^t$ for convenience. This white Gaussian process v^t has $E[v^t] = 0$ and $E[v^t v^s] = V\delta(t-s)$, for $t, s \in (0,1]$. Throughout this section, this process v^t is referred as the *innovation* of the source process. The initial condition x^0 is assumed to be zero-mean and Gaussian distributed with variance $\Lambda^0 > 0$. In addition, the Wiener process $w^{[0,1]}$ and the innovation process $v^{(0,1]}$ are assumed to be independent of the initial state x^0.

The process x^t in eq. (2.1) is a Gaussian process [21]. The probability measure on the state trajectory $x^{[0,t]}$ is induced by the probability measure on the initial state x^0 and the Wiener measure on the trajectory $w^{[0,t]}$. The probability measure on $x^{[0,t]}$ is *absolutely continuous* with respect to the Wiener measure on the space C of all continuous functions from $[0,1]$ into $\mathbf{R}$ (e.g., see Lemma 2 and Corollary 2 of [20]). The source process x^t is observed perfectly by the causal measurable encoder function at time t, denoted as f, which produces u^t as the input to the AWGN channel at time t. Let $f : [0,1] \times C \to \mathbf{R}$ be causal, i.e., f is not only $B \otimes \Gamma$ measurable but also measurable with respect to Γ_t for each fixed

$t \in [0,1)$. The encoder f can be parameterized as:

$$u^t = f(t, x^{[0,t]}) \tag{2.2}$$

where $x^{[0,t]}$ represents the trajectory of the source process as the full history up to time t. The channel input $u^t \in \mathbf{R}$ is chosen to deliver information to the decoder so that the decoder can produce an estimate of the state of the source process. The encoder function f can be time-varying and hence the parameter t. With the given trajectory of $x^{[0,t]}$, the trajectory of $w^{[0,t]}$ can be perfectly reconstructed for each t (e.g., see the discussion on pp. 355-358 and Theorem 1 of [20]). Therefore, $f(t,\cdot)$ is measurable with respect to the σ-algebra generated by the trajectory of $x^{[0,t]}$ and the trajectory of $w^{[0,t]}$ (and thus $v^{(0,t]}$ according to the generalized sense of derivative in [21]).

The AWGN channel output is the superposition of channel input u^t and the channel noise q^t:

$$y^t = u^t + q^t \tag{2.3}$$

where $y^t \in \mathbf{R}$ is the channel output at time t, and $q^t \in \mathbf{R}$ is a white Gaussian noise process independent of the source initial state x^0, the Wiener process $w^{[0,1]}$, and the innovation process $v^{(0,1]}$. The noise process q^t has $E[q^t] = 0$ and $E[q^t q^s] = Q^t \delta(t-s)$, $Q^t > 0$, for $t, s \in [0,1]$. We choose the formulation in eq. (2.3) instead of a stochastic differential form (e.g., eq. (2.1)) to match with most definitions of an AWGN channel [13-15]. The channel output y^t is observed by the decoder, denoted as g, which produces a real-time estimate of current state of the source process x^t. Let $g : [0,1] \times C \to \mathbf{R}$ be causal, i.e., g is not only $B \otimes \Gamma$ measurable but also measurable with respect to Γ_t for each fixed $t \in [0,1)$. The decoder g can be parameterized as:

$$\hat{x}^t = g(t, y^{[0,t]}) \tag{2.4}$$

where $\hat{x}^t \in \mathbf{R}$ is the estimate of x^t and $y^{[0,t]}$ is the full history of observed channel outputs up to time t. In this real-time tracking formulation, causality is imposed on the encoder f and decoder g. Once this estimate $\hat{x}^t$ is produced at time t, it is final and can not be improved later based on future channel outputs $y^{(t,1]}$. This decoder function g can also be time-varying and hence the parameter t.

The cost function $J_{(1)}$ is defined over a finite time horizon $t \in [0,1]$:

$$J_{(1)} \equiv \int_0^1 E[|x^t - \hat{x}^t|^2] dt \tag{2.5}$$

of which the expectation is taken with respect to the probability measure of the initial condition x^0, the Wiener process $w^{[0,1]}$, and the white Gaussian channel noise process $q^{[0,1]}$. For a given encoder-decoder pair, the real-time MSE $E[|x^t - \hat{x}^t|^2]$ can be calculated for each t. This cost function $J_{(1)} \in \mathbf{R}, J_{(1)} \geq 0$ is essentially the Lebesgue integral of the real-time MSE over the unit time interval $[0,1]$.

We define a finite time horizon optimization problem based on the cost function $J_{(1)}$ in eq. (2.5) to find an encoder-decoder pair, denoted as $\{f, g\}$, minimizing the cost function $J_{(1)}$:

$$\{f^*, g^*\} = \underset{E[|u^t|^2] \leq P^t, \forall t \in [0,1]}{\arg\min} J_{(1)} \tag{2.6}$$

where $\{f^*, g^*\}$ denotes the optimal encoder-decoder pair and $P^t < \infty$ is the finite power constraint on the channel input at each time t. The total transmission energy allowed is also finite over the same time horizon $t \in [0,1]$, i.e., $\int_0^1 P^t dt < \infty$. This power constraint P^t avoids the degenerate solution in which the encoder amplifies the channel input signal to an arbitrarily large value to *overwhelm* the channel noise q^t and the decoder can then restore the signal with an arbitrarily small error.

Preliminaries for the One-to-One Channel Formulation

Let $\bar{g} : [0,1] \times C \to \mathbf{R}$ be causal, i.e., $\bar{g}$ is not only $B \otimes \Gamma$ measurable but also measurable with respect to Γ_t for each fixed $t \in [0,1)$. We define a differential decoder for $\hat{x}^t$ (the real-time estimate of the source process) by the stochastic differential equation:

$$d\hat{x}^t = a^t \hat{x}^t dt + \bar{g}(t, y^{[0,t]})dt, \hat{x}^0 = \bar{g}(0, y^0) \tag{2.7}$$

where a^t is the same amplification factor in eq. (2.1) and the function $\bar{g}(t, y^{[0,t]})$ steers the evolution of $\hat{x}^t$. The similarity between eq. (2.1) and eq. (2.7) acknowledges the rationale that the decoder output $\hat{x}^t$ in eq. (2.7) incorporates the knowledge of the model of the source process x^t.

Lemma 2.1.1: For the real-time tracking problem in (2.6), there is no loss of optimality (in the MMSE sense for each $t \in [0,1]$) by assuming the differential decoder in eq. (2.7).

Proof: The form of the differential decoder in eq. (2.7) is MMSE optimal according to the nonlinear filtering analysis by Clark [11], Frost and Kailath [12], and Lo [17] (e.g., see Theorem 3 in [11], Theorem 3-5 in [12], and Theorem 1 in [17]). The finite channel input energy and Gaussian channel noise are the key elements guaranteeing the optimality of the differential decoder form in eq. (2.7). See specifically the discussion of Gauss-Markov Process and Linear Case on pp. 222 in [12]. ■

Theorem 2.1.2: Let $\Sigma^t \equiv E[(x^t - \hat{x}^t)^2]$ denote the tracking MSE at time t. For the optimal differential decoder (defined in eq. (2.7)), denoted as $\bar{g}^*(t, y^{[0,t]})$, the MMSE at time t, denoted as Σ^{*t}, can be described by the following differential equation. For $t \in (0,1]$,

$$d\Sigma^{*t} = 2a^t \Sigma^{*t} dt + E[(dw^t - \bar{g}^*(t, y^{[0,t]})dt)^2] \tag{2.8}$$

with the initial condition, $\Sigma^{*0} = E[(x^0 - \bar{g}^*(0, y^0))^2]$.

Proof: Let $e^t \equiv x^t - \hat{x}^t$. We get the differential equation of e^t based on eq. (2.1) and eq. (2.7):

$$de^t = a^t e^t dt + dw^t - \bar{g}(t, y^{[0,t]})dt. \tag{2.9}$$

With eq. (2.9) and the definition $\Sigma^t = E[(e^t)^2]$, the differential of the MMSE Σ^{*t} for the optimal differential decoder $\bar{g}^*$ can be derived as follows:

$d\Sigma^{*t} = \Sigma^{*(t+dt)} - \Sigma^{*t}$
$= E[(e^{*t} + de^{*t})^2] - E[(e^{*t})^2]$
$= 2E[e^{*t}de^{*t}] + E[(de^{*t})^2]$
$= 2a^t E[(e^{*t})^2]dt + 2E[e^{*t}(dw^t - \bar{g}^*(t, y^{[0,t]})dt)] + E[(a^t e^{*t}dt + dw^t - \bar{g}^*(t, y^{[0,t]})dt)^2]$
The last step is derived by substituting $de^{*t} = a^t e^{*t}dt + dw^t - \bar{g}^*(t, y^{[0,t]})dt$.
$= 2a^t E[(e^{*t})^2]dt - 2E[e^t \bar{g}^*(t, y^{[0,t]})dt] + (a^t)^2 E[(e^{*t})^2](dt)^2 + E[(dw^t - \bar{g}^*(t, y^{[0,t]})dt)^2]$
$-2a^t E[e^{*t}\bar{g}^*(t, y^{[0,t]})dt]dt$
The last step is true because the Wiener process has independent increments and thus dw^t is independent of e^{*t}.
$= 2a^t E[(e^{*t})^2]dt + (a^t)^2 E[(e^{*t})^2](dt)^2 + E[(dw^t - \bar{g}^*(t, y^{[0,t]})dt)^2]$
Due to a general form of Orthogonality Principle: the optimal tracking error is orthogonal to any function of all the past observations, e.g., see pp. 268 in [18].
$= 2a^t E[(e^{*t})^2]dt + E[(dw^t - \bar{g}^*(t, y^{[0,t]})dt)^2]$
The last step is derived by neglecting the higher order term associated with $(dt)^2$.

which leads to the differential equation in (2.8). ■

Corollary 2.1.3: For the real-time tracking problem in (2.6), an MMSE optimal differential decoder $\bar{g}^*$ can be expressed, for $t \in (0, 1]$, as

$$\bar{g}^*(t, y^{[0,t]}) = E[v^t | y^{[0,t]}] \tag{2.10}$$

with the initial condition, $\bar{g}^*(0, y^0) = E[x^0|y^0]$.

Proof: It has been noted that conditional expectation given observations minimizes the MSE (e.g., see the discussion on pp. 218 in [12]). From the differential form in eq. (2.8), observe that the MMSE Σ^{*t} can be minimized if all the previous $E[(dw^\tau - \bar{g}^*(\tau, y^{[0,\tau]})d\tau)^2]$ are minimized for all $0 < \tau \leq t$ and $E[(x^0 - \bar{g}^*(0, y^0))^2]$ is minimized for the initial condition. The differential decoder function $\bar{g}(t, \cdot)$ has all the channel observations $y^{[0,t]}$ and can be chosen for each t independently. This $\bar{g}(t, \cdot)$ does not depend on previous decoder functions $\bar{g}(\tau, \cdot), 0 \leq \tau < t$.

Because the conditional expectation $E[dw^\tau | y^{[0,\tau]}]$ minimizes this expectation for each τ, we get $\bar{g}^*(\tau, y^{[0,\tau]})d\tau = E[dw^\tau | y^{[0,\tau]}]$ and thus $\bar{g}^*(\tau, y^{[0,\tau]}) = E[\frac{d}{d\tau}w^\tau | y^{[0,\tau]}]$. Since the innovation process v^t is defined as the generalized sense of derivative of w^t, i.e., $v^t \equiv \frac{d}{dt}w^t$, we get eq. (2.10). At the initial condition, $t = 0$, the decoder is the conditional expectation of the source initial state x^0 given the available channel observation y^0. ■

Corollary 2.1.4: For the real-time tracking problem in (2.6) and $a^t \geq 0.5$, for each t, it is impossible to have asymptotic stable MSE, i.e., $\lim_{t\to\infty} \Sigma^t \to \infty$ for any encoder-decoder pair.

Proof: First partition infinite time line into segments of unit time length as in our formulation. In each unit time segment, the same differential equation (2.8) for Σ^{*t} still applies but with different initial conditions. Define the variable Ψ_1^t by

$$d\Psi_1^t = 2a^t \Psi_1^t dt, \Psi_1^0 = \Sigma^{*0} \tag{2.11}$$

and thus $\Psi_1^t \leq \Sigma^{*t}, \forall t > 0$ by comparing eq. (2.11) and eq. (2.8) and the fact that $E[(dw^t - \bar{g}^*(t, y^{[0,t]})dt)^2] > 0$ for nontrivial channel noise q^t, $\forall t > 0$. Now define another variable Ψ_2^t by

$$d\Psi_2^t = \Psi_2^t dt, \Psi_2^0 = \Sigma^{*0} \tag{2.12}$$

and thus, if $2a^t \geq 1, \forall t$, $\Psi_2^t \leq \Psi_1^t \leq \Sigma^{*t}, \forall t > 0$. The solution of the differential equation (2.12) can be expressed as $\Psi_2^t = \exp(t)\Psi_2^0$. Since $\Psi_2^0 = E[(x^0 - \bar{g}^*(0, y^0))^2] > 0$ for nontrivial channel noise q^0,

$$\infty = \lim_{t\to\infty} \Psi_2^t \leq \lim_{t\to\infty} \Psi_1^t \leq \lim_{t\to\infty} \Sigma^{*t}.$$

Therefore, in our formulation *without* channel feedback, if $2a^t \geq 1, \forall t$, no encoder-decoder pair can achieve stable MSE tracking asymptotically. ■

Main Results for the One-to-One Channel Formulation

In this subsection, we state an optimal encoder-decoder pair for the one-to-one channel formulation and the optimal tracking performance. With the Gaussian distributed source innovation v^t, the encoder is shown to be a linear innovation encoder and the associated decoder is a differential decoder that steers the state estimate $\hat{x}^t$ according to eq. (2.7).

Lemma 2.1.5: For the real-time tracking problem in (2.6), one optimal form of the encoder function and the differential decoder function (defined in eq. (2.7)) can be expressed as follows: for each $t \in (0, 1]$, the encoder is a function of v^t, denoted as $\bar{f}^*(t, v^t)$, and the associated differential decoder is denoted as $\bar{g}^*(t, y^t) = E[v^t|y^t]$. For the initial condition, $t = 0$, one optimal form can be written as $\bar{f}^*(0, x^0)$ and $\bar{g}^*(0, y^0) = E[x^0|y^0]$.

Proof: Assume an optimal encoder-decoder pair at t: $f^*(t, \cdot)$ and $\bar{g}^*(t, \cdot)$. The optimal differential decoder form $\bar{g}^*$ from Corollary 2.1.3 is:

$\bar{g}^*(t, y^{[0,t]}) = E[v^t|y^{[0,t]}] = E[v^t|y^t]$
Since v^t is independent of x^0, $v^{(0,t)}$, past channel outputs $y^{[0,t)}$ do not contain any information about v^t due to causality.
$= E[v^t|q^t + u^t]$
$= E[v^t|q^t + f^*(t, \{x^0, v^{(0,t)}, v^t\})]$
The source process, encoder f^*, noisy channel output, and decoder $\bar{g}^*$ form a Markov chain: $\{x^0, v^{(0,t)}, v^t\} \to u^t \to y^t \to E[v^t|y^t]$.
$= E[v^t|q^t + \bar{f}^*(t, v^t)]$ for some function $\bar{f}^*(t, \cdot)$
Since v^t is independent of x^0, $v^{(0,t)}$, v^t is as *informative* as the set $\{x^0, v^{(0,t)}, v^t\}$ for the decoder estimating v^t, e.g., see Theorem 3 and 4 in [24]. Thus one can design another function $\bar{f}^*(t, \cdot)$ to focus on delivering v^t without loss of optimality.

Therefore, without loss of optimality, the encoder at time $t \in (0, 1]$ can focus on delivering v^t to help the decoder better estimate the innovation v^t to steer the state estimate $\hat{x}^t$ according

to eq. (2.7). The decoder can be a function of current channel observation y^t mainly due to causality. ■

Theorem 2.1.6: For the real-time tracking problem in (2.6), one optimal encoder function $\bar{f}^*$ and its matched differential decoder $\bar{g}^*$ can be expressed, for $t \in (0, 1]$, as:

$$\bar{f}^*(t, v^t) = v^t \sqrt{\frac{P^t}{V}} \tag{2.13}$$

and

$$\bar{g}^*(t, y^t) = y^t \frac{\sqrt{VP^t}}{P^t + Q^t}. \tag{2.14}$$

At the initial condition, $t = 0$, the optimal form can be written as $\bar{f}^{*0}(x^0) = x^0 \sqrt{\frac{P^0}{\Lambda^0}}$ and $\bar{g}^{*0}(y^0) = y^0 \frac{\sqrt{\Lambda^0 P^0}}{P^0+Q^0}$.

Proof: Based on Lemma 2.1.5, the optimal encoder scales the Gaussian distributed innovation v^t to match with the channel input power constraint P^t (see pp. 561-562, 564 in Goblick [13] and pp. 1153 in Gastpar [14]), and this direct transmission can minimize the term $E[(dw^t - \bar{g}^*(t, y^{[0,t]})dt)^2]$ in eq. (2.8) for each $t \in (0, 1]$ and thus achieves MMSE optimal. The optimal differential decoder in eq. (2.14) is the conditional expectation of the source innovation v^t given y^t and the linear innovation encoder in eq. (2.13). The initial condition at $t = 0$ follows similarly. ■

Corollary 2.1.7: For the real-time tracking problem in (2.6), the optimal cost $J^*_{(1)}$ achievable is given by

$$J^*_{(1)} = \int_0^1 \Sigma^{*t} dt \tag{2.15}$$

where Σ^{*t} can be described by the differential equation:

$$\frac{d}{dt}\Sigma^{*t} = 2a^t \Sigma^{*t} + V(\frac{Q^t}{P^t + Q^t})^2, \Sigma^{*0} = \frac{\Lambda^0 Q^0}{P^0 + Q^0}. \tag{2.16}$$

Proof: Based on the optimal encoder and differential decoder in Theorem 2.1.6,

$E[(dw^t - \bar{g}^*(t, y^{[0,t]})dt)^2]$
$= E[(dw^t - (v^t \sqrt{\frac{P^t}{V}} + q^t) \frac{\sqrt{VP^t}}{P^t+Q^t} dt)^2]$
$= E[(dw^t - v^t dt \frac{P^t}{P^t+Q^t} - q^t dt \frac{\sqrt{VP^t}}{P^t+Q^t})^2]$
$= E[(dw^t \frac{Q^t}{P^t+Q^t} - q^t dt \frac{\sqrt{VP^t}}{P^t+Q^t})^2]$
$= E[(dw^t \frac{Q^t}{P^t+Q^t})^2] + E[(q^t dt \frac{\sqrt{VP^t}}{P^t+Q^t})^2]$
The last step is true because dw^t is independent of the channel noise q^t.
$= (\frac{Q^t}{P^t+Q^t})^2 E[(dw^t)^2] + \frac{VP^tQ^t}{(P^t+Q^t)^2}(dt)^2 = (\frac{Q^t}{P^t+Q^t})^2 V dt$
The last step is derived by neglecting the higher order term associated with $(dt)^2$.
Apply the property of the Wiener process $E[(dw^t)^2] = V dt$.

Combining the above with eq. (2.8), we get the differential form in eq. (2.16). The derivation for the initial condition is as follows:

$$E[(x^0 - \bar{g}^*(0, y^0))^2] = E[(x^0 - (x^0\sqrt{\tfrac{P^0}{\Lambda^0}} + q^0)\tfrac{\sqrt{\Lambda^0 P^0}}{P^0+Q^0})^2]$$
$$= E[(x^0\tfrac{Q^0}{P^0+Q^0} - q^0\tfrac{\sqrt{\Lambda^0 P^0}}{P^0+Q^0})^2]$$
$$= E[(x^0\tfrac{Q^0}{P^0+Q^0})^2] + E[(q^0\tfrac{\sqrt{\Lambda^0 P^0}}{P^0+Q^0})^2]$$
The last step is true because x^0 is independent of the channel noise q^0.
$$= (\tfrac{Q^0}{P^0+Q^0})^2\Lambda^0 + \tfrac{\Lambda^0 P^0}{(P^0+Q^0)^2}Q^0 = \tfrac{\Lambda^0 Q^0}{P^0+Q^0}$$

which leads to the Σ^{*0} term in eq. (2.16). ■

The simple form of the optimal encoder-decoder pair in eq. (2.13) and eq. (2.14) is mainly due to the fact that the Gaussian distributed source innovation v^t and Gaussian channel noise q^t are *matched* (see pp. 1152-1153 in Gastpar [14]). One can also observe from eq. (2.14) that, when the transmission power is zero (i.e., $P^t = 0$, no communication at all), the differential decoder will propagate the state estimate $\hat{x}^t$ in eq. (2.7) with $g^* = E[v^t] = 0$ and the MMSE is given by $\frac{d}{dt}\Sigma^{*t} = 2a^t\Sigma^{*t} + V$ as derived in [21]. The reduction from V to $V(\frac{Q^t}{P^t+Q^t})^2$ in eq. (2.16) can be viewed as the *benefit* when the encoder communicates v^t to the decoder.

2.1.2 Multiple-Access Channel Formulation

In this subsection, we extend the one-to-one channel formulation in Subsection 2.1.1 to a multiple-access channel formulation. There are two main differences: 1) $n \in \mathbf{N}$, $n \geq 2$ scalar linear processes are observed by n encoders individually which produce n channel inputs into a multiple-access AWGN channel; and 2) a single decoder reads the channel output and produces a vector of estimates for all n source processes in real-time. We are looking for an optimal set of encoders and decoder that achieves Minimum Sum of MSE (MSMSE) for tracking all the source processes. Figure 2.2 illustrates this formulation for $n = 2$.

Similar to the *Itô process* defined in eq. (2.1), each source process $x_i^t, i = 1, ..., n$, is a scalar linear continuous-time process described by the stochastic differential equation:

$$dx_i^t = a_i^t x_i^t dt + dw_i^t, x_i^0 \sim \mathbf{N}(0, \Lambda_i^0) \tag{2.17}$$

where $t \in [0, 1]$ is the time, $x_i^t \in \mathbf{R}$ is the process state, $a_i^t \in \mathbf{R}$ is the amplification factor, and $w_i^t \in \mathbf{R}$ is a Wiener process that steers the i-th source process. For $0 \leq s < t \leq 1$, $w_i^t - w_i^s \sim \mathbf{N}(0, V_i(t-s))$ for $V_i > 0$. This Wiener process w_i^t is equipped with a generalized sense of derivative $\frac{d}{dt}w_i^t$, denoted as the i-th innovation process $v_i^t \equiv \frac{d}{dt}w_i^t$. This white Gaussian process v_i^t has $E[v_i^t] = 0$ and $E[v_i^t v_i^s] = V_i\delta(t-s)$, for $t, s \in (0, 1]$. Within the n sources, for the same time index $t \in (0, 1]$ the v_i^t can be correlated with v_j^t for $i, j = 1, ..., n$ with the correlation coefficient ρ_{ij}^t, $i \neq j$, and $-1 \leq \rho_{ij}^t \leq 1$. The initial condition x_i^0 is assumed to be zero-mean and Gaussian distributed with variance $\Lambda_i^0 > 0$. Among n sources,

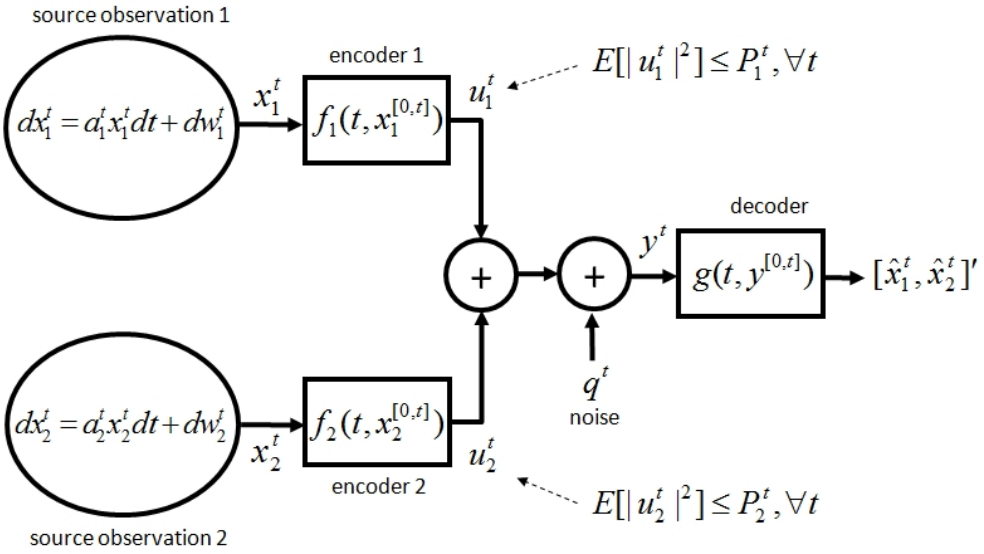

Figure 2.2. Analyzed multiple-access channel formulation: the real-time tracking of $n = 2$ linear processes over an AWGN channel *without* feedback

the initial condition x_i^0 can be correlated with x_j^0 for $i, j = 1, ..., n$ with the correlation coefficient ρ_{ij}^0, $i \neq j$, and $-1 \leq \rho_{ij}^0 \leq 1$. The probability measure induced by each source x_i^t is similar to that of the single source x^t in Subsection 2.2.1.

Each source process $x_i^t, i = 1, ..., n$, is observed perfectly by the i-th causal measurable encoder function f_i which produces $u_i^t \in \mathbf{R}$ as the i-th input to the AWGN channel. Let $f_i : [0,1] \times C \to \mathbf{R}$ be causal, i.e., f_i is not only $B \otimes \Gamma$ measurable but also measurable with respect to Γ_t for each fixed $t \in [0,1)$. The encoder f_i can be parameterized as:

$$u_i^t = f_i(t, x_i^{[0,t]}) \tag{2.18}$$

where $x_i^{[0,t]}$ represents the trajectory of the i-th source process as the full history up to time t. Note that the information structure of our formulation only allows the i-th encoder to observe the i-th source process.

The AWGN channel output is the superposition of the sum of the channel inputs $\sum_{i=1}^n u_i^t$ and the channel noise q^t:

$$y^t = \sum_{i=1}^{n} u_i^t + q^t \tag{2.19}$$

where $y^t \in \mathbf{R}$ is the channel output at time t, and $q^t \in \mathbf{R}$ is a white Gaussian noise process independent of $x_i^0, i = 1, ..., n$, $w_i^{[0,1]}, i = 1, ..., n$, and $v_i^{(0,1]}, i = 1, ..., n$. The noise process q^t has $E[q^t] = 0$ and $E[q^t q^s] = Q^t \delta(t-s)$, $Q^t > 0$, for $t, s \in [0,1]$. The channel output y^t is observed by the decoder g to produce a vector of estimates of $x_i^t, i = 1, ..., n$. Let $g : [0,1] \times C \to \mathbf{R}_{n \times 1}$ be causal, i.e., g is not only $B \otimes \Gamma$ measurable but also measurable with respect to Γ_t for each fixed $t \in [0,1)$. The decoder g can be parameterized as:

$$[\hat{x}_1^t, ..., \hat{x}_n^t]' = g(t, y^{[0,t]}) \tag{2.20}$$

where each $\hat{x}_i^t \in \mathbf{R}$ is the estimate of x_i^t and $y^{[0,t]}$ is the full history of observed channel outputs up to time t.

The cost function $J_{(n)}$ is defined over a finite time horizon $t \in [0,1]$:

$$J_{(n)} \equiv \int_0^1 \sum_{i=1}^{n} E[|x_i^t - \hat{x}_i^t|^2]dt \tag{2.21}$$

where n is the number of source processes and the expectation is taken with respect to the probability measure of the initial condition $x_i^0, i = 1, ..., n$, the Wiener processes $w_i^{[0,1]}, i = 1, ..., n$, and the channel noise process $q^{[0,1]}$. With a given set of encoders-decoder, the MSE $E[|x_i^t - \hat{x}_i^t|^2], \forall i$ can be calculated for each t. This cost function $J_{(n)} \in \mathbf{R}, J_{(n)} \geq 0$ is essentially the Lebesgue integral of the sum of all the real-time tracking MSE over the unit time interval $[0,1]$. The subscript in $J_{(n)}$ denotes that this multiple-access formulation considers the tracking of n sources, which is different from the cost function in eq. (2.5).

We define an optimization problem based on the cost function $J_{(n)}$ in eq. (2.21). It is to find the set of encoders and decoder for $t \in [0,1]$, denoted as $\{f_1, ..., f_n, g\}$, such that the cost function $J_{(n)}$ is minimized:

$$\{f_1^*, ..., f_n^*, g^*\} = \underset{E[|u_i^t|^2] \leq P_i^t, \forall i, \forall t \in [0,1]}{\arg\min} J_{(n)} \tag{2.22}$$

where f_i^* is the optimal encoder for the i-th source, g^* is the optimal decoder, and $P_i^t < \infty$ is the finite power constraint on u_i^t, the channel input producing the i-th encoder, at time $t \in [0,1]$, and the total energy is also finite: $\sum_{i=1}^n \int_0^1 P_i^t dt < \infty$. Again, the finite power and energy constraints avoid the degenerate solution mentioned in Subsection 2.1.1.

Preliminaries for the Multiple-Access Channel Formulation

Let $\mathbf{x}^t \equiv [x_1^t, ..., x_n^t]'$ denote the vector of the source states and similarly $\mathbf{w}^t \equiv [w_1^t, ..., w_n^t]'$. The source processes can then be described by the stochastic differential equation:

$$d\mathbf{x}^t = \mathbf{a}^t \mathbf{x}^t dt + d\mathbf{w}^t \tag{2.23}$$

with $\mathbf{a}^t \equiv diag(a_1^t, ..., a_n^t)$ where $diag$ represents a diagonal matrix with the indicated diagonal elements.

Let $\bar{g} : [0,1] \times C \to \mathbf{R}_{n \times 1}$ be causal, i.e., $\bar{g}$ is not only $B \otimes \Gamma$ measurable but also measurable with respect to Γ_t for each fixed $t \in [0,1)$. We define a differential decoder for the real-time estimate $\hat{\mathbf{x}}^t \equiv [\hat{x}_1^t, ..., \hat{x}_n^t]'$ by the stochastic differential equation:

$$d\hat{\mathbf{x}}^t = \mathbf{a}^t \hat{\mathbf{x}}^t dt + \bar{g}(t, y^{[0,t]})dt, \hat{\mathbf{x}}^0 = \bar{g}(0, y^0) \tag{2.24}$$

where $\mathbf{a}^t$ is the same amplification factor in eq. (2.23) and the function $\bar{g}(t, y^{[0,t]})$ produces the $n \times 1$ vector that steers the evolution of $\hat{\mathbf{x}}^t$, the decoder output.

Lemma 2.1.8: Given the multiple-access real-time tracking formulation in (2.22), there is no loss of optimality (in the MSMSE sense for each $t \in [0,1]$) by assuming the differential decoder in eq. (2.24).

Proof: Similar to the proof of Lemma 2.1.1. The differential form of eq. (2.24) is MSMSE optimal according to the nonlinear filtering analysis by Clark [11], Frost and Kailath [12], and Lo [17]. ■

Theorem 2.1.9: Let $\mathbf{\Sigma}^t \equiv E[(\mathbf{x}^t - \hat{\mathbf{x}}^t)(\mathbf{x}^t - \hat{\mathbf{x}}^t)']$ denote the tracking error covariance matrix at time t. The optimal error covariance $\mathbf{\Sigma}^{*t}$ (in the MSMSE sense) can be described by the differential equation:

$$d\mathbf{\Sigma}^{*t} = 2\mathbf{a}^t\mathbf{\Sigma}^{*t}dt + E[\Psi^t(\Psi^t)'] \tag{2.25}$$

where $\Psi^t \equiv d\mathbf{w}^t - \bar{g}^*(t, y^{[0,t]})dt$. The vector $\mathbf{w}^t$ is the vector of Wiener processes as defined in eq. (2.23). The function $\bar{g}^*(t, y^{[0,t]})$ is the optimal differential decoder with the form defined in eq. (2.24).

Proof: Let $\mathbf{e}^t \equiv \mathbf{x}^t - \hat{\mathbf{x}}^t$ denote the error vector. We get the differential equation of $\mathbf{e}^t$ based on eq. (2.23) and eq. (2.24):

$$d\mathbf{e}^t = \mathbf{a}^t\mathbf{e}^t dt + d\mathbf{w}^t - \bar{g}(t, y^{[0,t]})dt. \tag{2.26}$$

With eq. (2.26) and the definition $\mathbf{\Sigma}^t = E[\mathbf{e}^t(\mathbf{e}^t)']$, the differential of $\mathbf{\Sigma}^{*t}$ with the optimal differential decoder $\bar{g}^*$ can be expressed as eq. (2.25) using the similar arguments in the proof of Theorem 2.1.2. ■

Theorem 2.1.10: Let $tr(\cdot)$ denote the trace of the input matrix. Given the multiple-access real-time tracking formulation in (2.22), the optimal differential decoder $\bar{g}^*$ that achieves the Minimum Sum of MSE (MSMSE) $tr(\mathbf{\Sigma}^{*t})$ can be expressed, for $t \in (0, 1]$, as:

$$\bar{g}^*(t, y^t) = E[\mathbf{v}^t|y^t] \tag{2.27}$$

where the innovation vector $\mathbf{v}^t \equiv [v_1^t, ..., v_n^t]'$. One set of optimal form of encoders is the innovation encoders: for $t \in (0, 1]$, $\bar{f}_i^*(t, v_i^t), i = 1, ..., n$. For the initial condition, $t = 0$: one optimal decoder is $\bar{g}^*(0, y^0) = E[\mathbf{x}^0|y^0]$, and one optimal form of the encoders is $\bar{f}_i^*(0, x^0), i = 1, ..., n$.

Proof: Based on the differential form of $\mathbf{\Sigma}^{*t}$ in eq. (2.25) and similar arguments as in the proof of Corollary 2.1.3, to achieve MSMSE $tr(\mathbf{\Sigma}^{*t})$, $\bar{g}^*(t, y^{[0,t]})dt = E[d\mathbf{w}^t|y^{[0,t]}]$ and thus $\bar{g}^*(t, y^{[0,t]}) = E[\frac{d}{dt}\mathbf{w}^t|y^{[0,t]}]$. Since $v_i^t \equiv \frac{d}{dt}w_i^t, \forall i$, we get $\bar{g}^*(t, y^{[0,t]}) = E[\mathbf{v}^t|y^{[0,t]}]$. Based on the arguments in the proof of Lemma 2.1.5, $\bar{g}^*(t, y^{[0,t]}) = E[\mathbf{v}^t|y^t]$ due to causality. Since the i-th source innovation can only be observed by the i-th encoder, one optimal set of encoders is for each encoder to focus on delivering the innovation v_i^t at each time t as in the proof of Lemma 2.1.5. The initial condition at $t = 0$ follows similarly. ■

Theorem 2.1.10 says that, at each t, the i-th encoder can focus on communicating v_i^t to the decoder. However, how to design optimal encoders to communicate v_i^t over a shared channel to the decoder is an on-going research [25,26]. In the following, we study a simple case of tracking two identical linear sources and apply recent results in [25] to get the optimal encoders and the optimal tracking performance.

Tracking Two Identical Linear Sources over a Shared AWGN Channel

In this subsection, we assume the same multiple access tracking formulation with two identical linear sources and the same power constraint: $\forall t$, $a_1^t = a_2^t = a^t$, $P_1^t = P_2^t = P^t$, $V_1 = V_2 = V$, and $\Lambda_1^0 = \Lambda_2^0 = \Lambda^0$. Theorem 2.1.11 characterizes the optimal encoders when the Signal-to-Noise Ratio (SNR) P^t/Q^t is within a range decided by the source correlation factor ρ^t (see eq. (2.28)). The optimal encoder of the i-th source uses the uncoded transmission of the source innovation $v_i^t, i = 1, 2$, i.e., a linear scaling of the innovation to match with the power P^t. The optimal MSMSE is given in Corollary 2.1.12.

Theorem 2.1.11: For the real-time tracking problem in (2.22) with two identical linear sources and, $\forall t \in [0, 1]$,

$$0 < \frac{P^t}{Q^t} < \frac{|\rho^t|}{1 - |\rho^t|^2}, \tag{2.28}$$

one pair of optimal encoder functions $\bar{f}_1^*$, $\bar{f}_2^*$, and the associated differential decoder $\bar{g}^*$ (as defined in eq. (2.24)) can be expressed, for $t \in (0, 1]$, as,

$$\bar{f}_i^*(t, v_i^t) = v_i^t \sqrt{\frac{P^t}{V}}, i = 1, 2, \tag{2.29}$$

and

$$\bar{g}^*(t, y^t) = y^t \frac{\sqrt{VP^t}(1 + |\rho^t|)^2}{2P^t(1 + |\rho^t|) + Q^t}[1, 1]'. \tag{2.30}$$

For the initial condition, $t = 0$, the optimal form can be written as $\bar{f}_i^{*0}(x_i^0) = x_i^0 \sqrt{\frac{P^0}{\Lambda^0}}, i = 1, 2$ and $\bar{g}^{*0}(y^0) = y^0 \frac{\sqrt{\Lambda^0 P^0}(1+|\rho^0|)^2}{2P^0(1+|\rho^0|)+Q^0}[1, 1]'$.

Proof: Based on Theorem 2.1.10, the optimal encoder can focus on transmitting the source innovation v_i^t for each t. With the analysis by Lapidoth and Tinguely [25] (see specifically pp. 2720-2722 and Corollary IV.1 and IV.3), as long as the SNR P^t/Q^t satisfies eq. (2.28), the uncoded transmission of innovation in eq. (2.29) is optimal to minimize the distortion for each t. The optimal decoder in eq. (2.30) is the conditional expectation (see pp. 2729 in [25]) given the encoders in eq. (2.29). The initial condition $t = 0$ follows similarly. ■

Corollary 2.1.12: For the real-time tracking problem in (2.22) with two identical linear sources, and $\forall t \in [0, 1]$, SNR P^t/Q^t satisfies eq. (2.28), the optimal cost $J_{(2)}^*$ achievable is given by

$$J_{(2)}^* = 2 \int_0^1 \Sigma^{*t} dt \tag{2.31}$$

where Σ^{*t} can be described by the differential equation:

$$\frac{d}{dt}\Sigma^{*t} = 2a^t \Sigma^{*t} + V \frac{P^t(1 - |\rho^t|^2) + Q^t}{2P^t(1 + |\rho^t|) + Q^t}, \Sigma^{*0} = \Lambda^0 \frac{P^0(1 - |\rho^0|^2) + Q^0}{2P^0(1 + |\rho^0|) + Q^0}. \tag{2.32}$$

Proof: Based on Theorem 2.1.11 and Theorem 2.1.9, the achieved MSMSE can be described as the differential form in eq. (2.32). The derivation of the distortion of v_i^t for each t can be found on pp. 2722 of [25]. The initial condition $t = 0$ follows similarly. ■

When the SNR P^t/Q^t does not satisfy the condition in eq. (2.28), the form of the optimal encoder is still under investigation, e.g., see [25,26]. We provide the upper and lower bounds on the optimal real-time tracking performance.

Theorem 2.1.13: For the real-time tracking problem in (2.22) with two identical linear sources, when the SNR P^t/Q^t does not satisfy the condition in eq. (2.28), the optimal cost $J^*_{(2)}$ achievable is upper and lower bounded by

$$2\int_0^1 \underline{\Sigma}^{*t}dt \le J^*_{(2)} \le 2\int_0^1 \overline{\Sigma}^{*t}dt \tag{2.33}$$

where $\overline{\Sigma}^{*t}$ can be described by the differential equation:

$$\frac{d}{dt}\overline{\Sigma}^{*t} = 2a^t\overline{\Sigma}^{*t} + V\frac{P^t(1-|\rho^t|^2)+Q^t}{2P^t(1+|\rho^t|)+Q^t}, \overline{\Sigma}^{*0} = \Lambda^0\frac{P^0(1-|\rho^0|^2)+Q^0}{2P^0(1+|\rho^0|)+Q^0}, \tag{2.34}$$

and $\underline{\Sigma}^{*t}$ can be described by the differential equation:

$$\frac{d}{dt}\underline{\Sigma}^{*t} = 2a^t\underline{\Sigma}^{*t} + V\sqrt{\frac{Q^t(1-|\rho^t|)^2}{2P^t(1+|\rho^t|)+Q^t}}, \underline{\Sigma}^{*0} = \Lambda^0\sqrt{\frac{Q^0(1-|\rho^0|)^2}{2P^0(1+|\rho^0|)+Q^0}}. \tag{2.35}$$

Proof: This result is based on Theorem 2.1.10 and the analysis in [25] (see specifically Corollary IV.1 and IV.3): The upper bound $\overline{\Sigma}^{*t}$ can be achieved by uncoded transmission for each t as in Theorem 2.1.11. The lower bound $\underline{\Sigma}^{*t}$ can be achieved by a joint encoder function that takes both source innovations as input. ■

It is not yet known theoretically how close a distributed encoder design (i.e., each encoder only observes the corresponding source innovation) can approach the lower bound. However, some distributed encoders have been proposed to approach this bound for high SNR [25,26].

2.1.3 Short Summary

We first analyzed the real-time tracking MMSE of a scalar linear continuous-time source over a scalar AGWN channel *without* channel feedback. With the Gaussian distributed source innovation, the optimality of the linear innovation encoder and associated optimal tracking performance are proven for the one-to-one channel case. We then extend the one-to-one channel formulation to the case of tracking multiple sources over a shared AWGN channel and provideda stronger results for the case of tracking two identical linear sources. Our formulation can be considered as the continuous-time, continuous-state counterpart of the real-time tracking formulation by Teneketzis [9]. As a corollary, we show that it is impossible to achieve finite asymptotic MSE for real-time tracking an unstable process *without* feedback.

2.2 Real-Time Tracking over an Unreliable Channel: A Discrete-Time Continuous-State Approach with a Queueing Framework

In this section, we examine the problem of real-time tracking of an unstable, scalar, linear time-invariant (LTI) dynamical system over an unreliable queueing network. By *unreliable*, we mean that the transferred information could be corrupted and, even with re-transmission mechanisms, information delivery time (from the sender to the receiver) still has randomness. This kind of real-time tracking or control problem is well established in the literature, e.g., [3,4,9,38]. The multiple access problem is less well understood and current in the literature [8,37,41] with different assumptions on the network. [34,6,35] assume that state information (a real number) can be transferred by a packet without distortion. In this section, we remove this unrealistic assumption and try to understand how a network delay distribution impacts the bit stream the stability of real-time tracking.

Unlike the literature [4], we model an unreliable network with a G/G/1-∞ communication server (see Figure 2.3). This communication server handles network unreliability and re-transmits lost information based on network feedbacks. We do this to make the multiple access case more tractable. Another reason for this approach is that there are well defined statistical procedures to obtain the G/G/1-∞ queue model, e.g., [28,29,30], and its practical application to model a TCP/IP connection over Internet [30]. Unlike [4], we also assume separation of source and channel coding and have no analysis of the associated loss of optimality. However, under these assumptions, we are able to obtain necessary and sufficient conditions for stable tracking and use them to analyze a slotted wireless channel with different multiple access protocols.

More precisely, our results are as follows. The stability condition for real-time stable tracking of an unstable, scalar, LTI system is a bound on the entropy rate of the process. This bound is a function of the moment to be stabilized, encoder efficiency, quantization accuracy, and network parameters. This bound is sufficient under all load conditions. This bound is tight in the following sense: if the network is heavily utilized, this bound must be satisfied for stable tracking. Finally, we show how to use this stability bound to track multiple dynamical systems over a slotted wireless channel. For three commonly used channel access protocols, we give stability bounds based on the source entropy rate.

The contributions of this work are a framework with G/G/1-∞ queue, that covers many real-time tracking applications built on today's queue-based networking devices, and our quantitative discussion on stability conditions for real-time tracking over a multiple-access channel. Note that, there are practical reasons to develop a theoretical understanding of tracking unstable systems over multiple access networks. For our engineering work on tracking neighboring vehicles via a shared wireless channel, see [39,40,41]. Similar problems arise in the formations of UAVs (unmanned aerial vehicles), e.g., [5,32].

The organization of this section is as follows: Subsection 2.2.1 describes our problem formulation and main results. Subsection 2.2.2 is devoted to the analysis of three channel access

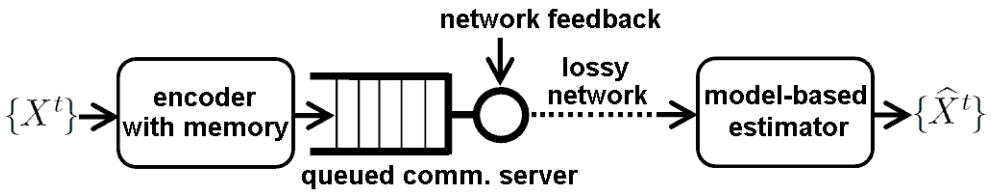

Figure 2.3. Proposed model for tracking over an unreliable network.

schemes for multiple-access networks. Subsection 2.2.3 provides the proofs and derivations. Subsection 2.2.4 summarizes this section.

2.2.1 Problem Formulation

In this subsection, we formulate the problem of tracking over an unreliable network (see Figure 2.3) and our main results on stable tracking. We start by stating definitions and properties from [27] for targeted unstable LTI process.

Definitions and Preliminaries

Def. 2.2.1: For a continuous random variable X with density function $f(x)$, if $f(x)$ is Riemann integrable, differential entropy is defined as

$$h(X) \equiv -\int_S f(x)\log_2 f(x)dx \tag{2.36}$$

where S is the support set of the random variable X.

Def. 2.2.2: For a random process $\mathcal{X} = \{X^t\}$, $t \in \mathbb{N}$, its joint entropy $h(X^t, X^{t-1}, ..., X^1)$ in a recursive form by the chain rule is

$$h(X^t, X^{t-1}, ..., X^1) = \sum_{i=1}^{t} h(X^i|X^{i-1}, ..., X^1). \tag{2.37}$$

Def. 2.2.3: Our definition for unstable scalar linear time-invariant (LTI) process $\mathcal{X} = \{X^t\}$ with $X^t \in \mathbb{R}$, $X^1 = 0$,

$$X^t = a \times X^{t-1} + \epsilon^{t-1} \tag{2.38}$$

where amplification factor $|a| > 1$ and ϵ^t is i.i.d. bounded noise process such that $|\epsilon^t| \leq W$ almost surely for some $W \in \mathbb{R}^+$. This bounded noise assumption follows [3,4].

For the process (2.38), its conditional entropy for each t can be simplified to be $h(X^t|X^{t-1}, ..., X^1) = h(X^t|X^{t-1})$ since it has a Markov structure.

Def. 2.2.4: Entropy rate for a process $\mathcal{X} = \{X^t\}$ is defined as the asymptotic conditional entropy:

$$h'(\mathcal{X}) \equiv \lim_{t\to\infty} h(X^t|X^{t-1}, ..., X^1). \tag{2.39}$$

If we divide $\mathbb{R}$ (the domain of X^t) into bins of length $\Delta = 2^{-\rho}$ such that $\rho \in \{0, 1, 2, ...\}$, i.e., ρ-bit quantization, the required number of bits is *on the average* $\cong h'(\mathcal{X}) + \rho$ to describe this process at each moment t as Δ is sufficiently small (by applying weak law of large number like the technique used in [27] for Asymptotic Equi-Partition).

Proposed Queueing Model for Remote Tracking

Figure 2.3 illustrates our proposed framework for tracking over a G/G/1-∞ queued communication system. We assume there is an unstable LTI process (2.38) serving as information source; the encoder releases state information at each moment and pushes those bits into a queue, waiting to be transmitted to the remote estimator via an unreliable network.

For the estimator to track the unstable process $\{X^t\}$ in real-time, bits are transmitted in the FIFO (first-in-first-out) order such that estimated states $\{\widehat{X}^t\}$ could be sequentially produced. If f represents the encoder function and g represents the estimator function, we require that, *when there is no delay in the system*, the encoder-estimator pair (f, g) must satisfy:

$$\{\widehat{x}^t\} = g(f(\{x^t\})) \text{ and } |\widehat{x}^t - x^t| \leq \Delta = 2^{-\rho}, \forall t. \tag{2.40}$$

At any time t, based on received information so far, this real-time estimator is forced to produce its best estimates $\{\widehat{x}^t\}$ up to current time index t. Due to the delay introduced in the network, the real-time tracking error could be larger than Δ.

A causal encoder has access to the observed process history $\mathcal{X} = \{X^t\}$ and produces a bit stream into the queue. Let $\nu^t(\mathcal{X})$ represent the number of bits produced while encoding x^t given $\{x^{t-1}, ..., x^1\}$ where $\{x^t, ..., x^1\}$ is one sample path (realization) of $\mathcal{X} = \{X^t, ..., X^1\}$. To satisfy the encoder-estimator pair (f, g) in (2.40), $E_{\mathcal{X}}[\nu^t(\mathcal{X})] \geq h'(\mathcal{X}) + \rho \geq \log_2 |a| + \rho$ bits to achieve $\Delta = 2^{-\rho}$ quantization accuracy (see [27], pp. 112-114). Let $\beta \in (0, 1]$ denote the efficiency of this encoder:

$$\beta \equiv \frac{h'(\mathcal{X})}{E_{\mathcal{X}}[\nu^t(\mathcal{X})] - \rho}$$

where $\beta = 1$ is the optimal case: $E_{\mathcal{X}}[\nu^t(\mathcal{X})] = h'(\mathcal{X}) + \rho$. We will use this specific definition of coding efficiency in our discussion throughout this section.

In [4], a fixed rate and a variable rate source codes for encoding the unstable LTI (2.38) have been proposed and both satisfy the requirement of (2.40). In general, the existence of such an encoder-estimator pair depends on the structure of the targeted LTI process and it needs to be analyzed in the future. For this work, we assume the existence of an encoder-estimator pair that satisfies (2.40).

Stability Bound on Entropy Rate

Here, we state our main results. The proofs are in Subsection 2.2.3. We consider a bit communication server in this subsection and then generalize it later in Subsection 2.2.2. Theorem 2.2.1 gives a stability bound on the entropy rate for real-time tracking via an

unreliable network. Corollary 2.2.1 comments on the trend of this bound with respect to stability requirement, encoder efficiency, quantization accuracy, server performance.

Theorem 2.2.1: Stability bound on entropy rate for bit communication systems. Given bit service rate $\mu_{bs} > 0$, bit service time variance $\sigma_{bs}^2 > 0$ of a communication system with a FIFO queue of infinite buffer, an unstable LTI process (2.38) $\mathcal{X} = \{X^t\}$, an encoder with quantization $\Delta = 2^{-\rho}$ and efficiency β such that it produces bit rate $(\frac{h'(\mathcal{X})}{\beta} + \rho)$ and inter-bit time variance $\sigma_{bt}^2 \geq 0$. If $(\frac{h'(\mathcal{X})}{\beta} + \rho) \uparrow \mu_{bs}$ (i.e., high utilization of the server), for $\eta > 0$,

$$h'(\mathcal{X}) < \Omega_b \Rightarrow \Pr(|\widehat{x}^t - x^t|^\eta < \infty) = 1 \tag{2.41}$$

and

$$h'(\mathcal{X}) < \Omega_b \Leftarrow E[|\widehat{x}^t - x^t|^\eta] < \infty \tag{2.42}$$

where, by letting $\xi \equiv \sigma_{bs}^2 + \sigma_{bt}^2$, the entropy bound Ω_b is given by

$$\Omega_b = \beta \times \frac{\{(\eta\rho\xi(\ln 2) + \mu_{bs}^{-1})^2 + \eta\xi(\ln 4)(1 - \rho\mu_{bs}^{-1} - \eta\rho^2\xi \ln 4)\}^{-2} - (\eta\rho\xi(\ln 2) + \mu_{bs}^{-1})}{\eta\xi \ln 2} \tag{2.43}$$

Else if $0 < (\frac{h'(\mathcal{X})}{\beta} + \rho) \ll \mu_{bs}$, above is weakened to a sufficient condition,

$$h'(\mathcal{X}) < \Omega_b \Rightarrow \Pr(|\widehat{x}^t - x^t|^\eta < \infty) = 1. \tag{2.44}$$

For the special case $\mu_{bs} > 0$ and $\sigma_{bs}^2 = \sigma_{bt}^2 = 0$, as long as $0 < (\frac{h'(\mathcal{X})}{\beta} + \rho) < \mu_{bs}$, $\Pr(|\widehat{x}^t - x^t|^\eta < \infty) = 1$ for any $\eta > 0$ for all t. ■

This Ω_b in (2.43) serves as a stability bound on the entropy rate $h'(\mathcal{X})$. This result is very useful since μ_{bs} and σ_{bs}^2 can be measured empirically for many bit communication systems. Given a communication system and the unstable LTI process, one can use this bound to check if designed encoder can support real-time tracking with desired stability.

Corollary 2.2.1: Properties of the stability bound. For the communication system and unstable LTI process described in Theorem 2.2.1, if we focus on stability instead of quantization accuracy and let $\Delta = 2^0$, i.e., $\rho = 0$, the stability bound Ω_b in (2.43) can be simplified to

$$\Omega_b(\eta, \beta, \mu_{bs}, \xi) = \beta \times \frac{(1 + \eta\mu_{bs}^2\xi \ln 4)^{\frac{1}{2}} - 1}{\eta\mu_{bs}\xi \ln 2} \tag{2.45}$$

which has following properties:

1. $0 \leq \Omega_b(\mu_{bs}) < \mu_{bs}$;
2. $\hat{\eta} > \check{\eta} \Leftrightarrow \Omega_b(\hat{\eta}) < \Omega_b(\check{\eta})$, i.e., $\eta \uparrow, \Omega_b \downarrow$;
3. $\hat{\beta} > \check{\beta} \Leftrightarrow \Omega_b(\hat{\beta}) > \Omega_b(\check{\beta})$, i.e., $\beta \uparrow, \Omega_b \uparrow$;
4. $\hat{\mu}_{bs} > \check{\mu}_{bs} \Leftrightarrow \Omega_b(\hat{\mu}_{bs}) > \Omega_b(\check{\mu}_{bs})$, i.e., $\mu_{bs} \uparrow, \Omega_b \uparrow$;
5. $\hat{\xi} > \check{\xi} \Leftrightarrow \Omega_b(\xi) < \Omega_b(\xi)$, i.e., $\xi \uparrow, \Omega_b \downarrow$;

for the range: $\eta > 0$, $\mu_{bs} > 0$, $\xi = \sigma_{bs}^2 + \sigma_{bt}^2 > 0$, and $0 < \beta \leq 1$. Note that these properties also hold for any $\rho > 0$. ■

That is, this bound Ω_b must be smaller than μ_{bs}, the service rate of the communication server. With a higher stability requirement η, this bound becomes smaller and thus further limits the entropy rate. With a higher coding efficiency β, this bound becomes lager. As the variance of the encoder's bit rate or service time variance increases, i.e., as ξ increases, this bound decreases.

2.2.2 Tracking over a Multiple-Access Network

Modern networking devices exchange information in a series of packets, i.e., bundles of bits, instead of a bit stream directly. In this subsection, we restrict our attention to the case $\Delta = 2^0$ as in Corollary 2.2.1 for ease of discussion.

In addition, for the packet stream produced by the encoder, inter-packet time variance is assumed to be much less than this network delay variance. That is, we assume network delay creates more randomness than the burstiness produced by the encoder (e.g., the fixed rate source code in [4]). This assumption helps simplify our Theorem 2.2.2 and our following discussions on tracking over a multiple-access channel.

Packet-Switched Formulation

We state a stability result for tracking an unstable LTI process (2.38) via a packet-switched network. The results can be extended to cases with $\rho > 0$.

Theorem 2.2.2: Stability bound on entropy rate for packet-switched systems. Given packet size L bits, packet service rate $\mu_{ps} > 0$, packet service time variance $\sigma_{ps}^2 > 0$ of a packet-switched system with a FIFO queue of infinite buffer, an unstable LTI process (2.38), an encoder with quantization $\Delta = 2^0$ and efficiency β such that it produces packet rate $h'(\mathcal{X})/(\beta L)$ and inter-packet time variance $\sigma_{pt}^2 \ll \sigma_{ps}^2$. If $\frac{h'(\mathcal{X})}{\beta L} \uparrow \mu_{ps}$ (i.e., high utilization of the server), for $\eta > 0$,

$$h'(\mathcal{X}) < \Omega_p \Rightarrow \Pr(|\widehat{x}^t - x^t|^\eta < \infty) = 1 \tag{2.46}$$

and

$$h'(\mathcal{X}) < \Omega_p \Leftarrow E[|\widehat{x}^t - x^t|^\eta] < \infty \tag{2.47}$$

where

$$\Omega_p(\eta, \beta, \mu_{ps}, \sigma_{ps}^2) = \beta L \times \frac{(1 + \eta\mu_{ps}^2\sigma_{ps}^2 \times \ln 4)^{\frac{1}{2}} - 1}{\eta\mu_{ps}\sigma_{ps}^2 \times \ln 2}. \tag{2.48}$$

Else if $0 < \frac{h'(\mathcal{X})}{\beta L} \ll \mu_{ps}$, above is weakened to a sufficient condition,

$$h'(\mathcal{X}) < \Omega_p \Rightarrow \Pr(|\widehat{x}^t - x^t|^\eta < \infty) = 1. \tag{2.49}$$

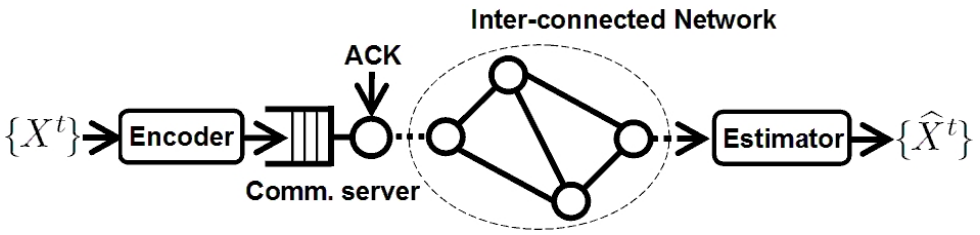

Figure 2.4. Theorem 2.2.2 can be applied to tracking over whatever inter-connected network as long as μ_{ps} and σ_{ps}^2 can be empirically measured. One possible solution is to perform remote tracking by unitizing a TCP/IP connection over Internet.

This stability bound Ω_p (13) has the same properties listed in Corollary 2.2.1. For the special case $\mu_{ps} > 0$ and $\sigma_{pt}^2 = \sigma_{ps}^2 = 0$, as long as $0 < \frac{h'(\mathcal{X})}{\beta L} < \mu_{ps}$, $\Pr(|\widehat{x}^t - x^t|^\eta < \infty) = 1$ for any $\eta > 0$ for all t. ■

Figure 2.4 illustrates remote tracking over an inter-connected network. As long as μ_{ps} and σ_{ps}^2 of the communication server can be measured, we can calculate this bound Ω_p and understand what level of stability is achievable for tracking over the particular network.

Assumptions for Modeling a Slotted Wireless Channel

Our preliminary analysis [41] indicates that different channel access protocols have huge impacts on tracking MSE (mean squared error) and stability over a shared channel. as the model of a slotted wireless medium in [23], we use following assumptions in stability analysis of three channel access protocols:

Channel data rate and slot: Let raw channel data rate be C bits per unit time, the packet size be L bits, and a slot length of shared wireless medium be $\zeta = L/C$.

Ternary feedback: At each time slot, the shared channel is assumed to provide instant feedback to all nodes, indicating either a success of transmission, failure (due to either a collision or channel error), or an idle slot.

Erasure probability: Even if a node wins channel access, its packet might still be erased by the lossy channel with PER (Packet Error Rate) τ_p during transmission, $\tau_p = 1-(1-\tau_b)^L$ where τ_b is the BER (Bit Error Rate) of physical layer modulation to support data rate C.

Re-Tx strategy: A bit within a packet can only be decoded after the whole packet is successfully received. Otherwise, the whole packet will be re-transmitted by the server. The packet header and redundancy bits are assumed to be negligible compared to its payload. On the receiver side, packets will be unpacked and fed into the estimator.

No hidden terminal: There are a fixed number of $n \geq 2$ nodes. All nodes are assumed to be within transmission range and can hear each other.

Stability Bounds for Three Channel Access Protocols

Three types of channel access schemes, i.e., decentralized, centralized, and hybrid cases, are described below and analyzed for their stability bounds Ω_p using (2.48).

Probabilistic (random access): This is a decentralized scheme. For $j = 1, 2, ..., n$, node j broadcasts its own state information with a fixed probability p_j at each time slot. Its channel access time is a geometric random variable with success probability of $(1 - \tau_p)p_j \prod_{i \neq j}(1 - p_i)$. One can get packet service rate $\mu_{ps}(P, j)$ and service time variance $\sigma^2_{ps}(P, j)$ for the j-th node:

$$\mu_{ps}(P, j) = (1 - \tau_p)p_j \prod_{i \neq j}(1 - p_i) \times \zeta^{-1} \tag{2.50}$$

and

$$\sigma^2_{ps}(P, j) = \frac{1 - (1 - \tau_p)p_j \prod_{i \neq j}(1 - p_i)}{(1 - \tau_p)^2 p_j^2 \prod_{i \neq j}(1 - p_i)^2} \times \zeta^2. \tag{2.51}$$

If we further assume homogeneous nodes, $p_j = p, \forall j$, packet service rate $\mu_{ps}(P)$ and service time variance $\sigma^2_{ps}(P)$ are given by

$$\mu_{ps}(P) = (1 - \tau_p)p(1 - p)^{n-1} \times \zeta^{-1} \tag{2.52}$$

and

$$\sigma^2_{ps}(P) = \frac{1 - (1 - \tau_p)p(1 - p)^{n-1}}{((1 - \tau_p)p(1 - p)^{n-1})^2} \times \zeta^2. \tag{2.53}$$

It can be shown that $p = 1/n$ maximizes $\mu_{ps}(P)$ and minimizes $\sigma^2_{ps}(P)$ at the same time. From Corollary 2.2.1, we know $p = 1/n$ also maximizes Ω_p in (2.48) given η and β.

From (2.50), (2.51), we can get the stability bound $\Omega_p(P, j)$ for this decentralized channel access scheme:

$$\Omega_p(P, j) = \beta T(P, j) \frac{(1 + \eta(1 - (1 - \tau_p)p_j \prod_{i \neq j}(1 - p_i)) \times \ln 4)^{\frac{1}{2}} - 1}{\eta(1 - (1 - \tau_p)p_j \prod_{i \neq j}(1 - p_i)) \times \ln 2} \tag{2.54}$$

where $T(P, j) = C \times (1 - \tau_p)p_j \prod_{i \neq j}(1 - p_i)$ is the effective bit throughput for the j-th node.

Deterministic (scheduling): As a centralized scheme, this design refers to the weighted round-robin scheduling to serve each node. Let $\phi_j \in [0, 1]$ be the portion of channel usage time for node j such that $\phi_j^{-1} \in \mathbb{N}$ and $\sum_{j=1}^{n} \phi_j = 1$. The channel access time for node j is a geometric random variable with success probability of $(1 - \tau_p)$ at every other ϕ_j^{-1} slots. One can get packet service rate $\mu_{ps}(D, j)$ and service time variance $\sigma^2_{ps}(D, j)$ for the j-th node:

$$\mu_{ps}(D, j) = \phi_j(1 - \tau_p) \times \zeta^{-1} \tag{2.55}$$

and

$$\sigma^2_{ps}(D, j) = \frac{\tau_p}{\phi_j^2(1 - \tau_p)^2} \times \zeta^2. \tag{2.56}$$

If we further assume homogeneous nodes, $\phi_j = 1/n, \forall j$, the same packet service rate $\mu_{ps}(D) = \frac{1-\tau_p}{n\zeta}$ and service time variance $\sigma^2_{ps}(D) = \frac{\tau_p n^2}{(1-\tau_p)^2} \times \zeta^2$ for all nodes. From (2.55), (2.56), we can get the stability bound $\Omega_p(D, j)$ for this centralized channel access scheme:

$$\Omega_p(D, j) = \beta T(D, j) \frac{(1 + \eta\tau_p \times \ln 4)^{\frac{1}{2}} - 1}{\eta\tau_p \times \ln 2} \tag{2.57}$$

where $T(D, j) = C \times \phi_j(1 - \tau_p)$ is the effective bit throughput for the j-th node.

Hybrid (grouped channel access): As a combination of the two previous schemes, this design bundles homogeneous nodes into one group and scheduled communication instants are given to different groups separately. Within the same group, nodes contend for channel access.

Assume that there are θ groups, the number of nodes in the r-th group, $r = \{1, 2, ..., \theta\}$, is denoted as m_r such that $\sum_{r=1}^{\theta} m_r = n$. Since all nodes in the r-th group are assumed to be homogeneous, the communication probability for each node is given by $p_r = 1/m_r$ when this group r is scheduled to use the channel. Otherwise, $p_r = 0$ while certain other group is assigned to use the channel.

Let $\phi_r \in [0, 1]$ be the portion of channel usage time for the r-th group such that $\phi_r^{-1} \in \mathbb{N}$ and $\sum_{r=1}^{\theta} \phi_r = 1$. For a node in group r, its channel access time is a geometric random variable with success probability of $(1 - \tau_p)p_r(1 - p_r)^{m_r-1}$ at every other ϕ_r^{-1} slots. One can get packet service rate $\mu_{ps}(H, r)$ and service time variance $\sigma^2_{ps}(H, r)$ for a node in the r-th group:

$$\mu_{ps}(H, r) = (1 - \tau_p)p_r(1 - p_r)^{m_r-1}\phi_r \times \zeta^{-1} \tag{2.58}$$

and

$$\sigma^2_{ps}(H, r) = \frac{1 - (1 - \tau_p)p_r(1 - p_r)^{m_r-1}}{((1 - \tau_p)p_r(1 - p_r)^{m_r-1}\phi_r)^2} \times \zeta^2. \tag{2.59}$$

From (2.58), (2.59), we can get the stability bound $\Omega_p(H, r)$ for this hybrid channel access scheme:

$$\Omega_p(H, r) = \beta T(H, r) \frac{(1 + \eta(1 - (1 - \tau_p)p_r(1 - p_r)^{m_r-1}) \times \ln 4)^{\frac{1}{2}} - 1}{\eta(1 - (1 - \tau_p)p_r(1 - p_r)^{m_r-1}) \times \ln 2} \tag{2.60}$$

where $T(H, r) = C \times \phi_r(1 - \tau_p)p_r(1 - p_r)^{m_r-1}$ is the effective bit throughput for a node in the r-th group.

From the form of (2.54), (2.57), (2.60), we see the bound Ω_p is proportionate to the effective bit throughput T, which depends on data rate C, the portion of channel usage time ϕ, and PER τ_p. These bounds and Theorem 2.2.2 together provide conditions for stable real-time tracking using these channel access protocols.

2.2.3 Derivations and Proofs

In this subsection, we present lemmas and proofs for the results in Subsections 2.2.1 and 2.2.2.

Def. 2.2.5: Chernoff type delay random variable q with decay rate α, $\exists M > 0$, $\exists \delta \in (0,1)$, satisfies below inequality for any k,

$$\delta \times 2^{-\alpha \times k} \leq \frac{\Pr(q > k)}{M} \leq 2^{-\alpha \times k}. \tag{2.61}$$

The FIFO queueing delay random variable has been shown to have this general form if we assume general arrival and service time distributions G/G/1-∞ [29].

Fact 2.2.1: Kingman's heavy-traffic approximation for G/G/1-∞ queue. Single server with service rate μ_s, service time variance σ_s^2, arrival rate λ, inter-arrival time variance σ_t^2, and a FIFO queue with infinite buffer. The waiting time in queue dominates end-to-end delay under heavy traffic condition, i.e., when $\lambda/\mu_s \uparrow 1$, and this delay random variable q has exactly an exponential distribution,

$$\Pr(q > k) = \exp(-k \times \frac{2(1-\lambda/\mu_s)}{\lambda(\sigma_s^2 + \sigma_t^2)}). \tag{2.62}$$

For non-heavy traffic condition, i.e., $0 < \lambda/\mu_s \ll 1$, there exists δ and M in the form (26) such that decay rate α:

$$\alpha \geq \log_2 e \times \frac{2(1-\lambda/\mu_s)}{\lambda(\sigma_s^2 + \sigma_t^2)}. \tag{2.63}$$

See [28,29] for proof. In general, under non-heavy traffic condition, delay distribution converges to zero faster (i.e., with a larger α value) than that under heavy traffic condition for a FIFO queue. ■

Prop. 2.2.1: Given a stationary bit delay distribution q_b in the form (2.61) with delay rate α, the delay distribution q_γ for a bundle of γ bits, $\gamma \in \mathbb{N}$, has the same decay rate α.

Proof:

$$\begin{aligned}
&\Pr(q_\gamma > k) = 1 - \Pr(q_\gamma \leq k) \\
&= 1 - (\Pr(q_b \leq k))^\gamma = 1 - (1 - \Pr(q_b > k))^\gamma \\
&= a_1 \Pr(q_b > k) + a_2 \Pr(q_b > k)^2 + ... + a_\gamma \Pr(q_b > k)^\gamma
\end{aligned}$$

where a_i are non-zero scalar coefficients, for $i = 1, 2, ..., \gamma$. We can see that the first term $a_1 \Pr(q_b > k)$ dominates the decaying behavior of $\Pr(q_\gamma > k)$. By plugging $\Pr(q_b > k)$ of the form (2.61) into (2.64), $\Pr(q_\gamma > k)$ can be organized into the same form (26) with the same α. ■

Since the same decay rate α works for either a single bit or a bundle of γ bits, from now on, we ignore the actual delay distribution and use a general form (2.61) to understand how decay rate α impacts the tracking error at estimator.

Prop. 2.2.2: Given a parameter Z and a stationary delay distribution of the form (2.61) with decay rate α,

$$E_k[2^{Z \times k}] < \infty \Rightarrow Z < \alpha. \tag{2.64}$$

Proof: If currently the latency between source and estimator is k, it means the delay random variable q is *at least* larger than k, and its probability is given by $\Pr(q > k)$ in (2.61).

$E_k[2^{Z\times k}] < \infty$
$\Rightarrow \sum_{k=0}^{\infty}(2^{Z\times k}) \times \Pr(q > k) < \infty$
$\Rightarrow \sum_{k=0}^{\infty}(2^{Z\times k}) \times 2^{-\alpha\times k} < \infty$
$\Rightarrow \sum_{k=0}^{\infty} 2^{(Z-\alpha)\times k} < \infty$
$\Rightarrow 2^{(Z-\alpha)} < 1$
$\Rightarrow Z < \alpha$

Note that the expectation in (2.65) is taken with respect to the latency k. ■

Lemma 2.2.1: Given an unstable LTI process (2.38) with $h'(\mathcal{X})$, encoder efficiency β, quantization size $\Delta = 2^{-\rho}$, and a stationary delay distribution of the form (2.61) with decay rate α, for $\eta > 0$,

$$h'(\mathcal{X}) < \beta(\alpha/\eta - \rho) \Leftarrow E[|\widehat{x}^t - x^t|^\eta] < \infty. \tag{2.65}$$

Proof: Let $\nu^t(\mathcal{X})$ represent the number of bits produced while encoding x^t given $\{x^{t-1}, ..., x^1\}$. Since the encoder efficiency is β, by our definition,

$$E_{\mathcal{X}}[\nu^t(\mathcal{X})] = h'(\mathcal{X})/\beta + \rho > 0. \tag{2.66}$$

Let $\{\widehat{x}^t, ..., \widehat{x}^1\}$ represent the estimates of corresponding sample path (realization) $\{x^t, ..., x^1\}$. If currently the latency between source and estimator is k, we denote estimated states $\{\widehat{x}^t, ..., \widehat{x}^1\}$ as $\{\widehat{x}^t(k), ..., \widehat{x}^{t-k+1}(k), \widehat{x}^{t-k}(k), ..., \widehat{x}^1(k)\}$. With (2.40), since the estimator has received information bits up to time $t-k$, for $1 \le s \le t-k$, $|\widehat{x}^s(k) - x^s| \le \Delta = 2^{-\rho}$.

The supremum of $|\widehat{x}^t(k) - x^t|$, i.e., the maximum estimation error due to latency k, is given by

$$\sup_{\mathcal{X}} |\widehat{x}^t(k) - x^t| \cong \prod_{l=0}^{k-1}(2^{\nu_{t-l}(\mathcal{X})}) \times \Delta = \prod_{l=0}^{k-1}(2^{\nu^{t-l}(\mathcal{X})}) \times 2^{-\rho} = 2^{\sum_{l=0}^{k-1}(\nu_{t-l}(\mathcal{X}))-\rho}$$

which is the uncertainty space expanded by those delayed information bits. Without further information, the estimated state $\widehat{x}^t(k)$ is uniformly distributed over all possible bins, thus the probability of $\widehat{x}^t(k)$ falls in the i-th bin of quantization Δ_i, for index $i \in \{1, 2, ..., 2^{\sum_{l=0}^{k-1}\nu_{t-l}(\mathcal{X})}\}$, is given by

$$\Pr(\widehat{x}^t(k) \in \Delta_i) = (2^{\sum_{l=0}^{k-1}\nu^{t-l}(\mathcal{X})})^{-1}. \tag{2.67}$$

Thus, we can calculate $E_{\mathcal{X}}[|\widehat{x}^t(k) - x^t|]$, i.e., the expected tracking error over all possible sample paths. By applying Jensen's inequality,

$E_{\mathcal{X}}[|\widehat{x}^t(k) - x^t|] \ge D \times 2^{E_{\mathcal{X}}[\sum_{l=0}^{k-1}\nu^{t-l}(\mathcal{X})]}$
$\ge D \times 2^{E_{\mathcal{X}}[\nu^t(\mathcal{X})]\times k}$

where D is a constant. Similarly, for any $\eta > 0$, $\exists D(\eta) \in \mathbb{R}^+$ such that

$$E_{\mathcal{X}}[|\widehat{x}^t(k) - x^t|^\eta] \ge D(\eta) \times 2^{E_{\mathcal{X}}[\nu^t(\mathcal{X})]\times k}. \tag{2.68}$$

Above expectation is taken with respect to the randomness of the process $\mathcal{X} = \{X^t\}$, and $E_{\mathcal{X}}[|\widehat{x}^t(k) - x^t|^\eta]$ is a function of latency k. Now take the expectation with respect to

latency k, i.e., the time difference between source and estimator (due to re-transmission and network delay),

$$E[|\widehat{x}^t - x^t|^\eta] = E_k[E_{\mathcal{X}}[|\widehat{x}^t(k) - x^t|^\eta]]$$

$\geq D(\eta) \times E_k[2^{E_{\mathcal{X}}[\nu^t(\mathcal{X})]\times k}]$.(2.69)Apply Prop. 2 to (2.72), for $\eta > 0$,

$E[|\widehat{x}^t - x^t|^\eta] < \infty \Rightarrow E_k[2^{E_{\mathcal{X}}[\nu^t(\mathcal{X})]\times k}] < \infty$
$\Rightarrow E_{\mathcal{X}}[\nu^t(\mathcal{X})] < \alpha/\eta \Rightarrow h'(\mathcal{X}) < \beta(\alpha/\eta - \rho)$.

We get desired result (2.66). ■

Lemma 2.2.2: Given an unstable LTI process (2.38) with $h'(\mathcal{X})$, encoder efficiency β, quantization size $\Delta = 2^{-\rho}$, and a stationary delay distribution of the form (2.61) with decay rate α, for $\eta > 0$,

$$h'(\mathcal{X}) < \beta(\alpha/\eta - \rho) \Rightarrow \Pr(|\widehat{x}^t - x^t|^\eta < \infty) = 1. \tag{2.70}$$

Proof: Given $\{x^t, ..., x^1\}$ and estimates $\{\widehat{x}^t(k), ..., \widehat{x}^{t-k+1}(k), \widehat{x}^{t-k}(k), ..., \widehat{x}^1(k)\}$ for latency $k > 0$ between source and estimator, from (2.68), we get below by applying Markov's inequality: for any $\pi > 0$,

$\Pr(\sup_{\mathcal{X}} |\widehat{x}^t(k) - x^t|^\eta \geq 2^\pi)$
$= \Pr((2^{\eta\times\sum_{l=0}^{k-1}\nu_{t-l}(\mathcal{X})}) \times \Delta^\eta \geq 2^\pi)$
$= \Pr(\eta \times \sum_{l=0}^{k-1}(\nu_{t-l}(\mathcal{X})) - \eta\rho \geq \pi)$
$= \Pr(\sum_{l=0}^{k-1}(\nu_{t-l}(\mathcal{X})) \geq \pi/\eta + \rho) \leq \frac{E[\sum_{l=0}^{k-1}\nu_{t-l}(\mathcal{X})]}{\pi/\eta+\rho}$
$= \frac{E_{\mathcal{X}}[\nu^t(\mathcal{X})]\times k}{\pi/\eta+\rho} = \frac{(\frac{h'(\mathcal{X})}{\beta}+\rho)\times k}{\pi/\eta+\rho} \leq \frac{\eta}{\pi} \times 2^{(\frac{h'(\mathcal{X})}{\beta}+\rho)\times k}$.

Now, we are ready to include the randomness of the stationary delay distribution in the form of (2.61):

$\Pr(\sup_{\mathcal{X}} |\widehat{x}^t - x^t|^\eta \geq 2^\pi)$
$= \sum_{k=0}^{t-1} \Pr(\sup_{\mathcal{X}} |\widehat{x}^t(k) - x^t|^\eta \geq 2^\pi) \times \Pr(q > k)$
$\leq \frac{\eta}{\pi} \sum_{k=0}^{t-1} 2^{(\frac{h'(\mathcal{X})}{\beta}+\rho)\times k} \times \Pr(q > k)$
$\leq \frac{\eta}{\pi} \sum_{k=0}^{t-1} 2^{(\frac{h'(\mathcal{X})}{\beta}+\rho)\times k} \times M \times 2^{-\alpha\times k}$
$= \frac{\eta M}{\pi} \sum_{k=0}^{t-1} 2^{((\frac{h'(\mathcal{X})}{\beta}+\rho)-\alpha)\times k}$

Since $(\frac{h'(\mathcal{X})}{\beta} + \rho) < \alpha$, $\sum_{k=0}^{t-1} 2^{((\frac{h'(\mathcal{X})}{\beta}+\rho)-\alpha)\times k} < \infty$, and

$\Pr(\sup_{\mathcal{X}} |\widehat{x}^t - x^t|^\eta \geq \infty)$
$= \lim_{\pi\to\infty} \Pr(\sup_{\mathcal{X}} |\widehat{x}^t - x^t|^\eta \geq 2^\pi)$
$\leq \lim_{\pi\to\infty} \frac{\eta M}{\pi} \sum_{k=0}^{t-1} 2^{((\frac{h'(\mathcal{X})}{\beta}+\rho)-\alpha)\times k} = 0.$

Therefore, $h'(\mathcal{X}) < \beta(\alpha/\eta - \rho) \Rightarrow \Pr(|\widehat{x}^t - x^t|^\eta < \infty) = 1$. We get desired result (2.73). ■

Proof of Thm. 2.2.1: From Fact 2.2.1, under heavy traffic condition, i.e., $\lambda = (\frac{h'(\mathcal{X})}{\beta} + \rho) \uparrow \mu_{bs}$, with $\xi = \sigma_{bs}^2 + \sigma_{bt}^2$, we have

$h'(\mathcal{X}) < \beta(\alpha/\eta - \rho)$
$\Leftrightarrow \frac{\eta}{\beta} \times h'(\mathcal{X}) < \log_2 e \times \frac{2(1-(h'(\mathcal{X})/\beta+\rho)/\mu_{bs})}{(h'(\mathcal{X})/\beta+\rho)\times\xi} - \eta\rho$
$\Leftrightarrow \frac{\eta\xi}{2\log_2 e}(\frac{h'(\mathcal{X})}{\beta})^2 + (\frac{1}{\mu_{bs}} + \frac{\eta\rho\xi}{\log_2 e})\frac{h'(\mathcal{X})}{\beta} < 1 - \frac{\rho}{\mu_{bs}} - \frac{\eta\rho^2\xi}{2\log_2 e}$

and thus we get the bound Ω_b in (8). From Lemmas 2.2.1 and 2.2.2, we get the necessary and sufficient conditions in (2.41) and (2.42). For non-heavy traffic condition, i.e., $0 < (\frac{h'(\mathcal{X})}{\beta} + \rho) \ll \mu_{bs}$,

$h'(\mathcal{X}) < \Omega_b$
$\Leftrightarrow (\frac{\eta}{\beta} \times h'(\mathcal{X}) + \eta\rho) < \log_2 e \times \frac{2(1-(h'(\mathcal{X})/\beta+\rho)/\mu_{bs})}{(h'(\mathcal{X})/\beta+\rho)\times\xi} \leq \alpha$
$\Rightarrow (\frac{\eta}{\beta} \times h'(\mathcal{X}) + \eta\rho) < \alpha \Rightarrow h'(\mathcal{X}) < \beta(\alpha/\eta - \rho)$
$\Rightarrow \Pr(|\widehat{x}^t - x^t|^\eta < \infty) = 1$

and we get the sufficient condition from Lemma 2.2.2. ■

Proof of Cor. 2.2.1: Property 1) can be shown by simple algebra. Property 3) is obvious. Now, take partial derivatives of (2.45) with respect to η, μ_{bs}, and ξ:

$$\frac{\partial\Omega_b}{\partial\eta} = \beta \times \frac{(1+\eta\mu_{bs}^2\sigma_{bs}^2\times\ln 4)^{\frac{1}{2}} - 1 - \eta\mu_{bs}^2\sigma_{bs}^2\times\ln 2}{\eta^2\mu_{bs}\sigma_{bs}^2\times(1+\eta\mu_{bs}^2\sigma_{bs}^2\times\ln 4)^{\frac{1}{2}}\times\ln 2},$$

$$\frac{\partial\Omega_b}{\partial\mu_{bs}} = \beta \times \frac{1-(1+\eta\mu_{bs}^2\sigma_{bs}^2\ln 4)^{-\frac{1}{2}}}{\eta\mu_{bs}^2\sigma_{bs}^2\ln 2},$$

$$\frac{\partial\Omega_b}{\partial\xi} = \beta \times \frac{(1+\eta\mu_{bs}^2\xi\times\ln 4)^{\frac{1}{2}} - 1 - \eta\mu_{bs}^2\xi\times\ln 2}{\eta\mu_{bs}\xi^2\times(1+\eta\mu_{bs}^2\xi\times\ln 4)^{\frac{1}{2}}\times\ln 2}.$$

Given the considered range of $(\eta, \beta, \mu_{bs}, \xi)$, we get strictly $\frac{\partial\Omega_b}{\partial\eta} < 0$, $\frac{\partial\Omega_b}{\partial\mu_{bs}} > 0$, $\frac{\partial\Omega_b}{\partial\xi} < 0$ and thus properties 2), 4), 5). Note that $\xi = \sigma_{bs}^2 + \sigma_{bt}^2$ in (41). ■

Proof of Thm. 2.2.2: Apply Theorem 2.2.1 and Corollary 2.2.1. ■

2.2.4 Short Summary

We derive a condition for stable real-time tracking of an unstable, scalar, LTI dynamical system. In particular, we use a G/G/1-∞ queue to model a broad class of unreliable networks. The communication server re-transmits lost information bits until they are received by the estimator. The stability condition is a bound on the entropy rate of the unstable process. The derived bound is a function of the moment to be stabilized, encoder efficiency, quantization accuracy, and network parameters. Finally, we show how to use this bound for stable real-time tracking of multiple dynamical systems over a slotted wireless medium using three channel access protocols.

Chapter 3

How Multiple Dynamical Systems Should Track Each Other in Real-Time over a Shared Channel

In this chapter, we address the question of how multiple dynamical systems should track each other in real-time over a shared channel with the additional assumption that a real scalar or a real vector can be delivered in a message with negligible distortion. This assumption is valid since practical applications usually do not require infinite precision of the source state. This assumption is dramatically different from that in Chapter 2 and used mainly to model the packet-switched nature of modern communication networks. In Section 3.1 and Section 3.2, we model with a slotted ALOHA channel and multiple LTI (linear time-invariant) dynamical systems. Non-adaptive channel access schemes are analyzed in Section 3.1 for the tracking stability and MSE (mean squared-error) tracking performance. Adaptive (error-dependent) transmission control schemes are analyzed in Section 3.2.

With preliminary Matlab simulations, a comparison is made in Section 3.3 for decentralized communication policies and a transmission rate control is proposed for intelligent vehicles to broadcast state information and to track each other in real-time for active safety. A microscopic traffic simulator and a network simulator are used to compare the tracking performance of the proposed design and the currently proposed 100-millisecond beaconing design. This error-dependent transmission rate control will be enhanced with a transmission power control for vehicular safety communications in Chapter 4.

3.1 The Tracking Performance of Non-Adaptive Channel Access Schemes over a Slotted ALOHA

In recent years, many control applications of distributed systems are built on top of networks for information exchange, such as AHS (Automated Highway Systems) and UAV (Unmanned Aerial Vehicles). Those systems are called Networked Control Systems (NCSs)

in which sensors, actuators, controllers communicate through a data network. In NCSs, estimation is known to be a critical step, and its accuracy directly affects the control performance. For example, imagine that there is a group of intelligent vehicles equipped with wireless transceivers, traveling on the highway. Each vehicle can estimate neighboring vehicles' position and speed information, via a shared channel, and uses this information to facilitate certain safety applications, such as collaborative collision avoidance and the electronic brake light system.

For control over lossy channel, a decade of research [3,4,5,32,42,43] shows that the right approach is probably to insert a model-based estimator in between controller and the sensor. If the channel does not deliver sensor measurements on time, the estimator uses its model to provide the controller with its best estimate of the state. When measurements are successfully received, the estimator uses them to improve its estimate for the state of the remote system. The controller is always fed by the estimator.

In NCSs, the question of how to use minimum bit rate to control/stabilize a system through feedback was first introduced in [44,45]. Towards better modeling of today's digital networks, i.e. state information is transferred via packets instead of bit streams, the minimum packet rate problem was investigated in [6,7,34,46]. In existing literature, estimation problem is usually formulated as the sender-receiver pair with one-to-one channel scenario. Channel losses are usually assumed to be independent events. However, this assumption is not realistic for most multiple-access networks since a collision happens when more than one node transmits data at the same time.

To better understand the performance of estimation/tracking over a multiple-access network, we propose a framework and analyze MSE (mean squared error) of model-based estimation on top of slotted ALOHA [23], a simple multiple-access network. Specifically, we compare the estimation performance of three channel access designs: 1) probabilistic design that utilizes fully random access to the channel; 2) deterministic design in which nodes are perfectly scheduled to transmit; and 3) hybrid design that is combined from probabilistic and deterministic channel access. Among three communication methods, probabilistic channel access is easier to implement in a decentralized fashion but would inevitably incur collisions. On the other hand, deterministic scheme can avoid collisions by scheduling but it may require out-of-band signaling for coordination or at least consensus among nodes. In our analysis, asymptotic behavior and stability conditions for estimation MSE using those channel access schemes are also derived.

The contribution of this study is its quantitative discussion on model-based estimation in a multiple-access channel setting. The organization of this section is the following: Subsection 3.1.1 states related work, and Subsection 3.1.2 describes our problem formulation. Subsection 3.1.3, 3.1.4, and 3.1.5 are devoted to the analysis of probabilistic, deterministic, and hybrid channel access designs respectively. Subsection 3.1.6 concludes this section with a summary.

3.1.1 Related Work on Networked Control Systems

Stability constraints for partial observations are investigated in [6,35]. In the problem formulation [6], raw sensor measurements are transmitted to remote estimators and the channel drops packets according to *i.i.d.* Bernoulli trials. On the receiver side, intermittent observations are processed with a time-varying Kalman filter. The threshold of channel loss probability to stabilize estimation error is also derived. In [8], multiple description (MD) codes, a type of network source codes, are designed to compensate for packet-dropping and communication delay for Kalman filtering.

In [34], the sender keeps track of successfully transmitted state information as well as performs estimation of its local process, which is assumed to reach the same estimation results by the receiver. Long-term average cost problem is formulated for this scenario. Optimal controlled communication policy is derived with the cost function defined as weighted summation of estimation MSE and packet rate. The optimal decision to broadcast status update at each moment turns out to be decided by the current estimation error. The optimal communication policy is also proved to be a threshold policy, in which a region is defined for the estimation error. When the error exceeds this region/threshold, a broadcast is triggered to update the state information on remote estimators.

In [7], authors suggest that each node should process raw measurements with a Kalman filter before sending them out. The stability condition of such pre-processing is compared with [6]. The minimum packet rate to stabilize the estimation error to the stochastic moments is given in [34,46] for uncontrolled communication logic triggered by one fixed-rate Poisson process. Controlled communication logic is also proposed based on the Doubly Stochastic Poisson Process (DSPP) [47] to trigger the transmission. At each moment, jump intensity of the DSPP is a function of current estimation error. This error-dependent policy is proven to effectively keep all finite moments of estimation errors and the communication rate bounded.

Classical information theory [27] deals with the encoding of long sequences of data and thus inherently needs to tolerate long latency. However, due to the interactivity of real-time control, the state information to be communicated is not known ahead in time and it is used to control the very process being encoded. A new metric for evaluating channels in terms of reliability, called Anytime Capacity, is defined on a sense of reliable transmission in [4] and extended to multiple-access channels in [48]. A summary of recent advances in NCSs can be found in [49].

3.1.2 Problem Formulation

In this section, we describe our mathematical framework of model-based estimation on top of multiple-access channel as foundation for analysis in following three sections.

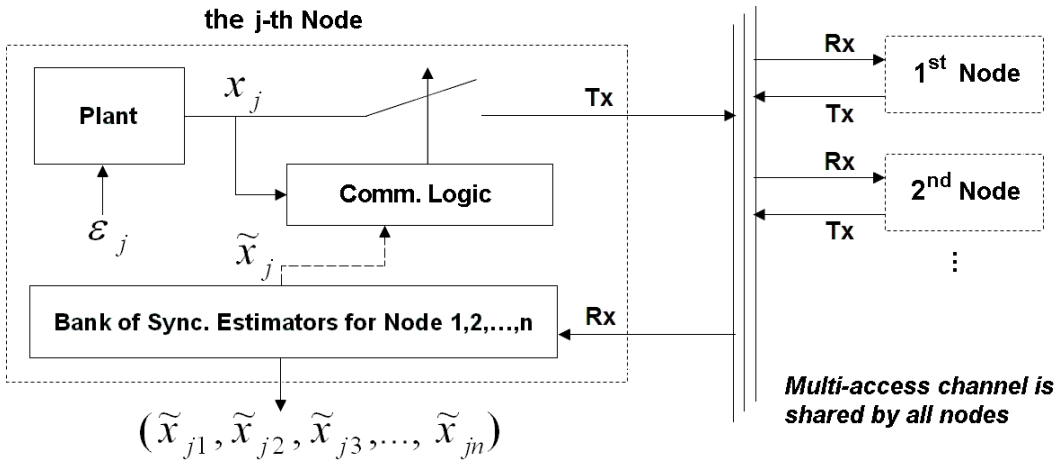

Figure 3.1. Node internal structure in analyzed real-time tracking problem.

NCS over a Multiple-Access Channel

Suppose there are n nodes sharing a slotted ALOHA network, $n = 2, 3, ...$, and each node contains a discrete-time LTI scalar process (3.1), a transmission control logic, and a bank of synchronized model-based estimators (see Figure 3.1). Each node will try to estimate the state on other nodes using received information from the shared channel.

In our setting, the dynamics of those spatially distributed processes are assumed to be completely decoupled. For notational convenience, let node $j \in \{1, 2, ..., n\}$ represent the j-th sender,

$$x_j(t) = a_j x_j(t-1) + \varepsilon_j(t-1) \tag{3.1}$$

where $x_j(t)$ is the scalar state of node j and $\varepsilon_j(t)$ is *i.i.d.* zero-mean noise process with finite variance σ_j^2, and t is the time index, $t \in N$.

Similar to the minimum packet rate formulation in [34,7], at each time index, the true state (a real number with acceptable distortion) of the sender j could be transferred to a receiver $i \neq j$, $i \in \{1, 2, ..., n\}$, via the shared and possibly lossy network. The transmission control logic decides whether to broadcast its own state information to others at each moment. Furthermore, the transmission time of state information, i.e. one slot length, is assumed to be the same as one discrete step of the process (3.1).

Model-Based Real-Time Tracking/Estimation

Let $\tilde{x}_{ij}(t)$ be the estimated state of sender j at receiver i. And, this estimated state is the expectation conditioned on all the previous received information from the lossy channel,

$$\tilde{x}_{ij}(t) = E[x_j | Y_i^1, Y_i^2, ..., Y_i^{t-1}] \tag{3.2}$$

where Y_i^t, $t = 1, 2, ...$, is the received information at moment t at the receiver i.

When channel is idle or has a collision at t, $Y_i^t = \emptyset$. Otherwise, $Y_i^t = x_s(t)$ from a certain successful sender $s \neq i$, $s \in \{1, 2, ..., n\}$. In our formulation, channel loss is only due to collisions. Neither fading nor hidden terminal problem are modeled for the multiple-access channel. Therefore, each node is assumed to get the same information from the channel.

Our performance metric is MSE (mean squared error) of the estimation process at the receiver side. The optimal MMSE model-based estimator, e.g., see [34,46,49], at receiver i switches between two modes:

- If no information regarding node j is received at $t-1$, i.e. $Y_i^{t-1} \neq x_j(t-1)$, use previous estimate $\tilde{x}_{ij}(t-1)$ and the known model (3.1) to carry on,

$$\tilde{x}_{ij}(t) = a_j \times \tilde{x}_{ij}(t-1) \tag{3.3}$$

- Else if state information of j is received at $t-1$, i.e. $Y_i^{t-1} = x_j(t-1)$, use it to reset estimation error,

$$\tilde{x}_{ij}(t) = a_j \times x_j(t-1) \tag{3.4}$$

Note that $\tilde{x}_{ij}(t)$ in (3.3), (3.4) is the optimal estimate, in MMSE sense, because noise process in (3.1) has zero mean.

For the estimator on node i, if an update is only received k steps before, $k = 1, 2, ...t-1$, when $\sigma_j^2 > 0$ and $a_j \neq 0$, the best estimate of x_j is

$$\tilde{x}_{ij}(t) = a_j^k x_j(t-k) \tag{3.5}$$

Let $\varphi_{ij}(t)$ denote the MSE of above estimation process, i.e. node j tries to estimate node i based on received information. $\varphi_{ij}(t)$ is given by definition,

$$\varphi_{ij}(t) = E[(x_j(t) - \tilde{x}_{ij}(t))^2] \tag{3.6}$$

By substituting $\tilde{x}_{ij}(t)$ derived in (3.5), conditioned on elapsed time step k since receiving the last update from j, we obtain

$$\varphi_{ij}(t) = E[E[(x_j(t) - a_j^k x_j(t-k))^2 | k < t]] \tag{3.7}$$

The inner part of (3.7) can be expressed as

$$x_j(t) - a_j^k x_j(t-k) = \sum_{l=1}^{k} a_j^{k-l} \varepsilon_j(t - (k-l+1)) \tag{3.8}$$

where $\varepsilon_j(t)$ is the noise process at moment t for node j.

Since the noise process $\varepsilon_j(t)$ are *i.i.d.* zero-mean random variables with finite variance σ_j^2, then (3.7), i.e. node i's estimate MSE for state j, can be organized as

$$\varphi_{ij}(t) = E[E[\sum_{l=1}^{k} a_j^{2(k-l)} | k < t]] \times \sigma_j^2 \tag{3.9}$$

where $E[\sum_{l=1}^{k} a_j^{2(k-l)} | k < t]$ can be further specified once the channel access design and the probability distribution of inter-arrival time k is known. In the following three sections, we will analyze the estimation performance of three different channel access schemes, namely probabilistic, deterministic, and hybrid methods, based on (3.9). Throughout this section, we further assume the process on each node is identical, i.e. $a_j = a$ and $\sigma_j = \sigma$ for all j.

3.1.3 Probabilistic Channel Access

In this section, we consider a purely random access scheme. Let each node broadcast its own state information with a fixed probability p_j at each time slot. To derive the optimal uniform probability p^* for all nodes, i.e. $p_j = p^*$ for all j, we need to consider several cases. Specifically, we denote the estimation MSE, defined in (3.6), while using the probabilistic method as φ_j^P. (We drop subscript i since all nodes can get the same copy of information from the channel and achieve the same estimation for node j.)

Case $|a| = 1$

Consider process (3.1) with bounded noise variance $\sigma^2 > 0$ and $|a| = 1$. First, let's focus on the case when $a = 1$,

$$x_j(t) = x_j(t-1) + \varepsilon_j(t-1) \tag{3.10}$$

which can be seen as a one-dimensional random walk with each step decided by the noise process. Without any broadcast of state information, i.e. $p_j = 0$ for all j, the best estimate of the state is given by

$$\tilde{x}_j(t) = E[x_j(0) + \sum_{l=0}^{t-1} \varepsilon_j(l)] = x_j(0) \tag{3.11}$$

if initial state $x_j(0)$ is given. However, estimation MSE of this process without any broadcast, denoted as $\bar{\varphi}_j(t)$, is given by

$$\bar{\varphi}_j(t) = E[(x_j(t) - \tilde{x}_j(t))^2] = E[\sum_{l=0}^{t-1} \varepsilon_j^2(l)] = t \times \sigma^2 \tag{3.12}$$

Thus, as $t \to \infty$, the estimation MSE will go unbounded, i.e. $\bar{\varphi}_j(t) \to \infty$, which shows the necessity for each node to broadcast state information to eliminate the estimation error, i.e. $0 < p_j \leq 1$.

To find the optimal broadcast probability $p_j = p^*$ for all j, let's focus on the estimation MSE for node j since all nodes are identical. In this case, (3.9) can specified as

$$\varphi_j^P(t) = E[E[\sum_{l=t-k}^{t-1} \varepsilon_j^2(l) | k < t]] = E[k | k < t] \times \sigma^2 \tag{3.13}$$

Considering $t \to \infty$, (3.13) implies the optimal probability p^* is the minimizer of mean inter-arrival time k of state information of j delivered to node i, i.e.

$$p^* = \arg\min_{0<p\leq 1} \; E[k] \tag{3.14}$$

Since all nodes share a slotted ALOHA network, the probability for receiver i to get an update from node j successfully, received at k slots ago, can be written as

$$P_{ij}(k = K) = p(1-p)^{n-1} \times [1 - p(1-p)^{n-1}]^{K-1} \tag{3.15}$$

where $K = 1, 2, ..., t-1$. With (15), $E[k|k < t]$ can be given by definition,

$$E[k|k < t] = \sum_{k=1}^{t-1} k \times p(1-p)^{n-1} \times [1 - p(1-p)^{n-1}]^{k-1}.$$

which can be organized into a closed form if $t \to \infty$,

$$E[k] = (p(1-p)^{n-1})^{-1}.$$

Therefore, to find the stationary solution p^*, (3.14) can be rewritten as

$$p^* = \arg\min_{0<p\leq 1} (p(1-p)^{n-1})^{-1} \tag{3.16}$$

The optimal (stationary) solution to above problem is the well-known result for slotted ALOHA [23]:

$$p^* = \frac{1}{n} \tag{3.17}$$

which maximizes the per node throughput $p(1-p)^{n-1}$. For the case $a = -1$, (3.17) can also be shown to be optimal.

Case $0 < |a| < 1$

Now consider the process (3.1) with bounded noise variance $\sigma^2 > 0$ and $0 < |a| < 1$. From (3.9), the general form of estimation MSE can be specified as

$$\varphi_j^P(t) = \sigma^2(\frac{1}{1-a^2} - \frac{E[a^{2k}|k < t]}{1-a^2}) \tag{3.18}$$

Since $a^2 < 1$, to minimize MSE, we focus on finding $p_j = p^*$, for all j, to maximize $E[a^{2k}|k < t]$ in (3.18). Now considering $t \to \infty$, we want to find p^* to maximize $E[a^{2k}]$,

$$p^* = \arg\max_{0<p\leq 1} E[a^{2k}]. \tag{3.19}$$

where the stationary formulation as $t \to \infty$,

$$E[a^{2k}] = \sum_{k=1}^{\infty} P_{ij}(k) \times a^{2k} \tag{3.20}$$

Substituting (3.15) into (3.20), we get

$$E[a^{2k}] = p(1-p)^{n-1} \times \sum_{k=1}^{\infty} [1-p(1-p)^{n-1}]^{k-1} \times a^{2k}.$$

Because $[1-p(1-p)^{n-1}] \times a^2 < 1$, above can be organized to a closed form,

$$E[a^{2k}] = \frac{p(1-p)^{n-1} \times a^2}{1-[1-p(1-p)^{n-1}] \times a^2} \tag{3.21}$$

Now let $q = p(1-p)^{n-1}$, which denotes the per node steady-state throughput in slotted ALOHA system. From the throughput analysis in [23], we know

$$0 < q \leq \frac{1}{n}(1-\frac{1}{n})^{n-1} < 1 \tag{3.22}$$

Thus (3.21) can be expressed as

$$E[a^{2k}] = \frac{q \times a^2}{1-(1-q) \times a^2} \tag{3.23}$$

Let $h_a(q)$ be a function of q with fixed a as its parameter,

$$h_a(q) = (1 + \frac{1-a^2}{qa^2})^{-1} = E[a^{2k}] \tag{3.24}$$

The fact that $0 < a^2 < 1$ together with (3.22) implies that $h_a(q)$ is monotone increasing as q increases. With (3.24), now the maximization problem (3.19) is equivalent to

$$q^* = \underset{0<q\leq \frac{1}{n}(1-\frac{1}{n})^{n-1}}{\arg\max} \quad h_a(q) \tag{3.25}$$

where optimal solution exists at $q^* = \frac{1}{n}(1-\frac{1}{n})^{n-1}$, which is the maximum per node throughput achieved in slotted ALOHA network. Therefore, the optimal broadcast probability is given by (3.17) for the case $0 < |a| < 1$.

Case $1 < |a| < \infty$

Now consider the process (3.1) with bounded noise variance $\sigma^2 > 0$ but $1 < |a| < \infty$. Since $1 < a^2 < \infty$, from (3.9) we can get the general form of MSE as (3.18). To get bounded MSE as $t \to \infty$, i.e. $\lim_{t\to\infty} \varphi_j^P(t) < \infty$, $E[a^{2k}]$ must be bounded. Similar to previous case, let $q = p(1-p)^{n-1}$, we have

$$E[a^{2k}] = q \times \sum_{k=1}^{\infty} (1-q)^{k-1} \times a^{2k}.$$

To have $E[a^{2k}]$ bounded, q and a must satisfy below condition,

$$(1-q) \times a^2 < 1 \tag{3.26}$$

Here we get a relationship between the per node steady-state throughput q and the parameter a if the estimation MSE is bounded for $t \to \infty$. Together with (3.22), to have $\lim_{t\to\infty} \varphi_j^P(t)$ bounded, a has to satisfy below condition:

$$|a| < (1 - \frac{1}{n}(1 - \frac{1}{n})^{n-1})^{-\frac{1}{2}} \tag{3.27}$$

where n is the number of nodes. This upper bound monotonically converges down to 1 when n is sufficiently large. If a satisfies (3.27), optimal broadcast probability can be shown to be (3.17). Otherwise, when $|a| \geq (1 - \frac{1}{n}(1 - \frac{1}{n})^{n-1})^{-\frac{1}{2}}$, the estimation process cannot have bounded MSE, as $t \to \infty$, by using a fixed broadcast probability for all nodes.

3.1.4 Deterministic Channel Access

Probabilistic design explored in Subsection 3.1.3 can be viewed as the completely randomized channel access. For multiple-access channel, one can also choose TDMA (Time Division Multiple Access) scheme for each node to broadcast state information without collisions in the shared channel.

In this section, deterministic design refers to the round-robin scheduling that fairly serves each node. All nodes are assumed to have this TDMA scheduling knowledge. At each moment, there will be only one node scheduled to broadcast its own state information and thus there is no collision (loss). In the following analysis, we denote the estimation MSE, defined in (3.6), while using round-robin scheme as φ_j^D.

Case $|a| = 1$

For the process (3.1) with bounded noise variance $\sigma^2 > 0$ and $|a| = 1$. Similarly, (3.9) can be specified as the form in (3.13). Now, with a deterministic communication scheduling, and the estimation MSE is bounded by

$$\sigma^2 \leq \varphi_j^D(t) \leq n \times \sigma^2 \tag{3.28}$$

depending on the moment t and scheduled communication instants for node j.

Recall that, from (3.13), (3.15) and (3.17), the steady-state *minimum* estimation MSE for probabilistic design, denoted as $\varphi_j^P(t)^*$, is given by

$$\varphi_j^P(t)^* = n(1 - \frac{1}{n})^{1-n} \times \sigma^2 \tag{3.29}$$

When n is sufficiently large, (3.29) can be approximated by

$$\varphi_j^P(t)^* \to ne \times \sigma^2 \tag{3.30}$$

which reveals that $\varphi_j^P(t)^*$ increases with the number of nodes n. By comparing (3.28) and (3.29), we can see that,

$$\varphi_j^P(t)^* > \varphi_j^D(t)$$

which shows that, in this simple case $|a| = 1$, using a deterministic channel access can achieve lower estimation MSE than that of probabilistic design as $t \to \infty$.

Case $0 < |a| < 1$

Now consider the process (3.1) with bounded noise variance $\sigma^2 > 0$ and $0 < |a| < 1$. From (3.9) we can get the general form of estimation MSE,

$$\varphi_j^D(t) = \frac{1 - a^{2L_j}}{1 - a^2} \times \sigma^2 \tag{3.31}$$

where L_j is the time from last transmission for node j, $L_j = 1, 2, ..., n$. Thus, the estimation MSE is bounded by

$$\underline{\varphi_j^D} \leq \varphi_j^D(t) \leq \overline{\varphi_j^D} \tag{3.32}$$

where lower bound is given by $\underline{\varphi_j^D} = \sigma^2$ and upper bound is given by $\overline{\varphi_j^D} = \frac{1-a^{2n}}{1-a^2} \times \sigma^2$.

From (3.17), (3.18) and (3.21), the minimum steady-state estimation MSE for probabilistic channel access, denoted as $\varphi_j^P(t)^*$, is given by

$$\varphi_j^P(t)^* = \frac{\sigma^2}{1 - a^2 + \frac{1}{n}(1 - \frac{1}{n})^{n-1} \times a^2} \tag{3.33}$$

when n is sufficiently large, (3.33) can be approximated by

$$\varphi_j^P(t)^* \to \frac{ne}{a^2 + ne(1 - a^2)} \times \sigma^2 \tag{3.34}$$

By comparing (3.32) and (3.33), numerical analysis shows that, for $0 < |a| < 1$,

$$\underline{\varphi_j^D} < \varphi_j^P(t)^* \leq \overline{\varphi_j^D}.$$

Therefore, when $0 < |a| < 1$, estimation MSE while using probabilistic design falls in the same range of that of using deterministic channel access as $t \to \infty$.

Case $1 < |a| < \infty$

For the process (3.1) with bounded noise variance $\sigma^2 > 0$ and $1 < |a| < \infty$, one can get (3.32) and (3.33) by going through similar derivation in previous case. Numerical analysis shows that, for the case $|a| > 1$,

$$\varphi_j^P(t)^* > \varphi_j^D(t)$$

which shows that, as $t \to \infty$, using a deterministic channel access can achieve strictly lower estimation MSE than that of probabilistic design when $|a| > 1$.

3.1.5 Hybrid Channel Access

A combined method from previous two designs may sometimes be proposed for scalability and flexibility reasons. In this section, the hybrid design bundles several nodes into one

group and scheduled communication instants are given to every group fairly in a round-robin fashion. Within the same group, each node use equal broadcast probability to contend for channel access.

Assume there are n nodes and θ groups, then the number of nodes in one group m is given by $m = \frac{n}{\theta}$. Of course, n, θ, m must be chosen to be positive integers to make this formulation meaningful. The communication probability p^θ for each node in the group is given by $p^\theta = \frac{1}{m}$ when this group is scheduled to use the channel; otherwise, $p^\theta = 0$. We denote the steady-state estimation MSE, defined in (3.6), while using the Hybrid-θ method as $\varphi_j^{H_\theta}$.

Case $|a| = 1$

For the process (3.1) with bounded noise variance $\sigma^2 > 0$ and $|a| = 1$. Since nodes within the same group will contend for channel access every θ slots, the probability for receiver i to get an update from node j successfully, received at k slots ago, can be written as

$$P_{ij}^\theta(k = L_j + r \times \theta) = p^\theta(1-p^\theta)^{m-1} \times [1 - p^\theta(1-p^\theta)^{m-1}]^r \tag{3.35}$$

where $r = 0, 1, 2, ...$ and L_j depends on the group communication instants of node j, $L_j = 1, 2, ..., \theta$. With (3.35), mean inter-arrival time $E[k]$ is bounded by

$$1 - \theta + n \times (1 - \frac{\theta}{n})^{1-\frac{n}{\theta}} \leq E[k] \leq n \times (1 - \frac{\theta}{n})^{1-\frac{n}{\theta}}.$$

As usual, (3.9) can be specified as similar form in (3.13). Therefore, the steady-state estimation MSE is bounded by

$$\underline{\varphi_j^{H_\theta}} \leq \varphi_j^{H_\theta}(t) \leq \overline{\varphi_j^{H_\theta}} \tag{3.36}$$

where lower bound is given by

$$\underline{\varphi_j^{H_\theta}} = (1 - \theta + n(1 - \frac{\theta}{n})^{1-\frac{n}{\theta}}) \times \sigma^2 \tag{3.37}$$

and upper bound is given by

$$\overline{\varphi_j^{H_\theta}} = n(1 - \frac{\theta}{n})^{1-\frac{n}{\theta}} \times \sigma^2 \tag{3.38}$$

When n is sufficiently large, the lower bound (3.37) can be approximated by

$$\underline{\varphi_j^{H_\theta}} \to (1 - \theta + ne) \times \sigma^2 \tag{3.39}$$

and upper bound (3.38) can be approximated by

$$\overline{\varphi_j^{H_\theta}} \to ne \times \sigma^2 \tag{3.40}$$

If $\theta = 1$, i.e. the probabilistic scheme, (3.37) and (3.38) reduce to (3.29). If $\theta = n$, i.e. the deterministic scheme, (3.36) reduces to (3.28).

Comparing (3.28), (3.29), and (3.36), numerical analysis shows that, when $|a| = 1$,

$$\varphi_j^P(t)^* > \varphi_j^{H_\theta}(t) > \varphi_j^D(t)$$

which says that, deterministic channel access is the one that minimizes MSE among three methods.

Case $0 < |a| < 1$

Now consider the process (3.1) with bounded noise variance $\sigma^2 > 0$, $0 < |a| < 1$. Plugging (3.35) into the same form of (3.20), and let $t \to \infty$, we can get the range of $E[a^{2k}]$

$$\underline{E[a^{2k}]} \leq E[a^{2k}] \leq \overline{E[a^{2k}]} \tag{3.41}$$

where lower bound is

$$\underline{E[a^{2k}]} = \frac{a^{2\theta} \times p^\theta (1-p^\theta)^{m-1}}{1 - (1 - p^\theta(1-p^\theta)^{m-1}) \times a^{2\theta}} \tag{3.42}$$

and upper bound is

$$\overline{E[a^{2k}]} = \frac{a^{2} \times p^\theta (1-p^\theta)^{m-1}}{1 - (1 - p^\theta(1-p^\theta)^{m-1}) \times a^{2\theta}} \tag{3.43}$$

With (3.9) and (3.41), and the steady-state estimation MSE is bounded by

$$\underline{\varphi_j^{H_\theta}} \leq \varphi_j^{H_\theta}(t) \leq \overline{\varphi_j^{H_\theta}} \tag{3.44}$$

where lower bound is given by

$$\underline{\varphi_j^{H_\theta}} = \frac{\sigma^2}{1-a^2} \times (1 - \frac{a^2 \times \frac{\theta}{n}(1-\frac{\theta}{n})^{\frac{n}{\theta}-1}}{1 - a^{2\theta} + a^{2\theta} \times \frac{\theta}{n}(1-\frac{\theta}{n})^{\frac{n}{\theta}-1}}) \tag{3.45}$$

and upper bound is given by

$$\overline{\varphi_j^{H_\theta}} = \frac{\sigma^2}{1-a^2} \times \frac{1 - a^{2\theta}}{1 - a^{2\theta} + a^{2\theta} \times \frac{\theta}{n}(1-\frac{\theta}{n})^{\frac{n}{\theta}-1}} \tag{3.46}$$

When n is sufficiently large, lower bound (3.45) can be approximated by

$$\underline{\varphi_j^{H_\theta}} \to \frac{\sigma^2}{1-a^2} \times (1 - \frac{a^2 \times \theta}{ne(1-a^{2\theta}) + a^{2\theta} \times \theta}) \tag{3.47}$$

and upper bound (3.46) can be approximated by

$$\overline{\varphi_j^{H_\theta}} \to \frac{\sigma^2}{1-a^2} \times \frac{ne(1-a^{2\theta})}{ne(1-a^{2\theta}) + a^{2\theta} \times \theta} \tag{3.48}$$

Similar to previous case, if $\theta = 1$, i.e. the probabilistic scheme, (3.45) and (3.46) reduce to (3.33). If $\theta = n$, i.e. the deterministic scheme, (3.44) reduces to (3.32).

Now comparing (3.32), (3.33) and (3.44), numerical analysis shows that, for the case $0 < |a| < 1$,

$$\underline{\varphi_j^D} < \underline{\varphi_j^{H_\theta}} \leq \varphi_j^P(t)^* \leq \overline{\varphi_j^{H_\theta}} \leq \overline{\varphi_j^D}$$

which shows that, as $t \to \infty$, three channel access designs have estimation MSE roughly within the same range.

Case $1 < |a| < \infty$

Now consider the process (3.1) with bounded noise variance $\sigma^2 > 0$, $1 < |a| < \infty$. One may go through similar derivation as previous case to get (3.44), (3.45) and (3.46). But note that, similar to (3.26), those results are valid only when

$$(1 - p^\theta(1 - p^\theta)^{m-1}) \times a^{2\theta} < 1.$$

In other words, to have bounded estimation MSE for hybrid design, parameters a, n, θ must satisfy below condition,

$$|a| < (1 - \frac{\theta}{n}(1 - \frac{\theta}{n})^{\frac{n}{\theta}-1})^{-\frac{1}{2\theta}} \tag{3.49}$$

where $1 \leq \theta < n$. (3.49) gives a relaxed condition than the limitation of probabilistic design given in (3.27). In Hybrid-θ channel access, the contention from all nodes, as what happens in probabilistic design, has been distributed to several small scale contentions within a group.

Comparing (3.32), (3.33) and (3.44), numerical analysis shows that, for the case $|a| > 1$,

$$\varphi_j^P(t)^* > \varphi_j^{H_\theta}(t) > \varphi_j^D(t).$$

That is, deterministic channel access can achieve strictly lower estimation MSE as $t \to \infty$.

3.1.6 Short Summary

Model-based estimation/tracking over the multiple-access network is studied in this section. A mathematical framework is proposed and the estimation MSE of three channel access schemes is analyzed. Asymptotic behavior and stability condition are also derived. Our results suggest that, while designing NCSs, the channel access scheme should be chosen based on $|a|$ of the dynamic process (3.1). If $|a| \geq 1$, the deterministic design (round-robin scheduling) can achieve strictly lower estimation MSE. Otherwise, for $0 < |a| < 1$, three methods have roughly the same range of MSE as $t \to \infty$. Meanwhile, [37] proves that, for a sender-receiver pair, optimal communication design should incorporate estimation error and such correlation can help improve estimation accuracy. We will explore this kind of *error-dependent* communication design for estimation in a multiple-access channel setting in next section.

3.2 The Tracking Performance of Error-Dependent Channel Access Schemes over a Slotted ALOHA

In this section, we compare the asymptotic time-averaged MSE (mean squared error) while using controlled and uncontrolled communication policies. Here, controlled communication means the decision to broadcast state information takes current estimation error as input. On the other hand, uncontrolled communication policy follows a pre-defined scheme instead of being dynamically adjusted by current estimation error.

Among three uncontrolled communication methods analyzed in Section 3.1, probabilistic design is easier to implement in a decentralized manner but would incur unnecessary collisions. On the other hand, deterministic scheme can avoid collisions by perfect scheduling but it may require out-of-band signaling for coordination or at least consensus among nodes.

The contribution of this section is its quantitative discussion on estimation performance of different communication policies in a multi-access channel setting. We show that it is possible for a decentralized policy to have estimation performance stayed *close* to a centralized one by properly choosing its parameter. An improved controlled communication policy is also proposed based on the analysis.

The organization of this section is the following: Subsection 3.2.1 describes our problem formulation. Subsection 3.2.2 and Subsection 3.2.3 are devoted to the analysis of uncontrolled and controlled communication policies respectively. Subsection 3.2.4 summarizes this section.

3.2.1 Problem Formulation with a Revised Performance Metric

In this subsection, we describe our mathematical framework and the performance metric for model-based estimation over a multi-access channel. A new performance metric, the Asymptotic Time-Averaged MSE defined in eq. (3.58), is used in this section and it is slightly different from the performance metric used in Section 3.1 so that different communication policies can be compared.

Scalar LTI Dynamical Systems

Suppose there are n nodes, $n = 2, 3, ...$, and the dynamics of those spatially distributed LTI processes are assumed to be completely decoupled. For notation convenience, for each node $j \in \{1, 2, ..., n\}$, its state transition is given by

$$x_j(t) = a_j \times x_j(t-1) + \varepsilon_j(t-1) \tag{3.50}$$

where $x_j(t)$ is the scalar state of node j and $\varepsilon_j(t)$ is i.i.d. zero-mean noise process with finite variance σ_j^2, and t is time index, $t \in N$.

Similar to the minimum packet rate formulation in [7,46], at each time index, the true state (a real number with acceptable distortion) of the sender j could be transferred to a receiver $i \neq j$, $i \in \{1, 2, ..., n\}$, via the shared and possibly lossy network. Furthermore, one

discrete step of the process (3.50) is adjusted to be the same as the transmission time of state information, i.e. one slot length.

Real-Time Tracking/Estimation over a Multi-Access Network

As illustrated in Figure 3.1, those n nodes share a slotted wireless channel, and each node contains a discrete-time LTI scalar process (3.50), a communication logic, and a bank of synchronized model-based estimators. The communication logic decides whether to broadcast its own state information at each moment. Each node will try to estimate the states on other nodes by received information.

Let $\tilde{x}_{ij}(t)$ be the estimated state of sender j at receiver i. And, this estimated state is the expectation conditioned on all the previous received information from the lossy channel,

$$\tilde{x}_{ij}(t) = E[x_j | Y_i^1, Y_i^2, ..., Y_i^{t-1}] \tag{3.51}$$

where Y_i^t, $t = 1, 2, ...$, is the received information at moment t at the receiver i.

When channel is idle or has a collision at t, $Y_i^t = \emptyset$. Otherwise, $Y_i^t = x_s(t)$ from a certain successful sender $s \in \{1, 2, ..., n\}$. In our formulation, channel loss is only due to collisions. Neither fade effect nor hidden terminal problem is modeled for the multi-access channel. Therefore, each node is assumed to get the same copy of information from the channel. Besides, all information contained in collided packets is treated as lost and there is no retransmission for lost packets.

As discussed in Section 3.1, the optimal model-based estimator at receiver i, e.g., see [34,46,49], switches between following two modes:

- If no information regarding node j is received at $t-1$, i.e. $Y_i^{t-1} \neq x_j(t-1)$, use previous estimate $\tilde{x}_{ij}(t-1)$ and the known model (3.50) to carry on,

$$\tilde{x}_{ij}(t) = a_j \times \tilde{x}_{ij}(t-1) \tag{3.52}$$

- Else if state information of j is received at $t-1$, i.e. $Y_i^{t-1} = x_j(t-1)$, use it to reset estimation error,

$$\tilde{x}_{ij}(t) = a_j \times x_j(t-1) \tag{3.53}$$

Note that $\tilde{x}_{ij}(t)$ in (3.52), (3.53) is the optimal estimate, in MMSE sense, due the fact that noise process has zero mean.

The estimation error $e_{ij}(t)$, i-th node's estimation error for state j, is defined as

$$e_{ij}(t) = x_j(t) - \tilde{x}_{ij}(t) \tag{3.54}$$

From the (3.52) and (3.53), if an update is only received k steps before, $k = 1, 2, ...t-1$, the best estimate of x_j at receiver i is given by

$$\tilde{x}_{ij}(t) = a_j^k \times x_j(t-k) \tag{3.55}$$

Assuming latest measurement arrives at receiver side at the $t-k$ moment, now let $\varphi_{ij}(t)$ be the MSE of above estimation process, i.e. node j tries to estimate node i based on received information at time t. Thus, $\varphi_{ij}(t)$ is given by definition,

$$\varphi_{ij}(t) = E[e_{ij}(t)^2] \tag{3.56}$$

By substituting $\tilde{x}_{ij}(t)$ in (3.55), conditioned on elapsed time step k since receiving an update from j-th node, (3.56) becomes

$$\varphi_{ij}(t) = E[E[(x_j(t) - a_j^k x_j(t-k))^2 | k < t]]$$

and its inner part can be expressed as

$$x_j(t) - a_j^k x_j(t-k) = \sum_{l=1}^{k} a_j^{k-l} \varepsilon_j(t-(k-l+1))$$

where $\varepsilon_j(t)$ is the noise process at moment t for node j.

Since the noise process $\varepsilon_j(t)$ are i.i.d. zero-mean random variables with finite variance σ_j^2, then (3.56), i.e. i-th node's estimation MSE for state j, can be organized as

$$\varphi_{ij}(t) = E[\sum_{l=1}^{k} a_j^{2(k-l)} | k < t] \times \sigma_j^2 \tag{3.57}$$

where $E[\sum_{l=1}^{k} a_j^{2(k-l)} | k < t]$ can be further specified once the communication design and the probability distribution of inter-arrival time k is known. In following analysis, we further assume the process on each node is identical, i.e. $a_j = a$ and $\sigma_j^2 = \sigma^2$ for all $j = 1, 2, ..., n$.

From now on, we use notation φ_j instead of φ_{ij} for all i since we assume all nodes can get the same copy of information from the channel. Throughout this section, the performance metric is **Asymptotic Time-Averaged MSE** of the estimation process,

$$\Phi_j = \lim_{T \to \infty} \frac{\sum_{t=1}^{T} \varphi_j(t)}{T}, \tag{3.58}$$

so that different communication policies can be compared later in Subsection 3.2.2 and 3.2.3.

3.2.2 Uncontrolled Transmission Policies: a Summary

In Section 3.1, we analyzed different types of uncontrolled communication schemes and results are summarized here.

Probabilistic (random access): Each node broadcasts its own state information with a fixed probability p at each time step. We denote its tracking MSE as Φ_j^P for (3.58). With bounded noise variance $\sigma^2 > 0$, the stability condition to have $\Phi_j^P < \infty$ is given by

$$0 < |a| < (1 - \frac{1}{n}(1 - \frac{1}{n})^{n-1})^{-\frac{1}{2}}. \tag{3.59}$$

Based on (3.59), when n is large enough, the channel can only support stable tracking of scalar dynamical systems with $|a| \leq 1$ if this policy is used. Under condition (3.59), the optimal broadcast probability is proven to be $p^* = \frac{1}{n}$ for all nodes. Otherwise, there is no bounded tracking MSE for this scheme. The minimum achievable Φ_j^P by this policy, denoted as $\Phi_j^{P^*}$, exists almost surely, $\forall j = 1, ..., n$,

$$\Phi_j^{P^*} = (1 - a^2 + \frac{1}{n}(1 - \frac{1}{n})^{n-1} \times a^2)^{-1} \times \sigma^2, \tag{3.60}$$

if $|a|$ satisfies the stability requirement in (3.59).

Deterministic (round-robin): Deterministic design refers to the round-robin scheduling to fairly serve each node. All n nodes are assumed to have this TDMA (time-division multiple access) scheduling knowledge and be perfectly synchronized. At each moment, there will be only one node scheduled to broadcast its own state information and thus there is no collision (message loss) in the channel. Since each node will definitely get a chance to broadcast its own state information after waiting a finite time (i.e., n slots), no finite $|a|$ will make tracking error grow unbounded between measurement arrivals. Therefore, there is no such upper-bound for $|a|$ as that in (3.59). We denote its tracking MSE as Φ_j^D for (3.58). Its asymptotic time-averaged MSE exists almost surely, $\forall j = 1, ..., n$, for $|a| = 1$,

$$\Phi_j^D = \frac{n+1}{2} \times \sigma^2, \tag{3.61}$$

and for $|a| \neq 1$ and $|a| < \infty$,

$$\Phi_j^D = \frac{n - \sum_{l=1}^{n} a^{2l}}{n(1 - a^2)} \times \sigma^2. \tag{3.62}$$

Hybrid (grouped channel access): This semi-centralized design bundles several nodes into one group and scheduled communication instants are given to each group fairly in a round-robin fashion. Channel contention only exists inside a group. This policy is sometimes used to reduce collisions and increase scalability when the node number is large. Assume there are n nodes and θ groups, and then the number of nodes in one group is given by $m \equiv \frac{n}{\theta}$. Of course, n, θ, m must be chosen to be positive integers. The communication probability p^θ for each node in the same group is given by $p^\theta = \frac{1}{m} = \frac{\theta}{n}$ when this group is scheduled to use the channel. Otherwise, $p^\theta = 0$ when other groups are using the channel.

This Hybrid-θ policy can be viewed as a multiple interleaved version of Probabilistic policy, and we denote its tracking MSE as $\Phi_j^{H_\theta}$ for (3.58). Similar to (3.59), the stability condition to have $\Phi_j^{H_\theta} < \infty$ is given by

$$0 < |a| < (1 - \frac{\theta}{n}(1 - \frac{\theta}{n})^{\frac{n}{\theta}-1})^{-\frac{1}{2\theta}} \tag{3.63}$$

where $1 \leq \theta \leq n$. Here, (3.63) gives a relaxed condition than the limitation of Probabilistic policy in (3.59) and these upper-bounds all monotonically converge down to 1 when n is sufficiently large, i.e., only stable plants can be tracked with bounded MSE by using these

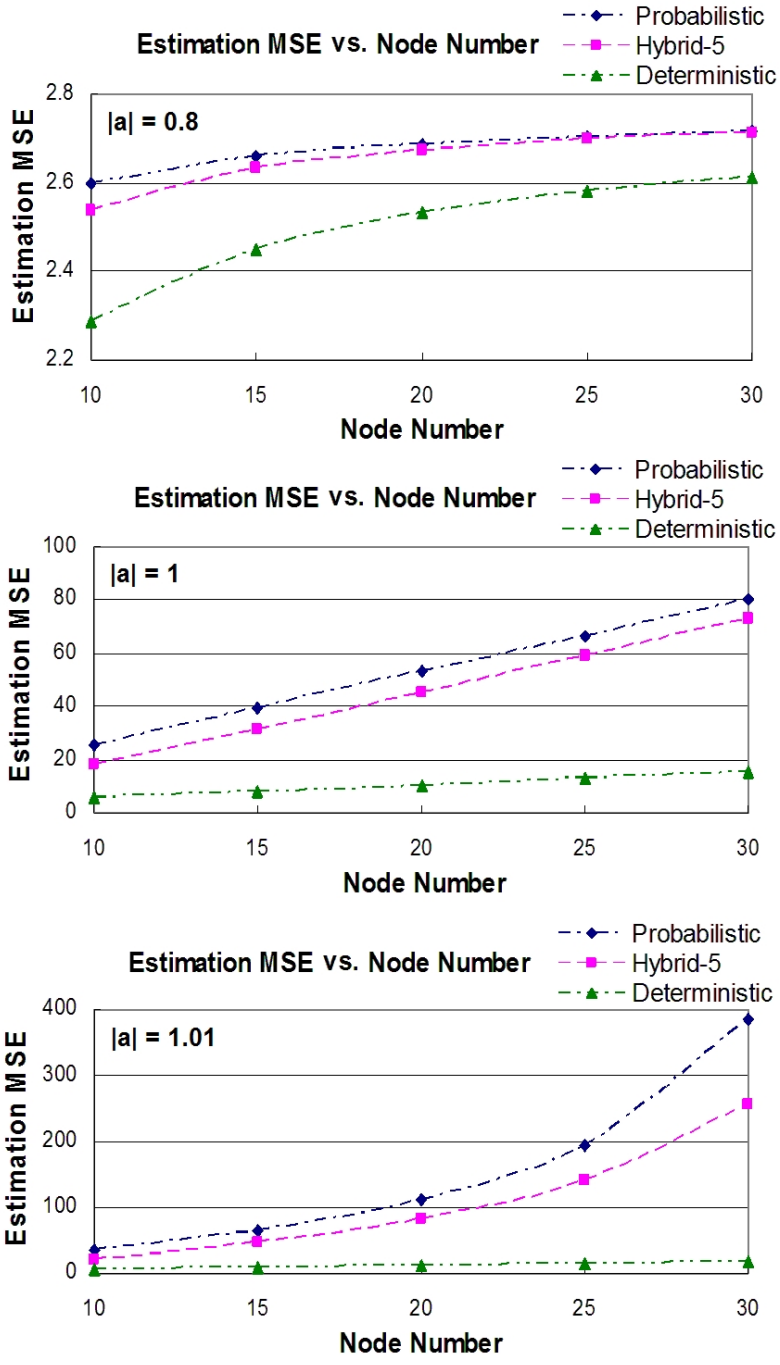

Figure 3.2. Performance comparison of three uncontrolled policies for $|a| = 0.8$, $|a| = 1$, and $|a| = 1.01$ (with $\sigma^2 = 1$).

randomized-access policies. The asymptotic time-averaged MSE of this Hybrid-θ policy exists almost surely, $\forall j = 1, ..., n$, for $|a| = 1$,

$$\Phi_j^{H_\theta} = (n(1 - \frac{\theta}{n})^{1-\frac{n}{\theta}} + \frac{1-\theta}{2}) \times \sigma^2, \tag{3.64}$$

and for $|a| \neq 1$ and it satisfies the stability requirement in (3.63),

$$\Phi_j^{H_\theta} = \{1 - \Omega\} \times \frac{\sigma^2}{1 - a^2} \tag{3.65}$$

where

$$\Omega \equiv \frac{a^2(1 - a^{2\theta}) \times \frac{\theta}{n}(1 - \frac{\theta}{n})^{\frac{n}{\theta}-1}}{\theta(1 - a^2)\{1 - a^{2\theta} + a^{2\theta} \times \frac{\theta}{n}(1 - \frac{\theta}{n})^{\frac{n}{\theta}-1}\}}.$$

Three examples of tracking MSE are plotted in Figure 3.2. By analyzing (3.60), (3.62), and (3.65), we learn the following facts: 1) when $0 < |a| < 1$, three uncontrolled policies have roughly the same tracking performance, $\Phi_j^D \leq \Phi_j^{H_\theta} \leq \Phi_j^P$; 2) when $|a| \geq 1$, strictly $\Phi_j^D < \Phi_j^{H_\theta} < \Phi_j^P$. One may notice the huge performance difference between Probabilistic policy and round-robin scheduling in Figure 3.2. However, round-robin scheduling requires perfect coordination, by either consensus among nodes or out-of-band signaling, and thus might not be feasible in some distributed systems, e.g., our CASS problem setting. In next subsection, we will show that it is possible for a decentralized policy, that utilizes a feedback control concept (inspired by [46]) to dynamically adapt its communication rate based on perceived tracking error, to achieve much better tracking performance than the Probabilistic policy.

3.2.3 Error-Dependent Transmission Control

In this subsection, we analyze a controlled communication policy, originally proposed in [46] for one-to-one channel setting, that takes current estimation error as input to decide its transmission probability. Using this policy, each node decides its own rate in a decentralized fashion. Based on analysis, we also propose an improved version of this policy and confirm its robustness by Matlab simulations.

Controlled Communication Policy

Error-Dependent: At the beginning of each slot, the communication probability is calculated in the following way. First, the communication intensity $\lambda_j(t)$ for node j at slot t is a function of the current estimation error $e_j(t)$,

$$\lambda_j(t) = \pi \times e_j^2(t) \tag{3.66}$$

where $0 < \pi < \infty$ is a positive real number, representing the sensitivity to estimation error $e_j(t)$. The calculation of $e_j(t)$ is possible because each node also keeps track of all successfully broadcast information and runs an estimator for its local plant to understand the estimation

error on other nodes. (This way, one node can know what other nodes *think* about its own state.)

As in [46], the communication intensity $\lambda_j(t)$ in (3.66) is then converted to the per slot transmission probability $p_j(t)$ by a continuous mapping from a non-negative real to $[0, 1]$,

$$p_j(t) = 1 - \exp(-\lambda_j(t)) \tag{3.67}$$

where the extreme case $p_j(t) = 1$ happens with probability measure zero for all t. We denote the estimation MSE while using this policy as φ_j^E and Φ_j^E. By Theorem II of [7], the existence of $\varphi_j^E(t)$ for all t is guaranteed for the process (1) with bounded noise variance $\sigma^2 > 0$ and $0 < |a| < \infty$.

Minimum Asymptotic Time-Averaged MSE

In this and next subsections, we first assume $0 < |a| < 1$ in discussion. As in last section, we start with asymptotic time-averaged MSE for error-dependent policy, i.e.

$$\Phi_j^E = \lim_{T\to\infty} \frac{\sum_{t=1}^{T} \varphi_j^E(t)}{T}.$$

Let Z_j^s be the time of s-th successful transmission from node j where $s \in N$. For simplicity, we assume initial state $x_j(0)$ is known and $Z_j^0 = 0$ for all j. Let $\omega_j(s)$ be defined as sum of $\varphi_j^E(t)$ between two successful transmissions,

$$\omega_j(s) = \sum_{t=Z_j^{s-1}+1}^{Z_j^s} \varphi_j^E(t) \tag{3.68}$$

Let $K_N = \inf\{s : Z_j^s > N\}$. Since the estimation error e_j has identical statistical behavior after each successful transmission of state information, we can further apply the theorem for renewal reward processes [19] and get a.s. convergence of Φ_j^E, i.e.

$$\Phi_j^E = \lim_{N\to\infty} \frac{1}{N} \sum_{s=1}^{K_N} \omega_j(s) = \frac{E[\sum_{t=Z_j^0+1}^{Z_j^1} \varphi_j^E(t)]}{E[Z_j^1 - Z_j^0]} \tag{3.69}$$

With (3.62), (3.69) can be written as

$$\Phi_j^E = \frac{\sigma^2}{1-a^2} \times \frac{E[\sum_{l=1}^{Z_j^1}(1-a^{2l})]}{E[Z_j^1]} \geq \frac{\sigma^2}{1-a^2} \times \frac{\sum_{l=1}^{E[Z_j^1]}(1-a^{2l})}{E[Z_j^1]} \tag{3.70}$$

where inequality is due to Jensen's inequality.

On the other hand, by elementary renewal theorem [19], j-th node's *successful* transmission probability, denoted as P_j^{suc}, converges a.s. to $E[Z_j^1]^{-1}$. Since the channel is shared by

n nodes and successful transmission is mutually exclusive among nodes, we can apply the normalization condition,

$$0 < \sum_{j=1}^{n} P_j^{suc} \leq 1 \tag{3.71}$$

which, by symmetric argument, implies $0 < P_j^{suc} \leq \frac{1}{n}$ for all j. Thus, the range for expected inter-arrival time can be written as

$$n \leq E[Z_j^1] < \infty \tag{3.72}$$

A piece of analysis of (3.70) shows that lower bound of Φ_j^E monotonically increases as $E[Z_j^1]$ increases. Together with (3.72), we can see that

$$\Phi_j^E \geq \frac{\sigma^2}{1-a^2} \times \frac{\sum_{l=1}^{n}(1-a^{2l})}{n} \tag{3.73}$$

of which the RHS is the Φ_j^D given in [41]. By (3.73), we show that error-dependent policy cannot outperform round-robin scheduling, i.e. $\Phi_j^E \geq \Phi_j^D$, and the equality is possible only when $E[Z_j^1] = n$. Otherwise, $\Phi_j^E > \Phi_j^D$ when $E[Z_j^1] > n$. The same observation can also be made for $|a| = 1$ and $1 < |a| < \infty$.

In fact, above analysis does not assume any specific communication policy, thus what we show is that the performance of round-robin scheduling Φ_j^D is the lower bound of all possible communication policies for the problem formulation descried in Subsection 3.2.1.

Optimal Sensitivity to Error

Intuitively, when π is too small, the communication logic is insensitive to error and thus not enough state information would be delivered to remote estimators. On the contrary, if π is too large, the communication logic is too sensitive to error and frequent transmissions from all nodes would cause unnecessary collisions in the shared channel and thus less state information is successfully delivered to remote estimators. Both extreme cases should be avoided.

In this subsection, we derive necessary range of π for $\Phi_j^E = \Phi_j^D$ and approximated form for optimal sensitivity π^* such that $\Phi_j^D \leq \Phi_j^E \ll \Phi_j^P$. Here, we start with the calculation of time-averaged communication probability for node j, denoted as P_j,

$$P_j = \lim_{T\to\infty} \frac{\sum_{t=1}^{T} \overline{p_j}(t)}{T} \tag{3.74}$$

where $\overline{p_j}(t)$ is the expected transmission probability at time t. Besides, with (3.61) and concave property of the mapping in (3.67), we can have below inequality for all t,

$$\overline{p_j}(t) = 1 - E[\exp(-\pi \times e_j(t)^2)] \leq 1 - \exp(-\pi \times \varphi_j^E(t)).$$

With (3.74), we can get the upper bound of P_j,

$$P_j \leq 1 - \exp(-\pi \times \lim_{T\to\infty} \frac{\sum_{t=1}^{T} \varphi_j^E(t)}{T}) = 1 - \exp(-\pi \times \Phi_j^E) \tag{3.75}$$

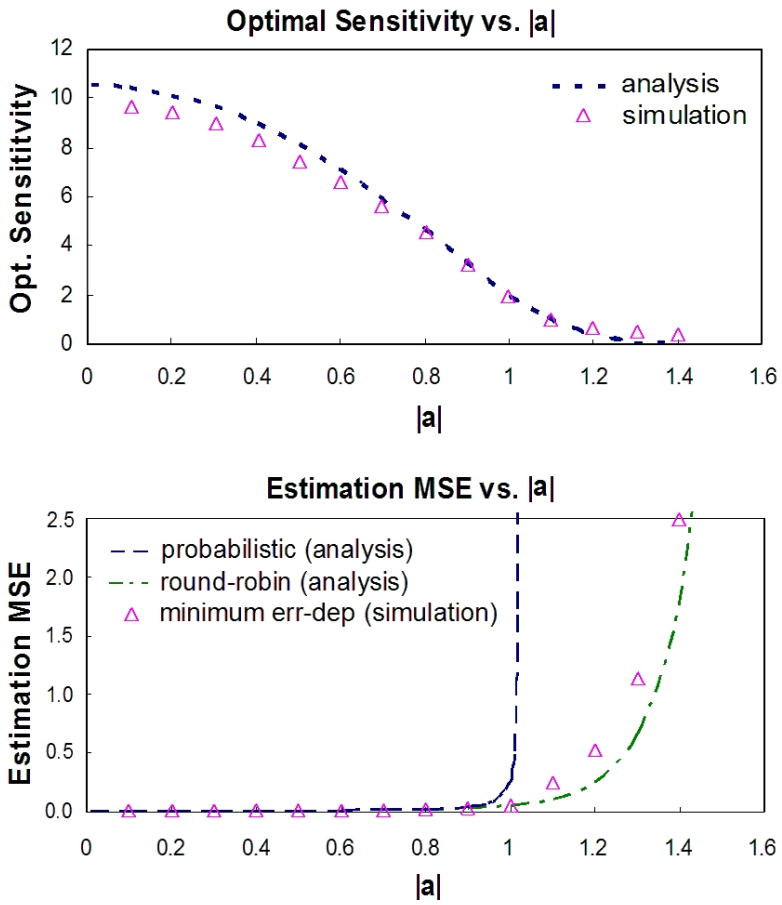

Figure 3.3. Optimal sensitivity and MSE tracking performance of Error-Dependent communication policies (with $n = 10$ and $\sigma^2 = 0.01$).

Since $P_j^{suc} \leq P_j < 1$, there exists δ and $1 < \delta < E[Z_j^1]$ s.t.

$$\frac{1}{E[Z_j^1]} \leq 1 - \exp(-\pi \times \Phi_j^E) \leq \frac{\delta}{E[Z_j^1]} \tag{3.76}$$

which is true for any $0 < \pi < \infty$ in (3.66).

From analysis in previous subsection, we know $E[Z_j^1] = n$ is the necessary condition for $\Phi_j^E = \Phi_j^D$. Therefore, at the optimal condition, (3.76) can be written as

$$\frac{1}{n} \leq 1 - \exp(-\pi \times \Phi_j^D) \leq \frac{\delta}{n}$$

where $1 < \delta < n$ and we get the range of π s.t. $\Phi_j^E = \Phi_j^D$ is possible,

$$\pi^* \leq \pi \leq \pi^* + \frac{1 - a^2}{\sigma^2} \times \frac{\ln(\frac{n-1}{n-\delta})}{1 - \frac{1}{n}\sum_{l=1}^{n} a^{2l}} \tag{3.77}$$

where π^* is the lower bound for π,

$$\pi^* = \frac{1-a^2}{\sigma^2} \times \frac{\ln(\frac{n}{n-1})}{1-\frac{1}{n}\sum_{l=1}^{n} a^{2l}} \tag{3.78}$$

Matlab simulations (see Figure 3.3) show that π^* is very close to optimal π. Above analysis can be readily generalized to cases $|a| = 1$ and $1 < |a| < \infty$.

However, one can tell from the form of (3.78) that $\pi^* \downarrow 0$ as n increases. In practice, the number of active nodes in the network might not be a constant and thus there is no fixed π^*. For example, in the active safety design for ITS mentioned in introduction, the number of neighboring vehicles might change with time, e.g. during peak or off-peak hours, and locations, e.g. on a highway or arterial. To address this problem, an improved policy is proposed.

Improvement to Error-Dependent Policy

Err-Coll-Dependent: This policy is modified from error-dependent method, and its communication intensity $\lambda_j(t)$ for node j at slot t is decided by a similar form of (3.66),

$$\lambda_j(t) = \xi(t) \times e_j(t)^2 \tag{3.79}$$

with $\xi(t)$ as a function of channel collision ratio $c(t)$,

$$\xi(t) = \frac{\pi}{1+\beta \times c(t)} \tag{3.80}$$

where $0 < \pi < \infty$ is a fixed positive real as defined in (3.66), $0 < \beta < \infty$ is the sensitivity to collisions, and $0 \le c(t) \le 1$ is the time-averaged channel collision ratio for immediate past γ time slots, $\gamma \in N$,

$$c(t) = \frac{1}{\gamma} \sum_{s=t-\gamma}^{t-1} I(s) \tag{3.81}$$

with $I(s)$ representing channel status of the s-th time slot: when there is a collision, $I(s) = 1$; otherwise, $I(s) = 0$. Similarly, $\lambda_j(t)$ is then converted to $p_j(t)$ by (3.67).

The idea behind (3.79) and (3.80) is that, when more nodes join in the shared network, potentially more collisions would happen and thus the sensitivity should be adjusted to account for such a change. As in many stabilization algorithms for multi-access networks [23], $c(t)$ is used as a indicator for the sender to infer the change of number of nodes in the network.

Matlab simulation parameters are $(a, \sigma^2, \pi, \beta, \gamma) = (-0.5, 0.01, 20, 29, 10)$. During 10 to 20 seconds, more nodes are joining in the network to share the limited bandwidth as shown in Figure 3.4(a). Figure 3.4(b) shows the robustness of Err-Coll-Dependent method against the channel congestion in terms of moderating its transmission probability to reduce collisions (see Figure 3.4(c) and 3.4(d)). Other sets of simulations also confirm the same observation: Err-Coll-Dependent policy can achieve a rather smooth estimation MSE curve and less fluctuation in packet rate and collision ratio than those of error-dependent policy.

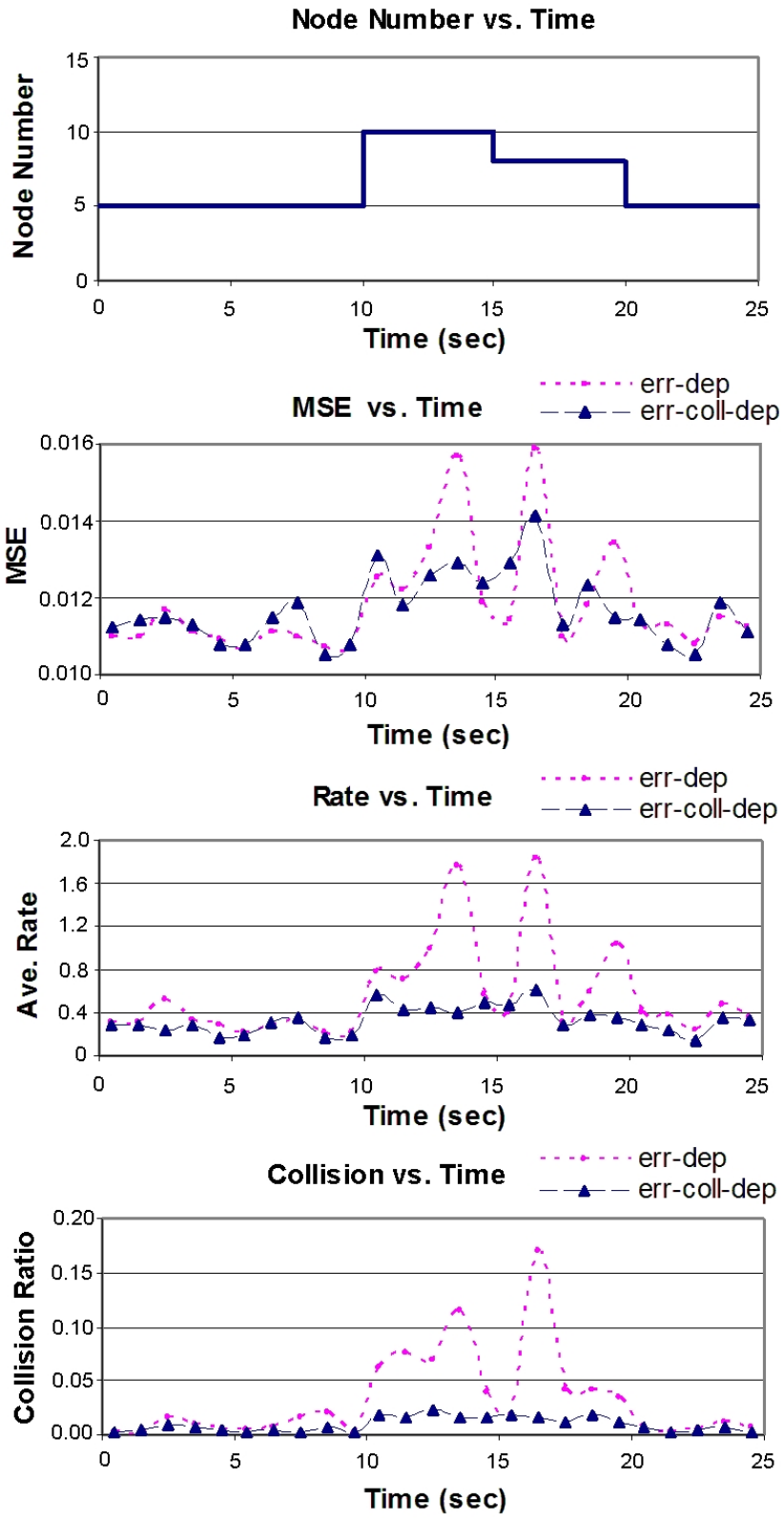

Figure 3.4. Tracking performance of Error-Dependent and Err-Coll-Dep policies with a time-varying number of active nodes.

3.2.4 Short Summary

A mathematical framework is proposed and the estimation MSE of error-dependent communication policy is analyzed and compared with uncontrolled ones. Based on analysis, Err-Coll-Dependent policy is proposed to achieve robust estimation performance. This result suggests that, while designing communication logic for vehicular safety applications, joint consideration of NCS system dynamics and channel congestion can lead to better estimation. This understanding will serve as the rationale behind our transmission rate control for vehicular safety communications.

3.3 Transmission Message Rate Control for Real-Time Vehicular Tracking over a Shared Channel

In this section, we apply the analysis in Section 3.1 and 3.2 to design an inter-vehicular communication control for vehicles to track each other in real-time and thus enhancing active safety.

Technology has always been the centerpiece of new developments for transportation systems. Advances in passive safety systems, such as the airbag and anti-lock brake system (ABS), contributed to a safer driving environment. Besides those passive safety mechanisms which protect the driver and passengers during a crash, active safety designs are proposed to prevent crashes from happening. For example, computer vision and associated filter designs are proposed to assist a driver in detecting critical motion of neighboring cars [67], identifying lanes and road boundaries [69], and even monitoring other drivers' attentiveness to predict their intentions [68]. However, the biggest promise yet is that of Intelligent Transportation Systems (ITSs) empowered by wireless technologies. Based on matured IEEE 802.11 standard, 802.11p transceivers [72], dubbed as DSRC (Dedicated Short Range Communication) or WAVE (Wireless Access in Vehicular Environments), are put on cars and make information exchange possible either in vehicle-to-vehicle (V2V) or vehicle-to-infrastructure (V2I) fashion. This kind of inter-vehicle communications (IVC) and Vehicular *Ad hoc* Networks (VANETs) have drawn much attention in recent years due to their important role in hosting safety, navigation, traffic management, and automation applications [55,76].

One of the most challenging mechanism planned for deployment over IVC is the Cooperative Active Safety System (CASS). See an illustration of proposed CASS in Figure 3.5. Each vehicle contains a communication control logic, a bank of estimators to track other vehicles, a plant (vehicle dynamics), a Global Positioning System (GPS) receiver, and other on-board sensors (producing vehicle state measurements. In this CASS concept, each vehicle broadcasts self-information (e.g., GPS position, speed, and heading) in the form of safety messages to neighboring vehicles via the DSRC channel. These V2V safety messages are in the format of WAVE short message (WSM) defined in IEEE 1609.3 for rapid and efficient information exchange [73]. The receiving vehicle can then use incoming messages to track the sending vehicle in real time. The estimated states of all neighboring vehicles (e.g., in a radius of 150 meters), called *Vehicle Neighborhood Mapping* in Figure 3.5, will be fed into ac-

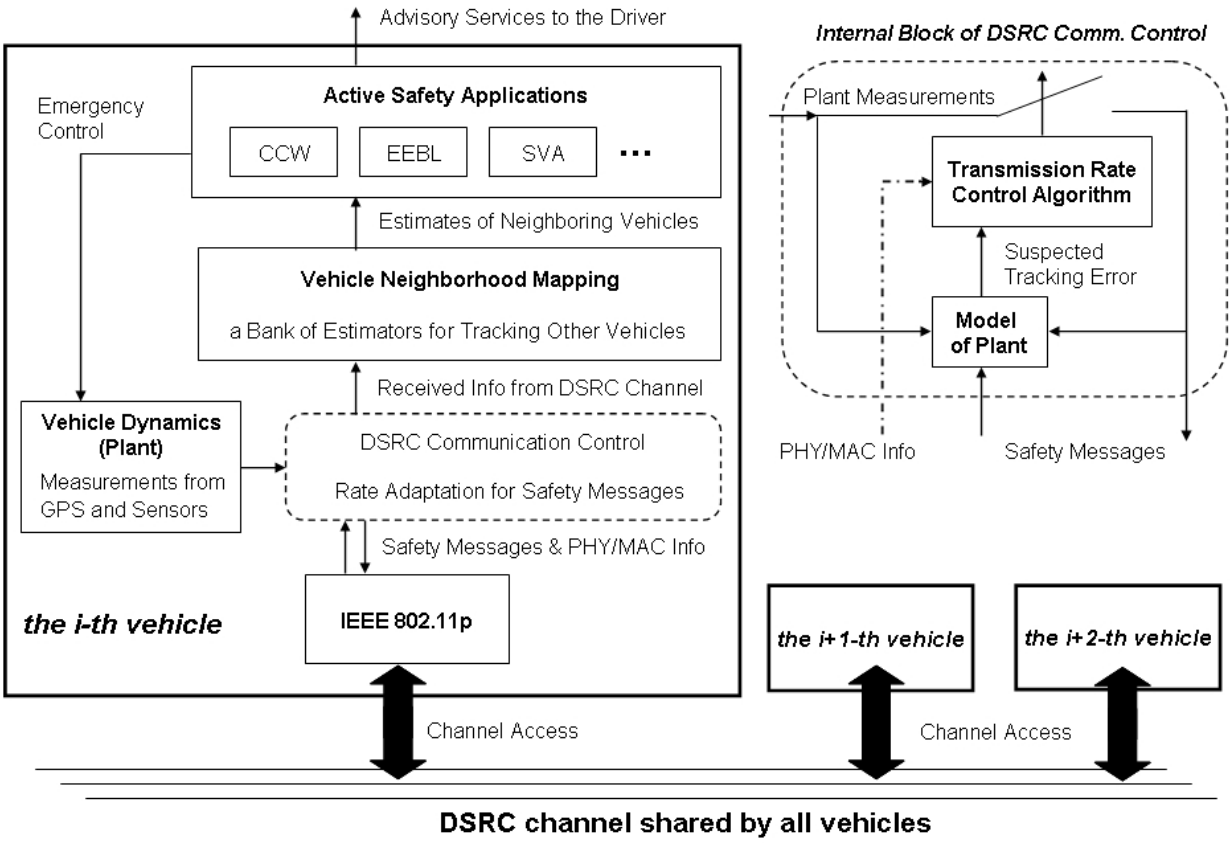

Figure 3.5. Functional blocks of proposed CASS in-vehicle unit.

tive safety applications, e.g., Cooperative Collision Warning (CCW), Electronic Emergency Brake Light (EEBL), and Slow/Stopped Vehicle Alert (SVA) [55]. These safety applications then provide warnings to the driver or take emergency control of the vehicle in case of an imminent danger. Note that our proposed rate control algorithm (illustrated in the upper right corner of Figure 3.5) works on top of the 802.11p transceiver and will be specified later in Subsection 3.3.3.

In Section 3.1 and 3.2, we already propose a mathematical framework where multiple scalar LTI dynamical systems can track each other over a multi-access channel and analyze different communication policies for self-information dissemination. This specific type of tracking problem is interesting because it is real-time and over a shared channel just like our CASS problem setting. Tracking performance is studied for three uncontrolled communication policies: probabilistic (random access), deterministic (round-robin scheduling), and combined (grouped channel access). In addition, two controlled communication policies are analyzed and their performances are compared using preliminary Matlab simulations. This theoretical exercise gives us insights into how to design CASS communication logic (i.e., the dashed box) in Figure 3.5.

Based on the analysis, we propose a decentralized transmission control algorithm to

decide how state information of a vehicle should be broadcast to neighboring vehicles for safety/tracking purposes. This algorithm has an *on-demand* nature since: 1) it increases communication rate when a vehicle suspects the estimation error of neighboring vehicles *toward itself* has increased; 2) it throttles rate during channel congestion to avoid further collisions (efficiency degradation and message losses). This simple yet intuitive design allows all vehicles to properly share available channel resource. Our proposed algorithm is shown to achieve tracking accuracy and robustness for different traffic scenarios. Its performance has been evaluated through realistic simulations, involving vehicle trajectories generated by SHIFT [74] traffic simulator and large-scale wireless network simulations using OPNET [75] with the best-known DSRC channel model reported in [54]. Our algorithm outperforms the standard solution suggested by Vehicle Safety Communications Consortium (VSCC) [76].

This section is organized as follows: Subsection 3.3.1 provides an overview of related work on IVC. Subsection 3.3.2 presents preliminary Matlab simulation results of different polices analyzed in Section 3.2 and provides insights into how to design a proper rate control in a shared channel. Subsection 3.3.3 describes our proposed transmission rate control algorithm. Subsection 3.3.4 states large-scale traffic/network simulation settings, implemented algorithms, and simulation results. Subsection 3.3.5 summarizes this section.

3.3.1 Related Work on Inter-Vehicle Communications

In [56,57], IVC is used to relay down-stream traffic information to up-stream drivers to expand their perception horizon. This kind of early warning system gives the driver more time to react to a hazardous situation and thus reduces injury/casualty rates. In [70], IVC is used to improve lane-level positioning based on Markov localization. In [58], an adaptive space-division multiplexing protocol is proposed for vehicles to share DSRC channel without control messages and to mitigate DoS (denial of service) attacks. A feasibility examination of V2V collision warning based on Differential GPS (DGPS) is provided in [59]. In this section, we assume such modestly accurate positioning information (e.g., sub-meter accuracy) is available on board and focus on the design of CASS communication logic.

For information propagation in wireless *ad hoc* networks, the analysis in [53] gives a fundamental bound on the product of rate and distance. The implication of such a capacity notion is that, when the network becomes denser, one needs to either throttle data rate or reduce transmission power so that limited channel resource can be properly shared by all nodes. Therefore, most existing designs for broadcasting safety messages focus on either rate or power adaption for different vehicular traffic conditions.

One such design trend is on transmission range (power) control for safety messages. For example, [60] proposes to fairly allocate transmission power across all cars in a max-min fashion, which helps reduce beacon load at every point of a formulated 1-D highway and thus reserves bandwidth for emergency messages with higher priorities. This method assumes a pre-defined maximum load as the target. By utilizing water-filling concept, [60] proves a centralized algorithm that achieves this fairness goal and gives a decentralized algorithm that approximates operations of the centralized one. Another work on transmission range adaptation is [61] in which estimated local vehicle density and traffic engineering

intuitions are used as algorithm inputs. The goal in [61], however, is to reduce DSRC channel interference while maintaining network connectivity among vehicles.

Another design trend for safety messages is on rate control. Since many applications require the same data elements from neighboring vehicles, the message dispatcher in [62] is proposed to reduce required data rate by removing duplicate elements. The message dispatcher at the sender side will group data elements from application layer (i.e., the information source) and decides how frequently each data element should be broadcast. At the receiver side, the message dispatcher pushes received data elements to designated applications (i.e., the sink). This design is similar to compression ideas in source coding [27].

For IVC-based CASS which relies heavily on tracking accuracy, our approach is to correlate communication behaviors with tracking error magnitude, which is fundamentally different from any previous designs. In [63,64], error threshold crossing is used as the transmission trigger; communication of the state information happens only when threshold is violated. However, this threshold crossing policy only works for a very reliable (lossless) channel and thus is not feasible for VANETs when the market penetration of on-board wireless devices is high (i.e., more contentions and packet collisions in the shared channel). Our on-demand design in this section follows the same rationale but adopts a stochastic rate control policy that considers both real-time tracking error and potential message losses. Unlike previous designs, our proposed algorithm is easy to implement; it also works in a decentralized fashion, which makes it more suitable for CASS.

3.3.2 Preliminary Matlab Simulations and Discussions

In this subsection, we analyze different communication policies to get insights into how tracking accuracy can be improved through controlling the rate of information dissemination in a shared channel. Since we are aiming at the design for VANETs and CASS, only decentralized policies are considered in this subsection: **Probabilistic**, **Error-Dependent**, and **Err-Coll-Dep** policies. They will be compared in terms of tracking accuracy, resulted collisions in the channel, and statistical multiplexing gain (i.e., channel sharing behaviors).

Monte Carlo simulations of different communication policies are conducted in Matlab/Simulink. Discrete time step length is set to 50 milliseconds. There are $n = 10$ nodes for the entire 100-second simulation duration. The same channel assumptions in Section 3.2 continue to hold here. As formulated in Section 3.1 and Section 3.2, all nodes contain an identical plant, with different RNs (random numbers) as simulation seeds, and a bank of model-based estimators. For the plant state, x_j is a scalar with $a_j = 0.5$ and $_j$ follows Gaussian distribution $N(0, 10^{-2})$ for all j. Each node kejpg tracking other nodes and broadcasting its own state information according to specified stochastic policy. Throughout Matlab simulations, values of (β, γ) in (3.79) and (3.80) are fixed at (30,10). By tuning the error sensitivity α in (3.66) and (3.79), we get different average packet rates for Error-Dependent and Err-Coll-Dep policies.

Time-Averaged Tracking Performance

The tracking performance (MSE in the sense of equation (3.56)) is plotted in Figure 3.6 with each point representing the statistics from one simulation run. First of all, three policies exhibit U-shape curves: 1) when the average rate is too low, tracking MSE is large because less state information is transmitted to remote estimators; 2) when the average rate is too high, MSE becomes large again because many transmitted packets get collided in the shared channel and thus the amount of available state information to remote estimators decreases. The observation that more state information transmitted results in higher tracking accuracy in [46] is not valid in a multi-access channel because of collisions. Corresponding collision ratios are also plotted in Figure 3.6 for comparison. Secondly, for Probabilistic policy, the minimum tracking MSE is achieved with average rate 2 pkt/node/sec (packets per node per second). This corresponds to transmission probability $p_j = \frac{1}{10}$, for all j, which matches with previous analysis $p^* = \frac{1}{n}$ where n is the node number. Thirdly, the Probabilistic policy, i.e., no rate control, cannot achieve the same minimum MSE as that of Error-Dependent and Err-Coll-Dep policies. Error-Dependent and Err-Coll-Dep policies achieve lower minimum MSE with a lower average rate (0.4 pkt/node/sec) than the Probabilistic policy.

Similar to the analysis in [46], controlled communication policies result in better tracking performance because timely delivered state information eliminates large estimation error. With the same average packet rate, Err-Coll-Dep policy can achieve lower MSE compared with that of Error-Dependent policy, especially when its packet rate is high. As shown in Figure 3.6, Err-Coll-Dep policy also achieves MSE close to the minimum for a wide range of rates (0.4 to 3 pkt/node/sec), i.e., that curve acts as if tracking MSE is not affected by the increasing packet rate and the gradually congested channel.

Collision Response in the Shared Channel

We compare short-term collision response while using different communication policies, which is a key performance indicator of a multi-access channel. Higher collision ratio means lower probability of successful transmission and thus lots of bandwidth wasted. Figure 3.7 shows the collision occurrence in 2000 time slots for three policies respectively. Their average packet rates are all around 0.2 pkt/node/sec, which means that the channel is only lightly loaded. In Figure 3.7, Error-Dependent policy has higher collision ratio and more *consecutive* collisions, which can also be observed in Figure 3.6 when the rate is small. For Error-Dependent, when a collision happens, it means that at least two nodes want to send out state information at the same slot because their estimation errors are relatively large. In next time slot, those nodes would still have high broadcast probabilities since their estimation errors are still large (because no state information is successfully transmitted due to previous collision). The same situation may go on, i.e., consecutive collisions, until all involved nodes can successfully transmit their state information.

The Error-Dependent design does not consider possible channel collisions and aggressively kejpg sending more packets until one successful transmission, which is the main cause of frequent consecutive collisions even when the channel is in lightly loaded condition. On

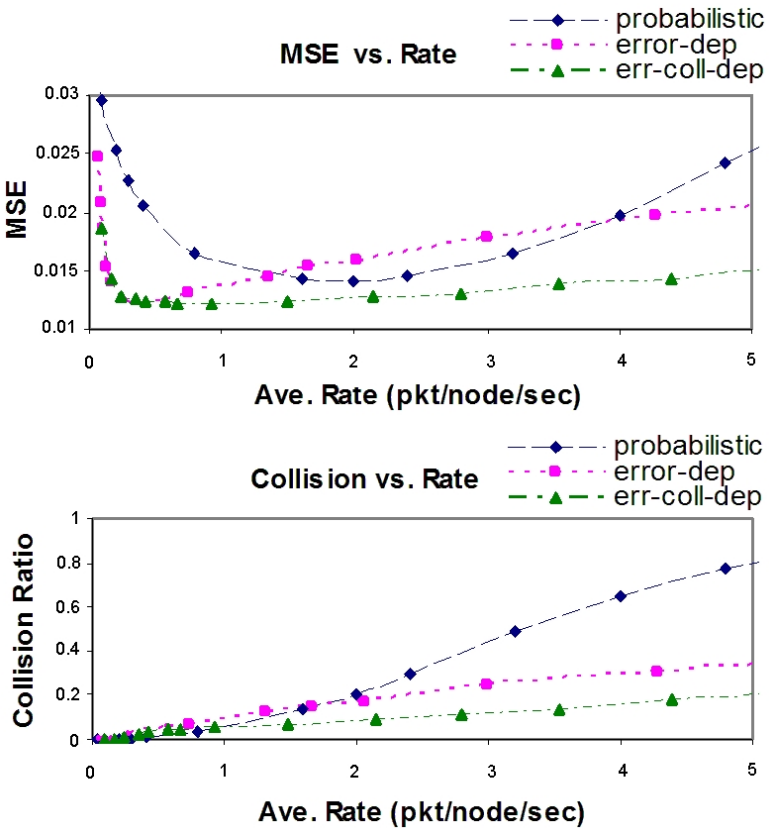

Figure 3.6. Tracking performance (MSE in the sense of equation (3.56)) and averaged collision ratio for three decentralized communication policies.

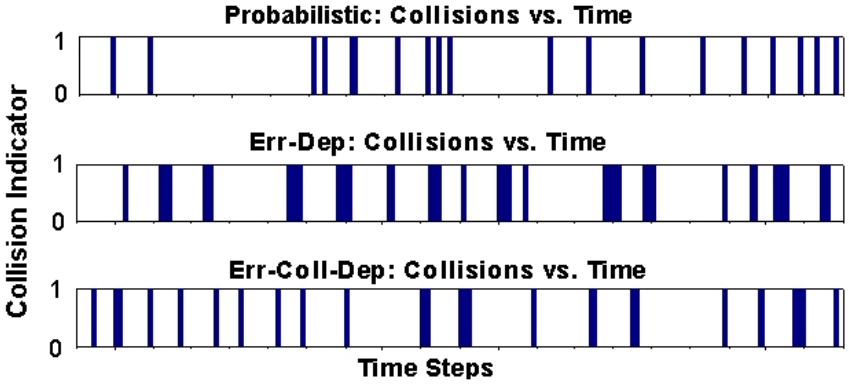

Figure 3.7. Collision occurrence for three decentralized policies in 2000 time slots with average rate around 0.2 pkt/node/sec, i.e., channel is only lightly loaded. Respective collision ratios are 0.95%, 2.55%, and 1.30%.

the contrary, Err-Coll-Dep policy alleviates this problem by considering channel collisions: when there is a collision, all nodes throttle their rates and *collaboratively* reduce consecutive collisions. Therefore, the collision ratio of Err-Coll-Dep design is always lower than that of Error-Dependent in Figure 3.7. Note that, although Figure 3.7 shows that Error-Dependent and Err-Coll-Dep policies have higher collision ratio in a lightly loaded channel, they still achieve lower tracking MSE than that of Probabilistic policy (compare their performance in Figure 3.7 when average rate is below 0.5 pkt/node/sec). Again this shows that, the effectiveness of using a controlled communication policy comes from the timely delivery of state information to eliminate large error even though some channel bandwidth is sacrificed.

Statistical Multiplexing Gain

Here, we study how efficient these communication policies can be in sharing the finite channel resource. Here, statistical multiplexing gain is defined as the tracking performance (MSE in the sense of equation (3.56)) improvement of using a shared channel with full bandwidth (i.e., accessed in an uncoordinated manner) instead of assigning a dedicated channel with equally partitioned bandwidth to every node (i.e., perfectly scheduled access). This multiplexing gain of three policies is compared in Figure 3.8. For each communication policy, we compare its performance in the following two scenarios: 1) 10 dedicated channels, each with 10% bandwidth, are assigned individually to 10 nodes for them to broadcast state information; 2) a multi-access channel, with 100% bandwidth, is simultaneously shared by all 10 nodes. A communication design that works well in the second scenario (i.e., it has statistical multiplexing gain in a shared channel) is more suitable for IVC-based CASS.

Figure 3.8 shows that there is no multiplexing gain for Probabilistic policy due to the lack of rate control and excessive collisions in the channel. On the contrary, the multiplexing gain exists when Error-Dependent's packet rate is less than 0.6 pkt/node/sec, and when Err-Coll-Dep's packet rate is less than 1.5 pkt/node/sec. Once average rate is higher than these values, channel collisions become dominant and their tracking performance degrades. The multiplexing gain for Error-Dependent and Err-Coll-Dep policies exists because plants on different nodes are decoupled, their tracking error magnitudes are different, and therefore not all nodes need to broadcast state information at the same time. This behavior comes from our design of on-demand rate control in (3.66) and (3.79).

In Figure 3.8, the Err-Coll-Dep policy also has a wide rate range of multiplexing gain than that of Error-Dependent policy because of lower collision ratio in the shared channel. By properly selecting parameters (β, γ) in (3.79) and (3.80) for Err-Coll-Dep, its tracking performance could be made very close to the case that each node is assigned a dedicated channel (as shown in Figure 3.8). Therefore, Err-Coll-Dep policy has a better rate control structure for tracking multiple dynamical systems to track each other over a shared channel and is more suitable for CASS.

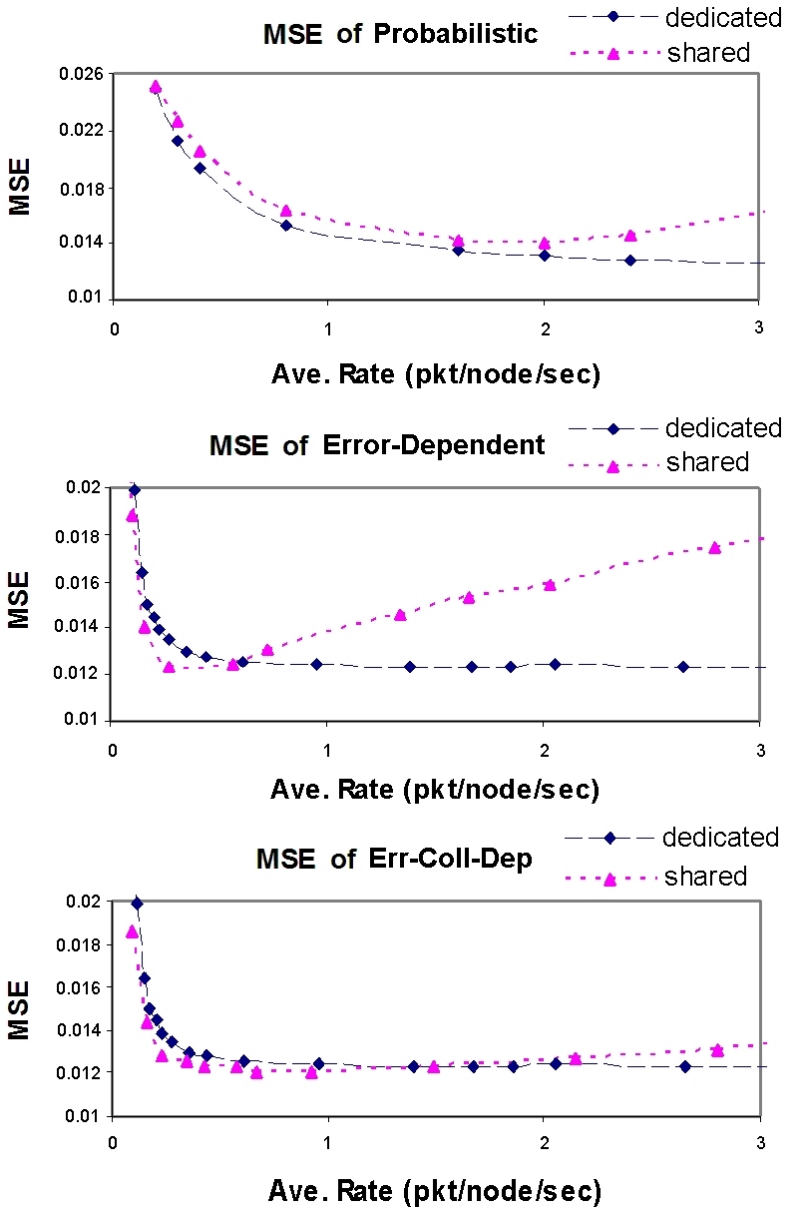

Figure 3.8. Tracking performance for three decentralized policies under dedicated channel (with 10% bandwidth) for each node (in total 10 nodes) and a shared channel (with 100% bandwidth) for all 10 nodes.

3.3.3 Proposed Vehicular Transmission Rate Control for Safety Messages

In this subsection, we propose a transmission rate control for CASS communication logic (i.e., the dashed box in Figure 3.5). Our rate control algorithm follows the same spirit of Err-Coll-Dep policy discussed in Subsection 3.2. Some minor modifications are introduced to address the fact that there is no explicit ACK (acknowledgment) for broadcast messages in DSRC [72]. Performance of our proposed algorithm will be evaluated in Subsection 3.3.4.

Our rate control algorithm runs on each vehicle every 50 milliseconds, which is due to the usual 20 Hz sampling frequency of on-board sensors [39]. At each time step $t \in \mathbb{N}$, i.e., multiples of 50 milliseconds, the j-th vehicle gets a measurement of its own state and calculates transmission probability $p_j(t)$ based on *suspected* tracking error $\tilde{e}_j(t)$ on neighboring vehicles toward its own position in Euclidean sense (i.e., the usual distance definition for Cartesian coordinate system). The calculation of $\tilde{e}_j(t)$ will be specified later. Similar to the rate control in (3.79), we use this scalar measure $\tilde{e}_j(t)$ to calculate the transmission probability by vehicle j at time step t, denoted as $p_j(t)$,

$$p_j(t) = 1 - \exp\left(\frac{-\alpha}{1 + \frac{\beta}{\gamma}\sum_{s=t-\gamma}^{t-1} \Lambda_j(s)} \times \tilde{e}_j(t)^2\right) \tag{3.82}$$

where α and β are sensitivity parameters as those in (3.79) and (3.80), and $\gamma = 20$ is the one-second time window to evaluate recent channel utilization. Later in simulations (Subsection 3.3.4), we use $\beta = 0$ for Error-Dependent and $\beta = 30$ for Err-Coll-Dep policy respectively. In (3.82), $\Lambda_j(s)$ represents CCA (Clear Channel Assessment) [72] reported by the j-th 802.11p MAC/PHY module: when channel is sensed busy, $\Lambda_j(s) = 1$; otherwise, $\Lambda_j(s) = 0$. Since a DSRC transceiver cannot detect collision, we use channel utilization in (3.82) as a substitute for $c(t)$ in (3.81). This substitution is adequate since collision ratio is a monotonically increasing function of channel utilization. Based on the $p_j(t)$ given by (3.82), the j-th vehicle stochastically generates a packet (i.e., a safety message) with its latest state information and places this packet in 802.11p MAC queue for transmission.

At each moment, the suspected error $\tilde{e}_j(t+1)$ (used in (3.82)) propagates from previous $\tilde{e}_j(t^+)$ based on the known plant model. Since there is no explicit ACK for broadcast-type transmission in DSRC, a subject vehicle uses perceived channel Packet Erasure Rate (PER) at time t, denoted as $\Omega_j(t)$, to stochastically decide the suspected error $\tilde{e}_j(t^+)$ *right after* each message transmission,

$$\tilde{e}_j(t^+) = (1 - \zeta_j(t)) \times \tilde{e}_j(t) \tag{3.83}$$

where $\zeta_j(t)$ is the Bernoulli trial with the failure probability $\Pr(\zeta_j(t) = 0) \equiv \Omega_j(t)$. If the outcome $\zeta_j(t) = 1$, this suspected error $\tilde{e}_j(t^+)$ is reset, i.e., $\tilde{e}_j(t^+) = 0$; otherwise, $\tilde{e}_j(t^+) = \tilde{e}_j(t)$. Note that, this suspected error $\tilde{e}_j(t)$ is *not* the actual tracking error; it is merely a measure used by the j-th vehicle to infer/simulate the tracking error evolution on its neighbors and to adjust its own message transmission rate in (3.82) accordingly.

The estimated PER, $\Omega_j(t)$, used by the Bernoulli trial in (3.83) is derived on-the-fly by checking the inconsistency in sequence number of recently received packets from all corresponding neighbors within 1-second history log of vehicle j. That is, the j-th vehicle uses the

number of lost packets divided by the number of total packets sent from a certain neighbor to estimate recent channel loss rate and $\Omega_j(t)$ is this empirical measure averaged over all its neighbors. Assuming network symmetry, $\Omega_j(t)$ tells the j-th vehicle the likelihood of its previous transmitted packet being erased in the channel.

The on-demand nature of (3.82) responds to the fact that a higher transmission rate, thus probability, is required for a subject vehicle that has more *unexpected* movements, which translate to higher tracking error at the neighboring vehicles. Besides, (3.82) takes channel status into account, as discussed in Subsection 3.3.2, to temporarily reduce the message rate of all vehicles in the same geographical area when channel congestion is detected, and thus this design increases the successful reception probability of messages from all vehicles.

3.3.4 Evaluations Using Large-Scale Traffic/Network Simulations

This subsection presents large-scale traffic/network simulations for IVC-based CASS and discussions on simulation results. We focus on the tracking performance while using different decentralized communication policies. Simulation results confirm that proposed algorithm in Subsection 3.3.3 achieves better accuracy than the standard solution by VSCC [76] and robustness under various traffic conditions.

Simulation Settings and Implemented Communication Policies

Our main simulation stage is a straight 1-Km highway. For vehicle dynamics, 20 Hz trajectory profiles of [position, speed, heading] are produced by SHIFT [74], a microscopic traffic simulator. Total simulation time is 30 seconds for each run. In the first part of our evaluations, we consider four lanes of identical traffic flows with an averaged velocity of 30 mph (miles per hour) and a mean gap of 0.8 second between vehicles in longitude direction. During the simulation, every 50 milliseconds, each vehicle gets a measurement of its own status and decides whether to generate a message or not, according to specified policy, to disseminate its own state information. The on-board measurement noise is modeled exactly the same way as in [63,64], which was in turn based on experimental data [39]. Upon receiving information from the channel, each vehicle updates its estimated states of neighboring vehicles using a first-order kinematic model, i.e., a constant speed predictor. Based on this model, a sending vehicle is assumed to run with the same speed and heading after its last safety message was received by the predictor on a receiving vehicle.

For OPNET [75] simulations, we modify the 802.11a PHY module to work at 5.9 GHz with 10 MHz bandwidth. We follow the DSRC channel model reported in [54] and simplify the far distances as Rayleigh fading, instead of pre-Rayleigh. The reason for this simplification is that we are considering a straight highway scenario while [54] considers urban scenarios with intersections and corners, which lead to pre-Rayleigh fading observations. We specify path loss exponent to be 2.31 (as suggested by [54]). The transceiver operates with 3 Mbps raw data rate, -87 dBm receiver sensitivity, and 600 mW transmission power. The payload size of each safety message is 300 bytes. Implemented algorithms run at every 50 milliseconds on top of 802.11p MAC/PHY (as depicted in Figure 3.5), namely the following:

- **Beaconing** at 100-millisecond interval, as suggested by VSCC [76];
- **Probabilistic** policy, which uses fixed transmission probability to generate messages;
- **Threshold** policy, which triggers communication when perceived tracking error violates a pre-defined threshold [63,64];
- ***Proposed*** on-demand rate control: 1) **Error-Dependent** (with $\beta = 0$), 2) **Err-Coll-Dep** (with $\beta = 30$) policies.

Simulation Results and Performance Comparison

Here, we present simulation results and compare the performance of different decentralized policies. The proximity or neighborhood of a subject vehicle is defined as the circular area of **150-meter radius** to satisfy most safety applications identified in [76].

After each simulation run, statistics are collected from neighboring vehicles and we calculate Euclidean positioning error over all vehicles to explore the law of large number. See Figure 3.9 for a typical tracking error distribution. Specifically, 95% cut-off error (as indicated by the arrow in Figure 3.9) means that 95% of Euclidean error population fall below this number (i.e., only 5% error population is larger than 1.07 meter), which represents the tracking accuracy of used communication policy. In this subsection, we use this measure, **95% Euclidean cut-off error**, as the main performance metric for CASS simulations. This metric is different from the MSE definition given in (3.56). The main advantage of this performance measure over (3.56) and others (e.g., mean or standard deviation of tracking error) is that it possesses a statistical sense similar to a Confidence Interval (CI). Note that presented error statistics in Figure 3.9 and Figure 3.10 is the *ground-truth* tracking error (in meters) collected during our simulations instead of the suspected error $\tilde{e}_j(t)$ perceived by vehicle j and used in formula (3.83).

The tracking performance (i.e., 95% cut-off error) of Beaconing in Figure 3.9 is used as the baseline for comparison. In Figure 3.10, the performance of different policies is plotted with second-order least squares fitting to indicate the trend. For Probabilistic policy, its tracking accuracy is shown with respect to different transmission probabilities; observed accuracy has a U-shape curve (similar to those in Figure 3.6) and the optimal probability for this traffic scenario is 0.6 with minimum 95% cut-off error around 0.8 meter. Probabilistic policy, though an uncontrolled policy, achieves better tracking performance than Beaconing by introducing randomness in its transmission behavior. For Threshold policy, its packet transmission rate is dependent on the selected error threshold. When this threshold decreases, it triggers more broadcasts and causes more collisions in the channel. Its 95% cut-off error also shows a U-shape curve and optimal threshold for this scenario is 0.4 meter with minimum 95% cut-off error around 0.6-0.7 meter, which is a further improvement from Probabilistic policy.

Performance of the Error-Dependent policy (i.e., proposed algorithm with $\beta = 0$) is also shown in Figure 3.10 with different error sensitivity α values and corresponding tracking accuracy. As we increase α, we increase the packet rate; optimal rate is around 4 pkt/node/sec when $\alpha = 5$. Its 95% cut-off error also shows a U-shape curve and this accuracy degrades

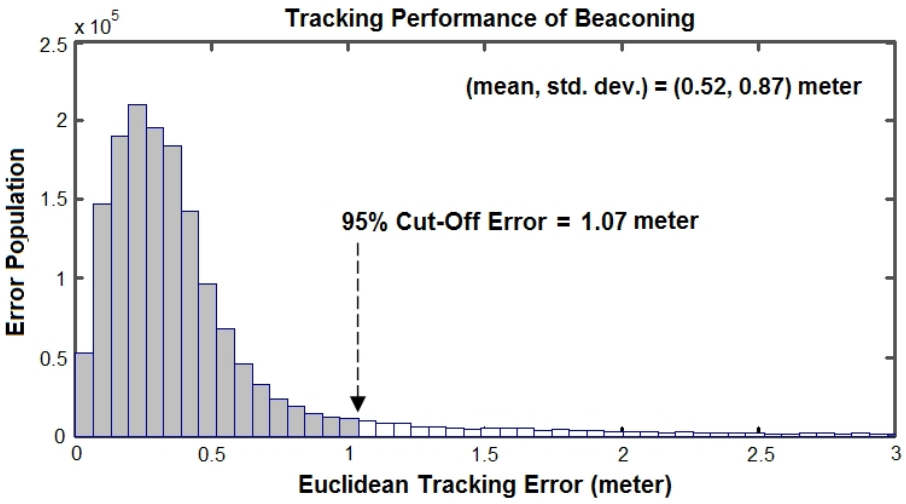

Figure 3.9. Statistical distribution of Euclidean tracking error while using 100-millisecond Beaconing proposed by [76].

as the average rate increases. Error-Dependent policy achieves similar minimum 95% error (i.e., 0.6-0.7 meter) as that of Threshold policy. Finally, the last plot in Figure 3.10 shows the tracking performance of Err-Coll-Dep policy (i.e., proposed algorithm with $\beta = 30$). Its 95% cut-off error has similar curve as that of Error-Dependent policy and achieves the same minimum 95% cut-off error when rate is around 4 pkt/node/sec. Compared with Beaconing, controlled communication policies (i.e., Threshold, Error-Dependent, and Err-Coll-Dep policies) all achieve significant improvement in tracking accuracy. However, the benefit of using Err-Coll-Dep policy needs to be understood from the following design perspective.

Although the 802.11p MAC layer helps reduce collisions, considered rate controls still have similar behaviors as those policies analyzed in Subsection 3.3.2. The reason is that collision still exists for broadcast-type safety messages and the hidden node phenomenon [53] degrades the effectiveness of CSMA/CA (Carrier Sense Multiple Access with Collision Avoidance) of the 802.11p MAC [72]. Therefore, the advantages of a controlled communication policy discussed in Subsection 3.3.2 still apply to VANETs here. Both Error-Dependent and Threshold policies could outperform Beaconing and Probabilistic policies *if* one properly chooses their parameters.

However, as suggested by (3.78), optimal sensitivity or threshold may vary greatly with vehicle densities; thus these parameters cannot be easily chosen by off-line calculations. Err-Coll-Dep policy alleviates above design problem and makes parameter selection easier. By comparing α values in Error-Dependent and Err-Coll-Dep policies in Figure 3.10, one can notice that, when $\beta = 30$, as long as we pick $\alpha \geq 20$, the tracking accuracy of Err-Coll-Dep policy can operate around optimal performance for a wide range of α.

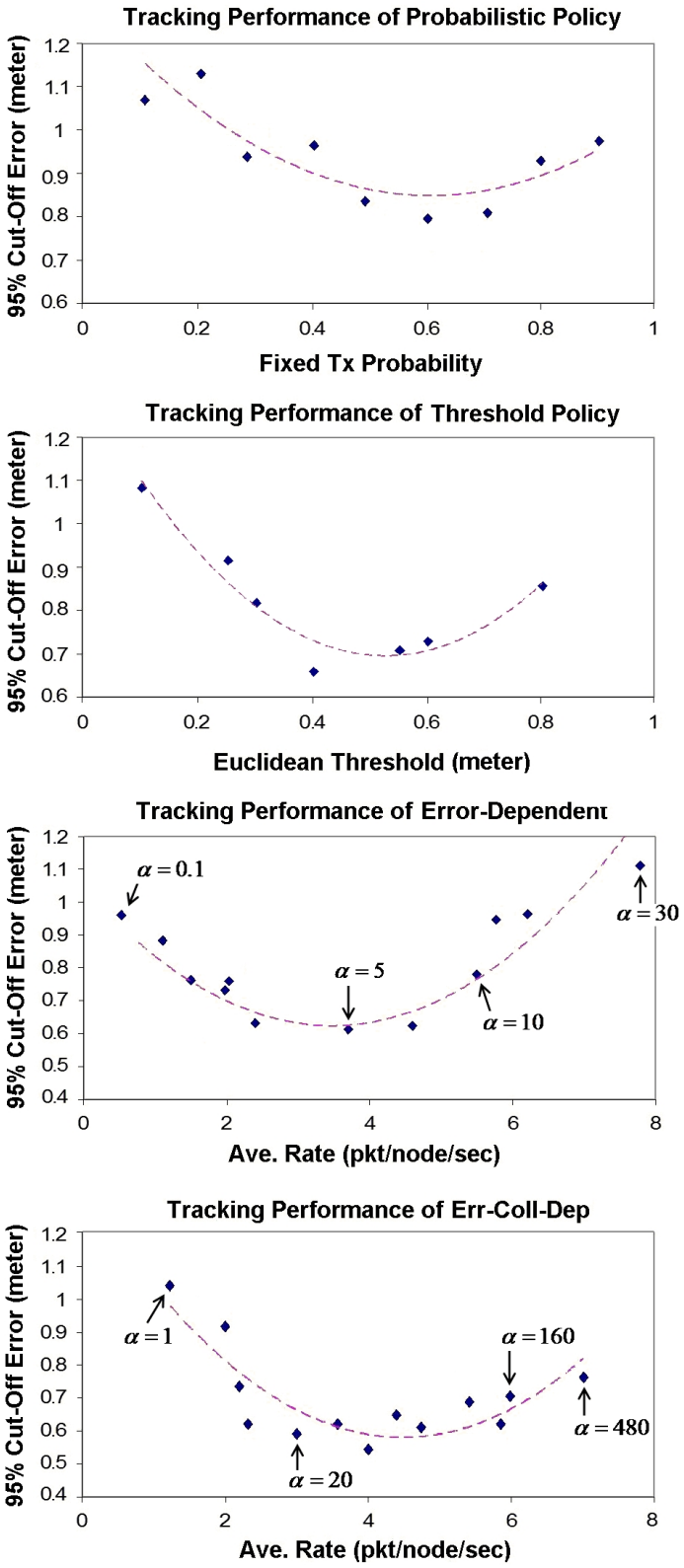

Figure 3.10. Tracking performance (95% cut-off error, in meters) of Probabilistic, Threshold, Error-Dependent (proposed algorithm with $\beta = 0$), and Err-Coll-Dep (proposed algorithm with $\beta = 30$) policies.

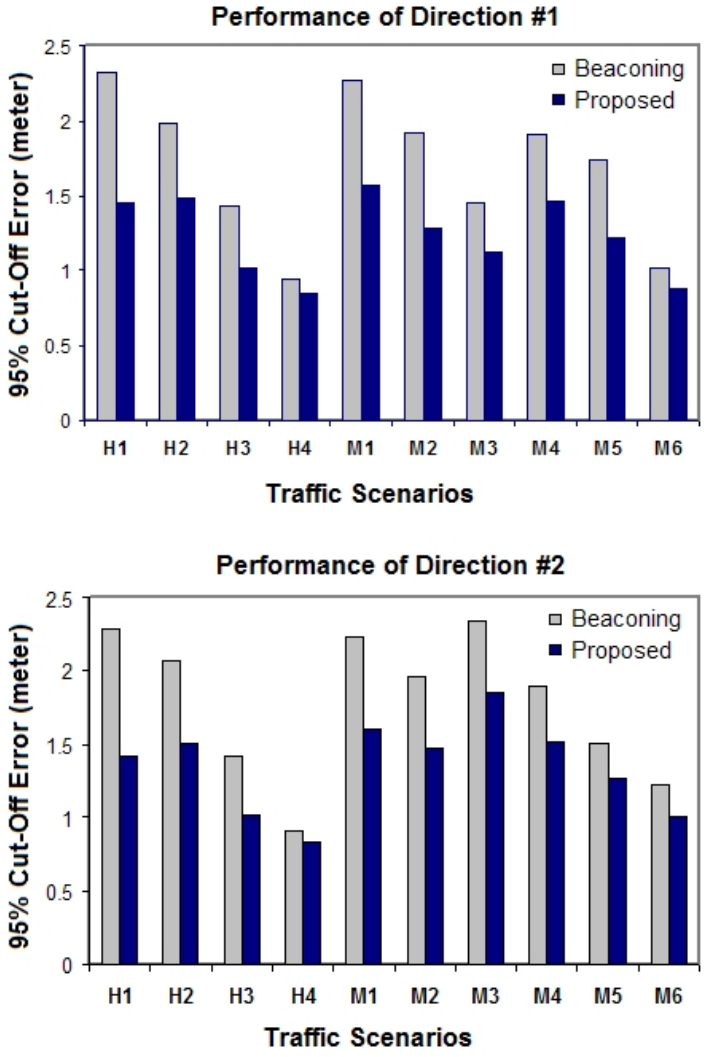

Figure 3.11. Tracking performance (95% cut-off error) of 100-millisecond Beaconing and Proposed algorithm with fixed parameters $(\alpha, \beta) = (20, 30)$ under different traffic conditions in TABLE 3.1.

Table 3.1. Simulated Bidirectional Highway Traffic Scenarios

Case ID	Dir#1 status (flow speed)	Dir#2 status (flow speed)
H1	congested (14 mph)	congested (14 mph)
H2	low speed (30 mph)	low speed (30 mph)
H3	medium speed (53 mph)	medium speed (53 mph)
H4	free flow (74 mph)	free flow (74 mph)
M1	congested (14 mph)	low speed (30 mph)
M2	congested (14 mph)	medium speed (53 mph)
M3	congested (14 mph)	free flow (74 mph)
M4	low speed (30 mph)	medium speed (53 mph)
M5	low speed (30 mph)	free flow (74 mph)
M6	medium speed (53 mph)	free flow (74 mph)

Robustness of Proposed Algorithm

To further verify the robustness of the Err-Coll-Dep policy, in the second part of our evaluations, we simulate 10 different traffic scenarios in a bi-directional 1-Km highway with four lanes of identical traffic in each direction (that is, eight lanes in total). As listed in Table 3.1, cases H1-H4 have homogeneous traffic in both directions, whereas cases M1-M6 have different traffic conditions for each direction (mean flow speed is listed for reference). Again, 100-millisecond Beaconing is used as the performance baseline; Figure 3.11 shows that it does not scale well in different traffic conditions due to excessive channel collisions. Our proposed algorithm, with fixed parameters $(\alpha, \beta) = (20, 30)$, is seen to be robust in achieving better tracking accuracy in all scenarios and its 95% cut-off error is always below 2 meters.

In addition, the worst-case scenario, in terms of tracking accuracy, is case M3 where one direction is congested and the other is free-flowing. This is the most challenging case because, on one hand, the high density of cars on the congested side means that the wireless medium is heavily loaded with huge amount of safety messages; on the other hand, vehicles on the free flow side are moving very fast and their states may change very quickly. In such situations, the already saturated DSRC channel is unable to support the more frequent information exchanges required by cars on the free flow side. Therefore, cars *on the free flow side* experience a poor tracking performance (see case M3 in Dir#2 of Figure 3.11). Interestingly, case M3 happens quite often during commute hours in metropolitan areas. With results in Figure 3.11, we show that it is possible to achieve a better tracking performance (than the uncontrolled, 100-ms beaconing proposed by VSCC [76]) using the proposed design with a fixed set of parameters (α, β). However, the appropriate values for (α, β) need further investigation and empirical tuning.

3.3.5 Short Summary

In Section 3.1 and 3.2, we first analyze the problem of how multiple scalar LTI dynamical systems track each other over a multi-access channel, which is motivated by the IVC-based Cooperative Active Safety System (CASS). Based on the analysis, we propose a transmission rate control algorithm in Section 3.3 for each vehicle to disseminate its state information. The proposed algorithm has an on-demand nature and adapts the V2V message rate for each vehicle in a decentralized fashion. Performance evaluations, both in Matlab and in large-scale traffic/network simulations, confirm that the proposed algorithm achieves better tracking accuracy than existing solutions and is more robust against channel congestion.

Throughout this section, we assume a uniform transmission power for all vehicles and adjust their individual message rates to enable statistical multiplexing and a better sharing of the wireless channel. As enlightened by [53,83], there could be further performance improvement if a variable transmission power is used by each vehicle to reduce interference and explore channel spatial reuse. In Chapter 4, we will explore such a joint design to adapt rate and power simultaneously for safety-driven information dissemination in VANETs.

Chapter 4

Transmission Rate and Power Control for Vehicle-to-Vehicle Safety Communications

In this chapter, we describe our real-time tracking formulation, assumptions, and proposed design for V2V (Vehicle-to-Vehicle) safety communications. In Section 4.1, we state our understanding of the V2V safety communications problem and our approach to adapt both transmission rate and power simultaneously. In Section 4.2, a transmission rate and power control is proposed for V2V safety communications and its performance is verified by a network simulator integrated with a microscopic traffic simulator. In our design, the error-dependent rate control in Chapter 3 is enhanced with an adaptive transmission power control for each out-going safety message. The power control on each vehicle is done based on sensed channel utilization (i.e., channel busy ratio) which serves as a side-information for each vehicle to infer the channel congestion. Its tracking accuracy is again shown to outperform the currently proposed 100-millisecond beaconing of messages. The prototype implementation of the proposed design along with small-scale real-world evaluations and protocol enhancements will be reported in Chapter 5.

4.1 Design Approach to Vehicular Safety Communications for Real-Time Tracking over a Shared Channel

In this section, we summarize our theoretical understanding of V2V safety communications problem and our approach to design our transmission rate and power control. The basic idea of safety communication is to put wireless radio and GPS on each vehicle so that all the vehicles on road can exchange vehicle state information. That is, wireless radio is used as an omni-directional sensor to provide proximity awareness to a host vehicle (HV) and to extend the perception horizon of the driver. To that purpose, each vehicle needs to

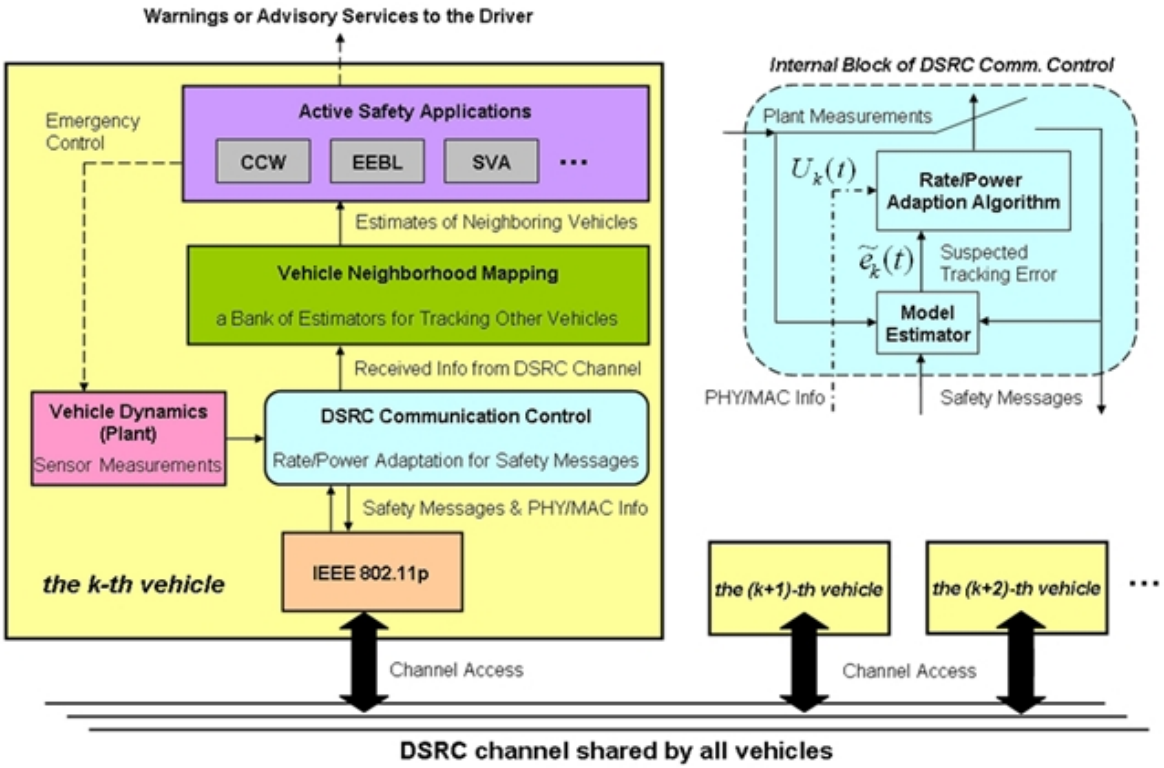

Figure 4.1. Proposed tracking framework for V2V transmission rate and power control

perform the following two tasks: 1) it needs to broadcast its own state information as safety messages to other vehicles in proximity; 2) it needs to listen to the channel and perform real-time tracking of all the neighboring vehicles based on received safety messages. Figure 4.1 depicts our view of this real-time tracking problem. Figure 4.1 is similar to Figure 3.5 except Figure 4.1 proposes a joint transmission rate and power control. Our design in this chapter is an extension of the proposed rate control in Section 3.3. An additional dimension of transmission control is the transmission power for each vehicle to broadcast each safety message. This specific view of V2V safety communication for tracking is quite different from other work in the literature, e.g. [56,57,58,60,61,62].

As shown in Figure 4.1, each vehicle is designed to contain a communication control logic, a bank of estimators to track other vehicles, and a plant (producing vehicle state information). The estimated states of neighboring vehicles will be fed to active safety applications, which in turn provide warnings to the driver or take emergency control of the vehicle in case of an imminent danger. The proposed rate and power control scheme is implemented in the communication control logic. The internal architecture of the communication control logic is shown in the upper right corner of Figure 4.1. Note that, produced safety messages are in WSM format [73], which allows specifying per-message power level for 802.11p radio. The detail of WSM format can be found in Chapter 5. For the rest of this section, we describe

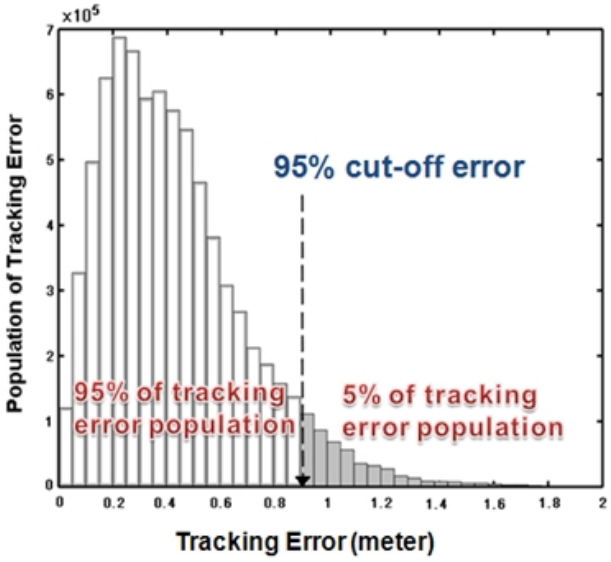

Figure 4.2. Illustration of proposed measure: 95% percentile of tracking error [25]

our design approach for V2V transmission control based on the framework in Figure 4.1. More details of our design and its implementation can be found in Chapter 5.

With the real-time tracking framework in Figure 4.1, there is one crucial question: How to allow multiple dynamical systems (i.e., intelligent vehicles) to track each other in real-time over a shared channel. As analyzed in Section 3.1 and Section 3.2, different message arrival patterns to a RV usually result in different real-time tracking error of a HV by this RV. Therefore, it is important to design a message generation mechanism that minimizes the tracking error. We have the following assumptions in our design: 1) A more accurate real-time tracking of other vehicles (i.e., better proximity awareness) results in better operations of V2V safety applications; 2) Each car is assumed to measure its own position by using GPS; 3) Nearby neighboring vehicles (RVs) should have better tracking accuracy towards a HV than farther vehicles (since nearby RVs are more physically involved with a HV and thus more critical to the safety of a HV).

Unlike other designs in the literature, e.g., [60,62], we use the real-time tracking accuracy as the performance metric instead of the message reception probability or the channel beaconing load. More specifically, we use a statistical measure called 95% percentile tracking error illustrated in Figure 4.2. This tracking error is the Euclidean distance between 1) the true position of a HV and 2) the estimated position of this HV by a RV:

$$e(t) = \sqrt{|x(t) - \hat{x}(t)|^2 + |y(t) - \hat{y}(t)|^2}$$

where $e(t)$ is the tracking error, $(x(t), y(t))$ are (long, lat) position of a HV, and $(\hat{x}(t), \hat{y}(t))$ are (long, lat) position of this HV estimated by a RV. As explained in Section 3.3, the rationale behind this 95% cut-off error is that 95% of the real-time tracking error population is below or equal to this number and it gives a sense of reliability and accuracy of the vehicle

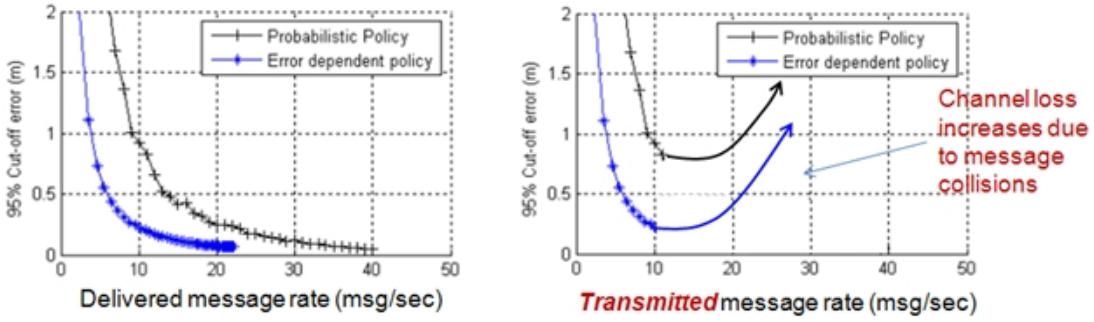

Figure 4.3. (a) Delivered message rate vs. 95% cut-off tracking error (Left) and (b) Illustrated transmitted message rate vs. 95% cut-off tracking error (Right)

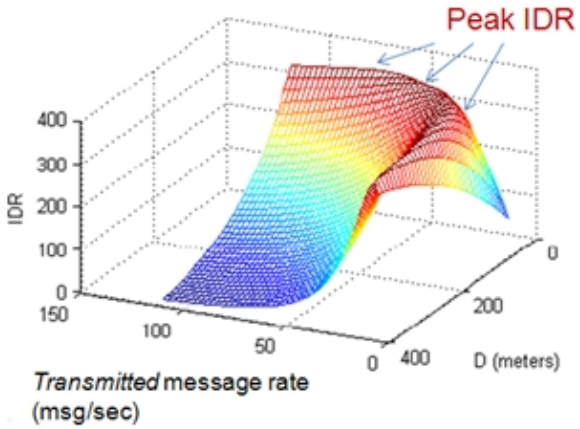

Figure 4.4. IDR: Rate of successful message delivery to all the neighboring vehicles

tracking. The same performance measure has been used in Section 3.3 for evaluating our V2V rate control design.

The relationship between the delivered message rate and this 95% cut-off tracking error is similar to the *Rate-Distortion function* in Information Theory [27]. One example is shown in Figure 4.3 (Left). As it is analyzed in Section 3.1 and Section 3.2, error dependent transmission is better than the uncontrolled probability transmission. Different message generation methods result in different tracking performance curves. However, Figure 4.3(a) does not consider the shared nature of the wireless channel. If one considers the network and the fact that all nodes need to contend to send out messages, the performance is illustrated in Figure 4.3(b). When all nodes generate too many messages at the same time (i.e., high message rate), the resulting tracking performance does not improve. Instead, the tracking error goes up due to too many message collisions in the shared channel and insufficient successful message arrival rate at the receiver side.

To understand the effect of a shared network, we analyzed the broadcast throughput, called Information Dissemination Rate (IDR), in [80,83]. This IDR is essentially the rate of

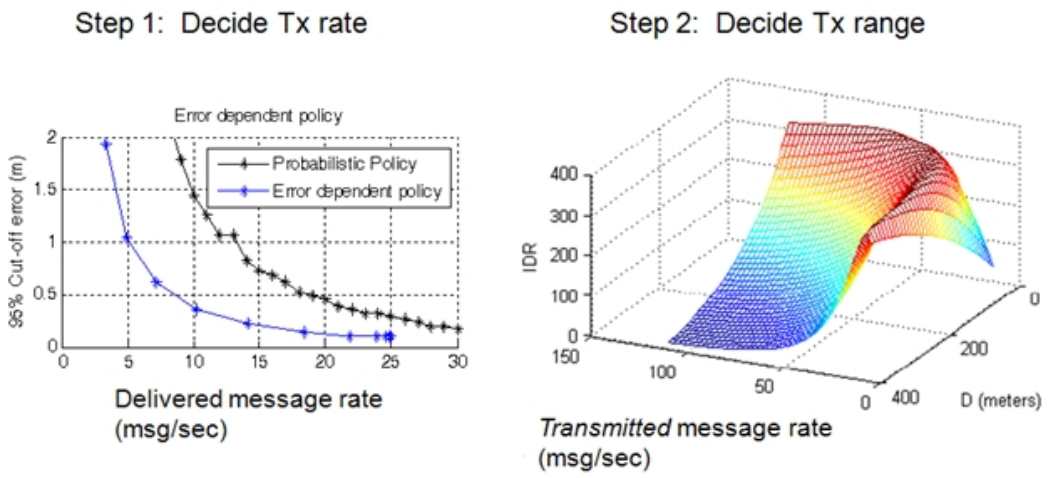

Figure 4.5. Our two-step approach of deciding Transmission rate and range

successful message delivery to all the neighboring vehicles (i.e., the broadcast throughput):

$$IDR = \sum_{i \in \{\text{Neighboring Vehicle within } D\}} R \times P_{succ}(i).$$

For a given traffic density, IDR can be simulated and plotted as the example in Figure 4.4 for different transmission Rate (R) and transmission Range (D) [83]. This IDR plot gives us a characterization of how the information broadcast behavior is constrained by a wireless channel shared by all nodes. As one can observe from Figure 4.4, for certain combinations of Rate (R) and Range (D), IDR can reach the peak (the red part of the plot). More details can be found in [83].

Based on the understanding of rate-distortion model in Figure 4.3 and the channel broadcast throughput (IDR) in Figure 4.4, our design follows two steps to first decide the message rate and then decide the transmission range (thus power). This idea is illustrated in Figure 4.5. For safety considerations, we propose to first control the message rate (R) based on vehicle dynamics and sensed tracking errors. Given a message rate, for network considerations, we propose to control the transmission range (D) to maximize IDR (i.e., the information broadcast throughput) for the current network condition. What is implied in this two step design is that our design assumes that accurate tracking at nearby vehicles is more desirable than poor tracking over a large neighborhood.

Therefore, our design responds to channel congestion by maintaining the same state information intensity (i.e., keeping the same message rate) to the nearest neighbors and (temporarily) stopping communication to farther vehicles (i.e., reducing transmission range/power). In essence, our design tries to maximize the number of neighbors that can track a HV with a specified accuracy. Our proposed V2V transmission rate and power control in Section 4.2 incorporates this design rationale and its implementation and evaluations can be found in Chapter 5.

4.2 Proposed Transmission Rate and Range Control and Simulation Verification

In this section, we state our transmission control for vehicular safety communications and the large-scale traffic/network simulation results. The simulations show that our design has a better structure and is more robust in different traffic conditions than the currently proposed 100 millisecond beaconing.

Intelligent Transportation Systems (ITSs), empowered by wireless communication, are expected to significantly improve the safety and efficiency of our transportation network. The idea is to inter-connect all the physical components of a transportation system in the cyber-space. Vehicles equipped with IEEE 802.11p transceivers [72], dubbed as DSRC (Dedicated Short Range Communication) or WAVE (Wireless Access for Vehicular Environments), can exchange information either in vehicle-to-vehicle (V2V) or vehicle-to-infrastructure (V2I) fashion. While V2I communication requires huge infrastructure investment, V2V communication is a more viable solution for the near future. Such V2V communication is the basis for the setup of Vehicular Ad-hoc Networks (VANETs). VANETs are expected to host new safety, navigation, and automation applications in vehicular environments.

The DSRC technology, based on IEEE 802.11p, is the centerpiece of VANETs. Formally, IEEE 802.11p defines high-speed short-range wireless communication among vehicles and surface transportation infrastructure. Similar to IEEE 802.11a, 802.11p radio is based on matured Orthogonal Frequency-Division Multiplexing (OFDM) technology. The MAC layer functionality is slightly modified to include provision for rapid communication of DSRC devices with no need for authentication or authorization processes as in the original 802.11 standard. In addition to the 802.11p standard, IEEE 1609 [73] defines higher layer functionalities such as networking and multi-channel operations for VANETs. The protocol stack depicted in Figure 4.6 describes how different protocols are involved in enabling vehicular communication. As part of these standards, a new type of message, WSM (WAVE Short Message) is defined in 1609.3, which supports frame-by-frame power and modulation assignment and thus provides new possibilities for cross-layer optimization. To ensure that DSRC applications are inter-operable, other standards may be employed in this architecture, e.g., SAE J2735, which is a message set dictionary (i.e., common language) for DSRC applications to understand each other, that describes DSRC message content. The standardization effort is equally supported by industry and government entities.

More related work on Inter-Vehicle Communication (IVC) and ITS applications can be found in Subsection 3.3.1. For the rest of this subsection, we will focus on the V2V safety communications for active safety.

DSRC and Cooperative Active Safety

Currently, prototype DSRC based applications are under test by different car manufacturers and research institutions. While these efforts show that DSRC based technology works in principle, deployment and performance issues are still under investigation, especially for high

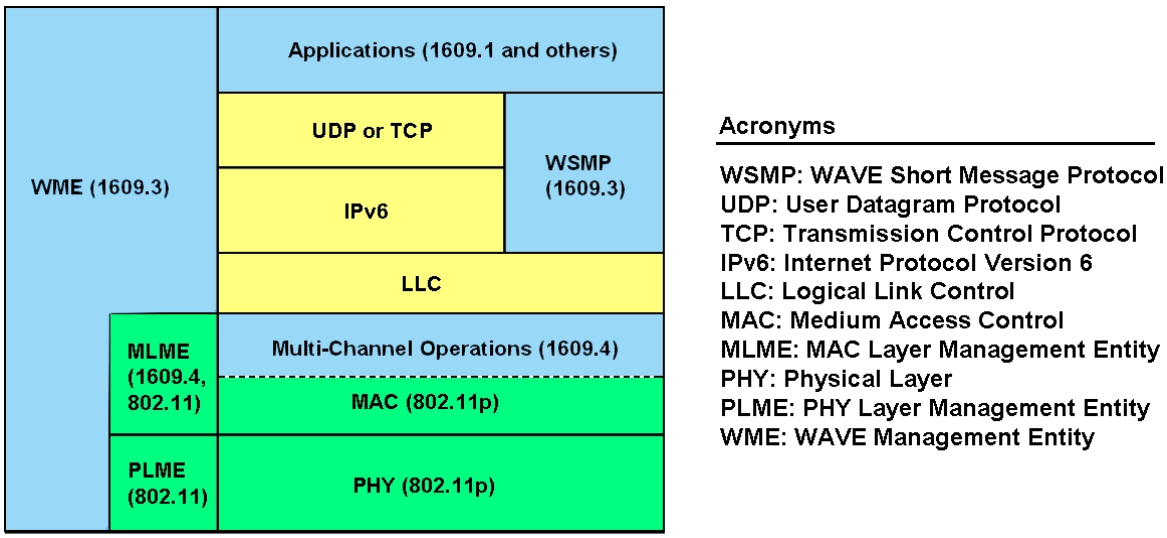

Figure 4.6. Protocol stack for WAVE (Wireless Access for Vehicular Environments), mainly composed of IEEE 802.11p [72] and IEEE 1609 family standard [73]: 1609.1 (resource manager), 1609.2 (security), 1609.3 (networking services), and 1609.4 (multi-channel operations). Note that, 1609.2 works jointly with 1609.3 and thus is not shown in above architecture.

market penetration case. For example, the issues facing cooperative safety applications are still active research subjects. Unlike research on Mobile Ad hoc Networks (MANETs) which focuses more on maximizing throughput or maintaining network connectivity, the distinct mission of VANETs is to enhance roadway safety through V2V communication [39,76]. To name a few, active safety applications include Cooperative Collision Warning (CCW), Electronic Emergency Brake Light (EEBL), and Slow/Stopped Vehicle Alert (SVA). In general, these active safety applications require that a subject vehicle have a good estimate of the position and state of the cars in its proximity. The availability of such proximity-awareness allows various safety applications to provide advisory services to the driver (via audio or visual human-machine interfaces) or perform emergency reactions to avoid hazardous situations.

For this safety/tracking purpose, each vehicle is assumed to be equipped with DSRC radio, GPS (Global Positioning System) receiver, and on-board sensors. Each vehicle is designed to continuously report its own status, e.g., position, speed, and heading, by broadcasting safety messages in WSM format. At the same time, each vehicle also tracks movements of neighboring vehicles based on information received from them over the shared channel. The question of how often and how far should these messages be broadcast, is one that drives this research.

In this section, we propose a joint rate-power control algorithm that describes how state information of a vehicle should be broadcast to its neighbors. Specifically, for different traffic scenarios, we compare the tracking accuracy of proposed algorithm with that of the currently proposed solution (beaconing with a constant interval, e.g., 100-millisecond or 500-

millisecond) suggested by Vehicle Safety Communications Consortium (VSCC) [76]. Simulation results indicate that our proposed algorithm is robust and achieves better tracking accuracy than the beaconing method in almost all traffic scenarios. In the context of safety-driven communication design for VANETs, this work provides a new perspective different from the existing methods that try to maximize throughput, achieve fairness or reduce message rate; the objective of our design is to reduce tracking error and improve the robustness and performance of the cooperative vehicle safety systems under different traffic conditions.

Overview of Existing Approaches for V2V Safety Communications

For information propagation in wireless ad hoc networks, the work in [53] gives a fundamental bound on the product of rate and distance (due to the shared nature of considered wireless medium). The implication of such a capacity notion is that, when the network becomes denser, one needs to either throttle data rate or reduce transmission power so that limited channel resource can be properly shared by all nodes. This bound applies to VANETs too and most existing designs for broadcasting safety messages focus on either rate or power adaption so that the network could operate properly when traffic density (number of vehicles) changes.

For safety applications in VANETs, [60] proposes to fairly allocate transmission power across all cars in a max-min fashion, which helps reduce beacon load at every point of a formulated 1-D highway and thus reserves bandwidth for emergency messages with higher priorities. This method assumes a predefined maximum load as the target. By utilizing water-filling concept, [60] proves a centralized algorithm that achieves this fairness goal and gives a decentralized algorithm that approximates operations of the centralized one.

Since many applications require the same data elements from other vehicles, message dispatcher in [62] is proposed to reduce required data rate by removing duplicate elements. The message dispatcher at the sender side will group data elements from application layer (i.e., the source) and decides how frequently each data element should be broadcast. At the receiver side, the message dispatcher pushes received data elements to designated applications (i.e., the sink). This design is similar to compression ideas in source coding.

Since our primary focus is on cooperative vehicle safety, our approach is to correlate communication behaviors with tracking error magnitude. In [63], error threshold crossing is used as the transmission trigger; broadcast of the state information happens only when threshold is violated. In [66], we propose a rate-control design that has advantages over others in a shared channel: 1) it increases communication rate when a vehicle suspects the estimation error of neighboring vehicles *toward itself* has increased; 2) it throttles rate during channel congestion to avoid further efficiency degradation and message loss. These two principles and their combined effect govern transmission behaviors on each vehicle and provide improved robustness to the tracking process. Our proposed rate-power control in this section follows this line of design rationale, and adds another adaptation dimension: the transmission range.

4.2.1 VANET Tracking Problem and Proposed Design

Channel access in DSRC, especially for safety applications, is performed in a random manner, following CSMA/CA (Carrier Sense Multiple Access with Collision Avoidance) rules [72] with no centralized coordination. Therefore, vehicle tracking problem is essentially a remote estimation problem over a random access channel. In this section, we will first state VANET tracking problem at an abstract level and then describe our proposed design.

As shown in Figure 4.1, each vehicle is designed to contain a communication control logic, a bank of estimators to track other vehicles, and a plant (producing vehicle state information). The estimated states of neighboring vehicles will be fed to active safety applications, which in turn provide warnings to the driver or take emergency control of the vehicle in case of an imminent danger. The proposed rate and power control scheme is implemented in the communication control logic. The internal architecture of the communication control logic is shown in the upper right corner of Figure 4.1. Note that, produced safety messages are in WSM format, which allows specifying per-message power level for 802.11p radio. For the rest of this section, we describe our proposed algorithm for decentralized self-information dissemination based on the design in Figure 4.1.

Tracking over a Multiple-Access Network

To better understand the problem at hand, assume that a number of vehicles ($n \geq 2$) share the same wireless channel, and each vehicle contains a transmission control logic, a plant generating state information $x_j(t)$, and a bank of model-based estimators for tracking neighboring vehicles. On each vehicle, there are a balanced control input $u_j(t)$ to model driver's accelerating/decelerating behavior and a noise input $\varepsilon_j(t)$ to model the mechanical disturbance within a car. The transmission control logic decides whether to broadcast self-information vector $x_j(t)$ (i.e., the state) at each moment. Each subject vehicle will try to estimate the states of other cars based on received information from the shared channel.

The estimated state (e.g., position) of sender j at receiver i, $\tilde{x}_{ij}(t)$, is the expectation conditioned on all the previous received information over the lossy channel. Packet loss in the channel could be due to collision, or channel error and fading. For presentation convenience, let's assume the dynamics of a vehicle can be sampled at discrete time step and approximated as a LTI (linear-time invariant) system of appropriate dimensions as follows:

$$x_j(t) = a_j \times x_j(t-1) + b_j \times u_j(t-1) + \varepsilon_j(t-1) \tag{4.1}$$

where a_j, b_j represent the mechanical characteristics and physical laws that govern vehicle j. The model-based estimator at a receiver i switches between two modes. At time $t-1$, if state information of vehicle j is received, the receiver uses this information to reset the estimate: $\tilde{x}_{ij}(t) = a_j \times x_j(t-1)$. Otherwise, if no information regarding vehicle j is received, the receiver i uses known model (4.1) to carry on and estimate the new state: $\tilde{x}_{ij}(t) = a_j \times \tilde{x}_{ij}(t-1)$.

In the tracking problem described above, the arrival of a new measurement from sender j to a receiver i resets the tracking error similar to that in a renewal process. Between measurement arrivals, the real-time tracking error could grow due to noise and disturbance.

Note that the above calculation of $\tilde{x}_{ij}(t)$ is MMSE (minimum mean squared error) optimal estimate, if we assume $u_j(t)$ and $\varepsilon_j(t)$ have zero mean. The tracking error $e_{ij}(t)$, i-th vehicle's estimation error toward vehicle j, is defined as $e_{ij}(t) = x_j(t) - \tilde{x}_{ij}(t)$. Due to hidden node problem or channel fading, this tracking error might vary for different vehicles.

Given the multi-access nature of the DSRC channel, the packet loss ratio and therefore the real-time tracking error depend on the number of vehicles that share the channel. This dependence means that at high transmission rates and ranges, the random access channel will become congested and consecutive collisions will make the channel useless. On the other hand, higher transmission rate and range, if successfully achieved, will directly result in better tracking performance and lower error. The question is, therefore, how to control each vehicle's transmission behavior to avoid channel collision failure while maximizing the use of the wireless medium for tracking purpose. Moreover, the maximum achievable values of rate and range before excessive collision happens are different for different vehicular traffic densities. This fact motivates the need for adaptive transmission control protocol or algorithm which is described in the next subsection.

Proposed Adaptive Vehicular Transmission Control for Safety Messages

In this subsection, we present a joint rate-power control algorithm for the VANET tracking problem. The algorithm is comprised of two parts: 1) rate control, i.e., a message generation control, which decides how frequently a subject vehicle should broadcast its own state information; 2) power control, which decides how far the state information should be broadcast to, thus determining the power level for the 802.11p radio. The functional components of the proposed algorithm are shown in Figure 4.1. The following describes these methods formally and in more detail:

Transmission Rate Control: At each time step $t \in N$, the j-th vehicle's communication logic calculates transmission probability $p_j(t)$ based on *suspected* tracking error $\tilde{e}_j(t)$ on neighboring vehicles toward its own position in *Euclidean* sense (i.e., usual distance definition for Cartesian coordinate system). If suspected error $\tilde{e}_j(t)$ is smaller than e_{th} (the error threshold), there is no transmission at all from vehicle j, i.e., $p_j(t) = 0$. This threshold design leaves the channel to be used by other vehicles when the suspected error by vehicle j is within the tolerable range. Else if suspected error is larger than this threshold, the probability of transmission in that time step t is computed as follows:

$$p_j(t) = 1 - \exp(-\alpha \times |\tilde{e}_j(t) - e_{th}|^2) \tag{4.2}$$

where $\alpha > 0$ is the sensitivity to suspected tracking error. The rationale behind this formula is that, a subject vehicle j increases transmission probability p_j when it suspects tracking error on other vehicles (toward its own state) has exceeded the threshold. The more this error violates the threshold, the higher the transmission probability becomes.

The *on-demand* nature of (4.2) responds to the fact that a higher transmission rate, thus probability, is required for a subject vehicle that has more *unexpected* movements (as estimated by other vehicles). In information theoretical terms, a vehicle with higher entropy (a measure of surprise) needs higher communication rate to describe its stochastic behavior.

On the contrary, when the suspected error is small or under the threshold, a vehicle tends to stay quiet, and this allows the channel to be used by those vehicles having larger suspected error. This design also implicitly acts as transmission error correction as explained below.

Since there is no explicit ACK (acknowledgment) for broadcast in DSRC, after each transmission, we use the PER (Packet Erasure Rate) to stochastically decide the *suspected* error $\tilde{e}_j(t)$ in (4.2): $\tilde{e}_j(t^+) = (1-\zeta) \times \tilde{e}_j(t)$ where ζ is a Bernoulli trial (similar to coin tossing) with success probability 1-PER to address potential channel loss. If successful, the suspected error is reset; otherwise, suspected error accumulates from $\tilde{e}_j(t)$ based on known state model, e.g., (4.1). Note that, this suspected error is *not* the actual estimation error; instead, it is only a measure used by a subject vehicle to adjust its own communication rate (the higher this probability, the higher the communication rate of the vehicle). Based on $p_j(t)$ in (4.2), a subject vehicle stochastically generates a packet (i.e., a safety message containing its own state information) and places it in the queue of the 802.11 MAC layer.

Finally, the PER used by the above Bernoulli trials is estimated on-the-fly by checking the inconsistency in sequence number of recently received packets (by a subject vehicle) from all corresponding senders (with at least two messages received) within a 1-second history log. That is, a subject vehicle uses the number of lost packets divided by the number of total packets initiated from a certain sender to infer recent channel loss rate; PER is this measure averaged over all its senders within a geographical area. Assuming network symmetry, PER tells a subject vehicle the likelihood of the loss of its previous transmission at the receivers. Note that this PER is in fact an average and rough measure of the real error probability of individual links between the subject vehicle and other vehicles within the spatial neighborhood. The exact value of link error probability is not practically measurable under the assumptions of proposed active safety systems in Figure 4.1 since all safety messages are in the broadcast mode.

Transmission Power Control: The transmission range $L_j(t)$ is adjusted based on the observed channel status. Here, instead of using explicit feedback, usually done through piggy-back information exchange as in [60], we propose a simple design to scale transmission range linearly with averaged channel occupancy. This method is scalable and easy to implement. The average channel occupancy, $U_j(t)$, is a real number between 0 and 1. $U_j(t)$ is computed for each vehicle j by observing the CCA (Clear Channel Assessment) reports that are available from PHY to the MAC layer of 802.11. This occupancy measure is the time-average of recently sampled CCA within 1-second time window. Since there is no explicit ACK for broadcast in DSRC, we use this side information, channel occupancy, to infer channel status and adjust targeted communication range.

In the proposed algorithm, if channel occupancy is higher than U_{max}, minimum transmission range L_{min} is used; else if channel occupancy is lower than U_{min}, maximum transmission range L_{max} is used; otherwise, the range is selected as follows:

$$L_j(t) = L_{min} + \frac{U_{max} - U_j(t)}{U_{max} - U_{min}} \times (L_{max} - L_{min}). \tag{4.3}$$

In (4.3), L_{min} and L_{max} are communication range lower/upper bounds, which are usually determined from safety specification for vehicular environments. Besides, U_{min} and U_{max}

represent the desired linear operating range of channel occupancy and are selected based on experimental or analytical data. Since the granularity of power levels for DSRC is 0.5 dBm [72], to convert $L_j(t)$ to power, we apply a power-range mapping (with step size 0.5 dBm) based on the empirical channel model reported in [54]. The basic assumption of proposed power control is that vehicles in proximity would perceive roughly the same CCA and the same amount of averaged channel occupancy. Therefore, in our design, vehicles in proximity coordinate their transmission power by using the same side information (i.e., the observed channel occupancy). In [80,83], we show that for different combination of message rate and vehicular traffic density, optimal information dissemination exists between channel occupancy 0.4 and 0.8, which will be used as U_{min} and U_{max} in our simulations later.

The idea behind our rate-power control algorithm is that nearby vehicles are assumed to be physically more related to a subject vehicle. In fact, it is potentially more dangerous if a subject vehicle does not know the state (e.g., position and speed) of its immediate neighbors. In proposed power control, when channel is congested, a vehicle tries to make sure that its nearby cars can still hear its state information by reducing the transmission power, which results in temporarily giving up far-away cars. According to [53], adapting power properly can help reduce interference and increase successful reception probability of nearby nodes. In short, the proposed algorithm does not compromise information rate intensity while facing channel congestion; instead, it reduces power to maintain decent tracking accuracy of its immediate neighboring vehicles to ensure safety.

4.2.2 Evaluations Using Large-Scale Traffic/Network Simulations

To evaluate the performance of the proposed design, we have conducted several simulation experiments with realistic settings using a network simulator and a microscopic traffic simulator. The main stage for simulations is a bidirectional 2-Km highway, with each direction containing 4 lanes of identical traffics. We only collect statistics from vehicles within 0.5 Km to 1.5 Km segment to avoid boundary effects in simulations. Our simulations consider traffic scenarios listed in Table 3.1: Cases H1-H4 represent scenarios with homogeneous traffic flows in both directions while Cases M1-M6 contain mixed traffic conditions. Mean flow speed, in the unit of miles per hour (mph), is also listed in Table 3.1 for reference.

Simulation Settings

For network simulations in OPNET [75], we use modified 802.11a PHY module working at 5.9 GHz with 10 MHz bandwidth. We follow the DSRC channel model reported in [54] and simplify the far distances as Rayleigh fading, instead of pre-Rayleigh. The reason for this simplification is that we are considering a straight highway scenario while [54] considers urban scenarios with intersections and corners, which lead to pre-Rayleigh fading observations. In addition, we assume that path loss exponent is always 2.31. The transceiver operates with -87 dBm receiver sensitivity, 3 Mbps raw data rate, and a fixed 28 dBm transmission power (which roughly covers the radius of 250 meters) for 100-millisecond (ms) and 500-millisecond beaconing, which is the standard solution suggested by VSCC [76]. The payload size of each

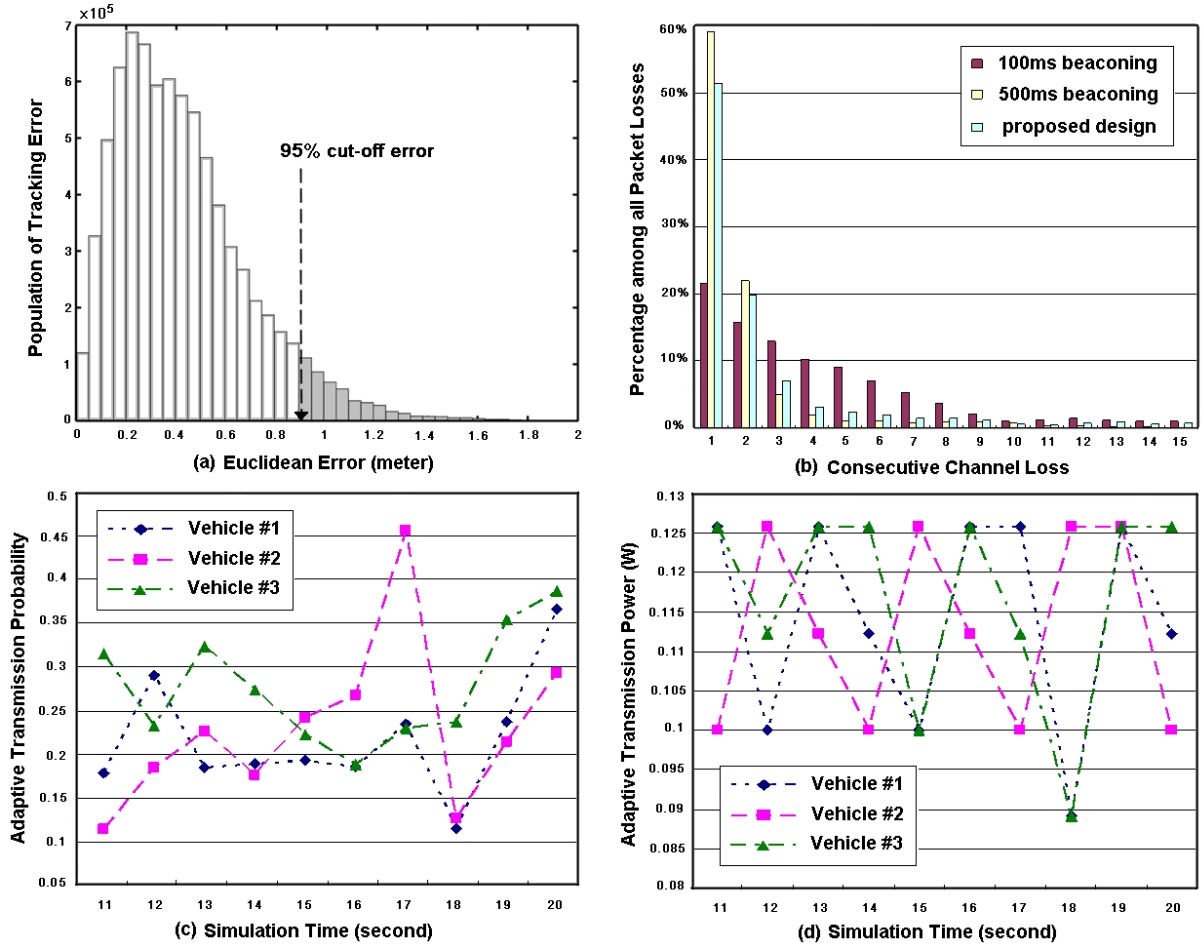

Figure 4.7. (a) Histogram of tracking error (in meters) collected within 150-meter radius of each subject vehicle while using 100-ms beaconing (in H4 case). (b) Percentage of consecutive losses collected within 30-meter radius of each subject vehicle during simulation (in M3 case). (c) Samples of three vehicles' adaptive transmission probability for 10 seconds (in M3 case). (d) Samples of three vehicles' adaptive transmission power for 10 seconds (in M3 case).

safety message is 300 bytes. Throughout OPNET simulations, the CSMA/CA of the 802.11 MAC layer is kept intact.

For vehicle dynamics, we use trajectory files of [position, speed, heading] sampled at 20 Hz, produced by a microscopic traffic simulator, SHIFT [74]. Total simulation time is 30 seconds for each run. During the simulation, at 50-millisecond time step, each vehicle gets a measurement of its own status from on-board sensors and decides whether to generate a packet or not, according to the specified communication policy. The on-board measurement noise is modeled exactly the same way as in [40], which was in turn based on experiment data [39]. Upon receiving information from the shared channel, each vehicle updates its estimation of cars in proximity. We choose a simple first-order kinematic model, i.e., a constant speed predictor, for tracking neighboring vehicles. By using this predictor, a vehicle is assumed to run with the same speed and heading after its last successful information broadcast is received by this predictor.

Tracking Accuracy Measure

After each simulation run, statistics are collected from neighbors within indicated distance interval in Figure 4.8 and we calculate **Euclidean tracking error** over all vehicles to explore law of large number. See Figure 4.7(a) for an example of typical tracking error distribution. Specifically, 95% cut-off error (indicated by the arrow in Figure 4.7(a)) means that 95% of Euclidean errors fall below this number (i.e., only 5% population is on the right side of the arrow), which represents the tracking accuracy of used communication policy. We will use this measure, 95% cut-off error, as the main performance metric for comparisons in Figure 4.8. The main advantage of this performance measure over others (e.g., mean or standard deviation of error) is that it gives a statistical sense similar to that of a confidence interval. Note that presented tracking error in Figure 4.7(a) and Figure 4.8 is the *ground-truth* tracking error (in meters) during simulations instead of the *suspected error* $\tilde{e}_j(t)$ perceived by vehicle j in (4.2).

Robustness of the Proposed Design

In this subsection, we present simulation results and compare the performance of the 100-ms and 500-ms beaconing of safety messages with that of the proposed communication algorithm for different traffic conditions listed in Table 3.1. The following parameters are used for the proposed rate-power control: $\alpha = 2$ meter^{-2}, $e_{th} = 0.2$ meter, $L_{min} = 50$ meters, $L_{max} = 250$ meters, $U_{min} = 0.4$, and $U_{max} = 0.8$ in (4.2) and (4.3). In this subsection, we focus on the robustness of proposed design: with a *fixed* set of parameters, our design can work well in different traffic scenarios compared with the non-controlled beaconing.

Figure 4.7(b) shows a typical distribution of consecutive losses in one particular simulation run for each communication design respectively. Note that the shown percentage is calculated based on *all communication losses* instead of all communication instants. The reason for analyzing this data is to understand how efficient the channel is shared by all vehicles and how effective broadcasting behaviors of vehicles are. It is seen that the 100-ms

beaconing method causes significantly more consecutive losses because each vehicle keeps transmitting the same amount of messages without considering whether the channel could support such high volume of data or not. Using our proposed design, there are fewer consecutive losses in the channel. Figure 4.7(c) and 4.7(d) show an example of the adaptive behavior of transmission rate and power for three vehicles in proximity for 10 simulation seconds. For simplicity of presentation, only values on integer seconds are plotted in Figure 4.7(c) and 4.7(d); during simulation, the transmission power and rate for each vehicle is adapted every 50 millisecond based on our algorithm.

The tracking accuracy (**95% cut-off Euclidean error**, see an illustration in Figure 4.7(a)) for both 100-ms/500-ms beaconing and our proposed solution is plotted in Figure 4.8 with respect to various traffic conditions in Table 3.1. Each subplot shows the tracking accuracy of three communication policies at different distances, presented in 30-meter bins between 0-240 meters. The reason for such presentation is to illustrate how tracking accuracy degrades as the distance from a subject vehicle increases. Due to space limitation, only results from cases H1, H2, M3, M5, and M6 are presented in Figure 4.8. For cases H1 and H2, only tracking accuracy in direction#1 is presented since traffics in both directions are homogeneous; for cases M3, M5, and M6, tracking accuracy in both direction#1 (left) and direction#2 (right) is presented.

The message rate for 100-ms beaconing is fixed at 10 packet per second (pkt/sec) while that is 2 pkt/sec for 500-ms beaconing. The message rate of our proposed design is also shown in Figure 4.8 for each case, ranging from 2 to 3 pkt/sec. On average, our proposed design achieves better (or equal) tracking accuracy than beaconing. As it is observed from Figure 4.8, the 100-ms beaconing method does not scale well when facing different traffic conditions, especially when there is a high density of cars. This *uncontrolled* method suffers from more consecutive losses (as indicated by Figure 4.7(b)) and thus higher tracking error.

For the 500-ms beaconing, it does not suffer channel congestion in most cases (see one example in Figure 4.7(b)) because its transmission behaviors is not as frequent as that of 100-ms beaconing. Therefore, in some cases, 500-ms beaconing achieves a better tracking performance than 100-ms beaconing due to fewer collisions in the channel. However, its sending interval (one message every 0.5 second) is too long and thus not enough information intensity available for neighboring vehicles to track a subject vehicle in real-time. Therefore, tracking error of 500-ms beaconing is still larger than our proposed algorithm in most scenarios. Although the channel congestion level of our proposed algorithm is similar to that of 500-ms beaconing (e.g., see Figure 4.7(b)), our proposed algorithm is more efficient and uses timely transmission of state information to eliminate large tracking error on neighboring vehicles. A higher transmission probability is utilized when a subject vehicle suspects other vehicles have higher error toward itself; otherwise, a subject vehicle leaves the shared channel to other vehicles that have larger suspected tracking error to broadcast safety messages.

Furthermore, our proposed design adapts its power according to channel occupancy and thus its tracking error stays flat for a certain range or distance (this range depends on vehicular traffic condition and network congestion). Take H1 case (in Figure 4.8) for example, the 95% Euclidean tracking error stays roughly the same within 90-meter radius; beyond that, the tracking error goes up quickly as distance increases. In other words, the immediate

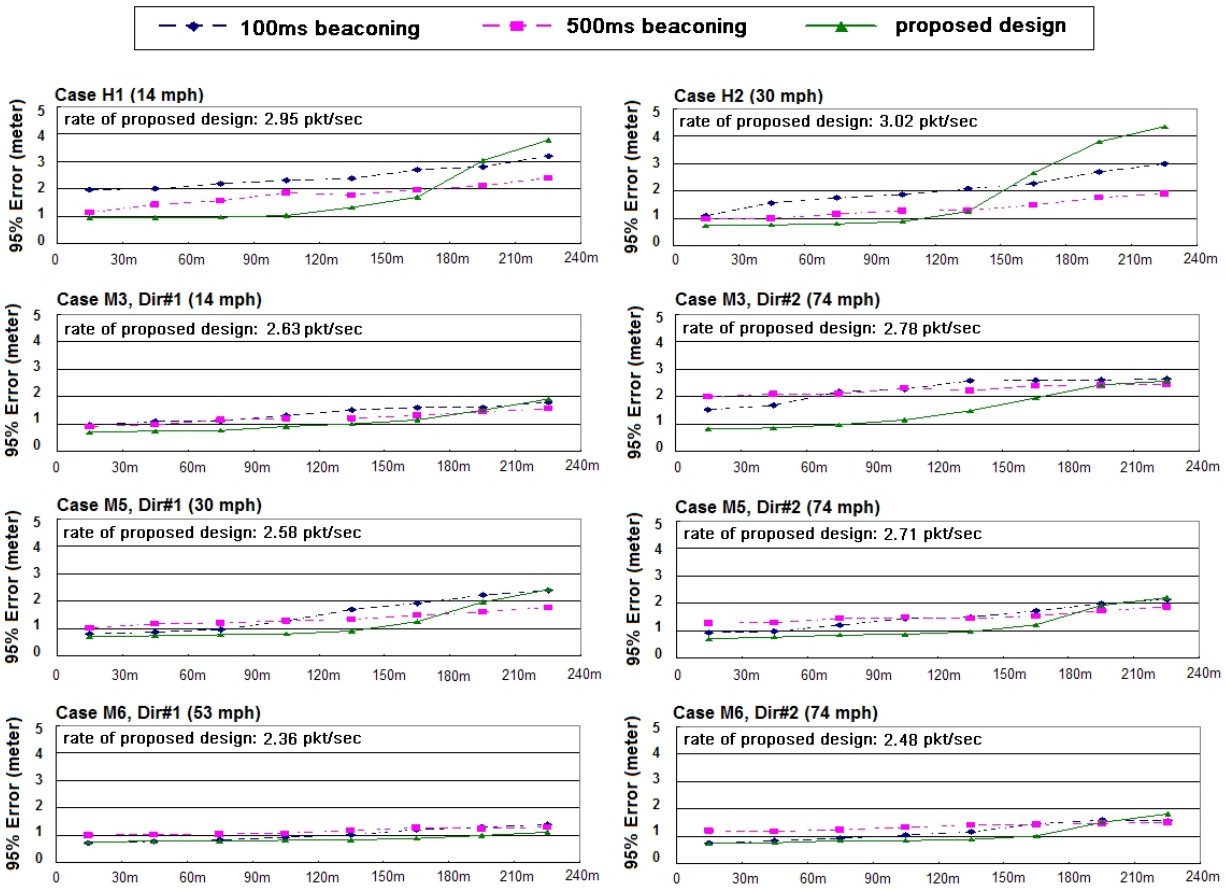

Figure 4.8. Tracking Accuracy (95% Euclidean error, in meters) in 8 distance ranges for 1) the 100-ms beaconing method (*Blue Dash* curve), 2) the 500-ms beaconing method (*Pink Dash* curve), 3) the proposed rate-power control (*Green Solid* curve).

neighbors have better tracking accuracy than others. This result is simply because the proposed design temporarily gives up far-away cars during channel congestion and tries to maintain the same amount of state information available to its closer neighbors. Our design pays the price of higher tracking error on remote vehicles to gain better tracking accuracy on nearby vehicles to ensure safety.

4.2.3 Short Summary

Cooperative active safety applications are among the most important services provided by ITSs. Such cooperative safety systems require that each vehicle track its neighboring vehicles in real-time and detect hazardous situations. The uncontrolled transmission of state information by each vehicle is shown to produce excessive data traffics that could choke the vehicular wireless network and fail all applications. In this section, we propose a joint rate-power control algorithm for broadcast of self-information which enables neighbor tracking in VANETs. We evaluated the presented solution through realistic network and microscopic traffic simulations. We also defined a statistical performance measure for tracking accuracy. To verify the robustness of the algorithm, we simulate the tracking performance of the proposed algorithm that adapts transmission power and rate in different traffic scenarios. Simulation results confirm that the proposed design is robust and can considerably reduce the tracking error compared to that of the currently proposed solution (beaconing with 100-millisecond or 500-millisecond interval).

Chapter 5

Implementation and Evaluations of Proposed Vehicle-to-Vehicle Safety Transmission Control

In this chapter, we present the prototype implementation, real-world evaluations, and enhancements of the V2V (Vehicle-to-Vehicle) communications design proposed in Chapter 4. The implementation details are presented in Section 5.1 as message generation and power assignment functional blocks. Section 5.2 provides our evaluations for outdoor vehicle mobility and scalability. The real-world evaluations conducted in General Motors Technical Center show that our design works well in practice and is a promising solution to address the scalability of V2V safety communications. In Section 5.3, we provide updated performance metrics, identified challenging traffic scenarios, and our updated simulation results for these challenging scenarios. Overall, the prototype evaluations and simulation results prove the robustness of our V2V transmission control and its superior tracking performance over the currently proposed 100-millisecond beaconing design.

5.1 Implemented Functional Blocks

We have implemented the proposed rate and range control algorithms for this deliverable following the software architecture and implementation plan. We have used Denso Wireless Safety Units (WSUs) [81,82] as the platform to implement and compare different algorithms. The cross compile build environment for the WSU was set up and the implmentation code is written in C. We have used the API provided by Denso to access various WSU functionalities for positioning and radio parameters. In this section, we will describe the functional software blocks in detail.

Similar to Figure 4.1, Figure 5.1 summarizes the rate and range control framework while introducing all the critical blocks like sensor inputs, neighborhood vehicle mapping, radio interface, the message generator and the range controller. Figure 5.2 and Figure 5.4 show the Message Generation and Power Assignment functional blocks respectively along with the

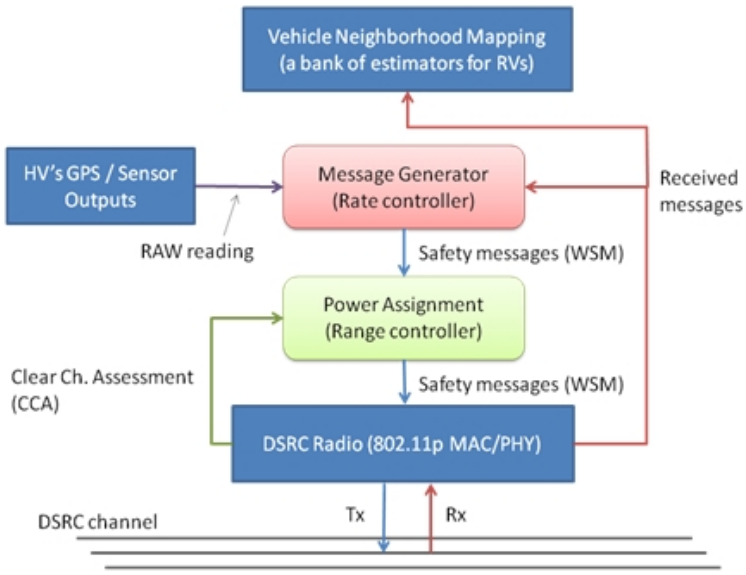

Figure 5.1. High level illustration of our transmission rate and power control

member functions. Figure 5.5 combines the Message Generation blocks (as in Figure 5.2) and Power Assignment blocks (as in Figure 5.4) to provide an overview of the transmission rate/power framework along with the interaction between the various functional blocks and the device. Now with the overall software hierarchy presented, we describe the individual functional blocks in further details.

Message Generation Functional Blocks

1) **Function:** Local Estimator for HV (Host Vehicle). **Member of:** Message Generation Functional (see Figure 5.2). This functional block estimates the current state information for a HV. Based on the latest GPS sensory data, current state of a HV is calculated based on constant speed and constant heading assumptions, i.e., coasting. This coasting operation can take many forms and one example is given below for ease of discussion. Let t be the time of latest state information with $x(t)$, $y(t)$, $v(t)$, $\theta(t)$ as the longitudinal position, lateral position, speed, and heading of this HV measured at time t. Let t' be current time and

$$\begin{aligned}
\hat{x}(t') &= x(t) + v(t)\cos(\theta(t)) \times (t' - t) \\
\hat{y}(t') &= x(t) + v(t)\sin(\theta(t)) \times (t' - t) \\
\hat{v}(t') &= v(t) \\
\hat{\theta}(t') &= \theta(t)
\end{aligned}$$

where $\hat{x}(t')$, $\hat{y}(t')$, $\hat{v}(t')$, $\hat{\theta}(t')$ are the estimated longitudinal position, lateral position, speed, and heading of this HV at time t'. The reason of this coasting formula is that there is usually

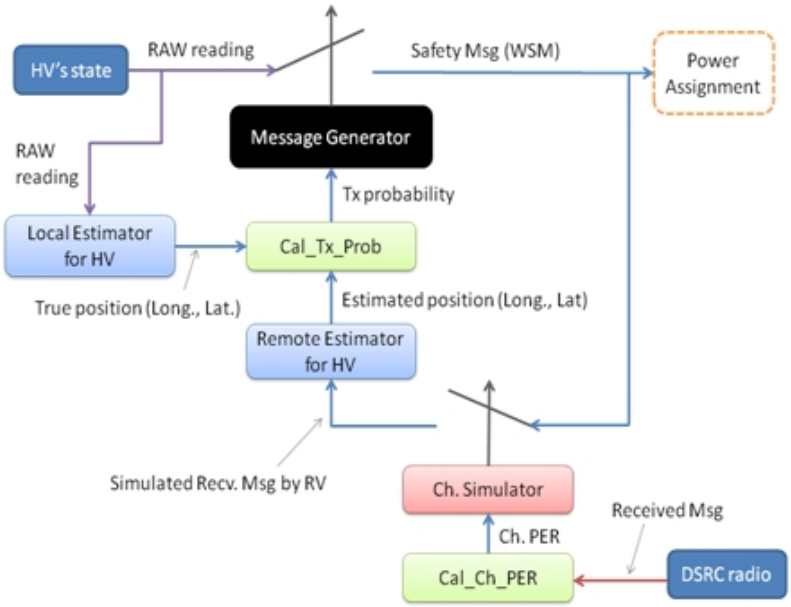

Figure 5.2. Functional blocks of proposed transmission rate (message generation) control

a small time difference between the moment when GPS measurement is taken (e.g., at t) and the moment when current state information is required (e.g., at t') to make a transmission decision.

2) **Function:** Calculate Channel PER (Cal_Ch_PER). **Member of:** Message Generation Functional (see Figure 5.2). This functional block estimates the DSRC channel quality and derives a channel packet error rate (PER) for every pre-defined interval, e.g., one second. Due the outdoor environment and different scales of fading in DSRC channel, it is in general hard to apply any mathematical model to get this PER. Therefore, this functional block uses an empirical approach described below. First, by inspecting the missing sequence number of received messages from all neighboring vehicles within a defined range, e.g., a radius of 100 meters,

$$\pi(t) = \frac{1}{N(t)} \sum_{i=1}^{N(t)} \frac{\text{missed seq. number from vehicle } i \text{ during } (t-,t]}{\text{total seq. number from vehicle } i \text{ during } (t-,t]}$$

where δ is the length of the evaluation interval, $\imath(t)$ is the estimate channel unreliability for the time interval from $t-\delta$ to t , $N(t)$ is the number of neighboring vehicles within a defined range at time t. This $\pi(t)$ from above formula is then smoothened by an Auto-Regressive-1 (AR-1) model below to further filter out temporal noise or disturbance in this measurement:

$$\Pi(t) = \lambda \times \pi(t) + (1-\lambda) \times \Pi(t-\delta)$$

where λ is the weight factor (e.g., $\lambda = 0.9$), $Pi(t)$ is the PER metric that will be used by the next functional block.

3) **Function:** Channel Simulator (Ch. Simulator). **Member of:** Message Generation Functional (see Figure 5.2). This functional block helps a HV *guess* the latest state information received by RVs in its proximity. By using the PER metric $\Pi(t)$ from the **Cal_Ch_PER** functional block, after each transmission, this functional block uses a uniform random number generator to infer whether a previous transmission is successful or not. After each transmission, a Bernoulli trial with $\Pi(t)$ is used to infer whether this previous transmission is successful. If the outcome of this Bernoulli trial is positive, this functional block assumes previous transmission is successful and updates the latest received information by RVs as the state information contained in previous transmission. Otherwise, if the outcome of this Bernoulli trial is negative, this function block treats the previous transmission as a failure and does not update the latest state information received by RVs.

To express the idea more precisely, let $\begin{bmatrix} t \\ x \\ y \\ v \\ \theta \end{bmatrix}_{Latest}$ be the HV's assumed latest state information received by RVs and $\begin{bmatrix} t \\ x \\ y \\ v \\ \theta \end{bmatrix}_{Pre-Tx}$ be the HV's state information contained in the message of its previous transmission (where t is the time when the longitudinal position x , lateral position y , speed v , and heading θ are measured). The HV's assumed latest state information received by RVs is updated after each transmission based on below formula:

$$\begin{bmatrix} t \\ x \\ y \\ v \\ \theta \end{bmatrix}_{Latest} = 1(rand() \geq \Pi(t)) \times \begin{bmatrix} t \\ x \\ y \\ v \\ \theta \end{bmatrix}_{Pre-Tx} + 1(rand() < \Pi(t)) \times \begin{bmatrix} t \\ x \\ y \\ v \\ \theta \end{bmatrix}_{Latest}$$

where $rand()$ is a uniform random number generator and $\Pi(t)$ is the estimated channel PER from the **Cal_Ch_PER** functional block. Note that, above calculation only helps a HV *guess* the latest state information received by RVs. The actual latest state information received by RVs might be different for each RV due to different scales of fading and unreliability in wireless channel and they might also be different from this HV's assumed latest state information received by RVs. The derived latest state information from above formula only serves as the *simulated* tracking error perceived by a HV and is used for a HV to adapt its transmission rate.

4) **Function:** Remote Estimator for HV (Host Vehicle). **Member of:** Message Generation Functional (see Figure 5.2). This functional block uses constant speed and constant

1	1	1	1	1	4	2	Variable
WSM Version	Security Type	Channel Number	Data Rate	TxPwr_ Level	Provider Service Identifier	WSM Length	WSM Data

Figure 5.3. WSM format and where HV data will be put in

heading assumptions to calculate the HV's current state being estimated by other RVs, i.e. coasting. That is, this functional block helps an HV to infer what RVs *think* about its own state based on the outcome of the **Ch. Simulator** functional block. The formula used here is basically the same as the formula used in the **Local Estimator for HV**. Let the latest state information assumed to be received by RVs contains $x(t)$, $y(t)$, $v(t)$, $\theta(t)$ as the longitudinal position, lateral position, speed, and heading of the HV at time t. Let t' be current time and

$$\begin{aligned}
\widetilde{x}(t') &= x(t) + v(t)\cos(\theta(t)) \times (t' - t) \\
\widetilde{y}(t') &= x(t) + v(t)\sin(\theta(t)) \times (t' - t) \\
\widetilde{v}(t') &= v(t) \\
\widetilde{\theta}(t') &= \theta(t)
\end{aligned}$$

where $\widetilde{x}(t')$, $\widetilde{y}(t')$, $\widetilde{v}(t')$, $\widetilde{\theta}(t')$ are the estimated HV's longitudinal position, lateral position, speed, and heading of this HV at time t' by RVs. The reason of the coasting in above calculation is that there is usually a significant time difference (due to channel access delay, transmission delay, and possible channel losses) between the moment when GPS measurement is taken (e.g., at t) and the moment when an HV's state information is received by RVs and used to update state estimation towards that HV (e.g., at t'). Due to this longer latency between assumed message receptions, the accuracy of the position calculation in this functional block is usually poorer than that of the position calculation in the **Local Estimator for HV** functional block.

5) **Function:** Message Generator. **Member of:** Message Generation Functional (see Figure 5.2). This functional block calculates the suspected tracking error and then uses that to decide a transmission probability that will be used to generate a message by the Message Generator functional block. The suspected tracking error is calculated as the Euclidean distance between $(\hat{x}(t), \hat{y}(t))$ from formula (1) and $(\widetilde{x}(t), \widetilde{y}(t))$ from formula (5):

$$\widetilde{e}(t) = \sqrt{|\hat{x}(t) - \widetilde{x}(t)|^2 + |\hat{y}(t) - \widetilde{y}(t)|^2}$$

where $\widetilde{e}(t)$ is the suspected tracking error, $(\hat{x}(t), \hat{y}(t))$ are (longitudinal, lateral) position from the **Local Estimator for HV** functional block, and $(\widetilde{x}(t), \widetilde{y}(t))$ are (longitudinal, lateral) position from the **Remote Estimator for HV** functional block.

This suspected tracking error $\widetilde{e}(t)$ from above formulation is then used to decide the

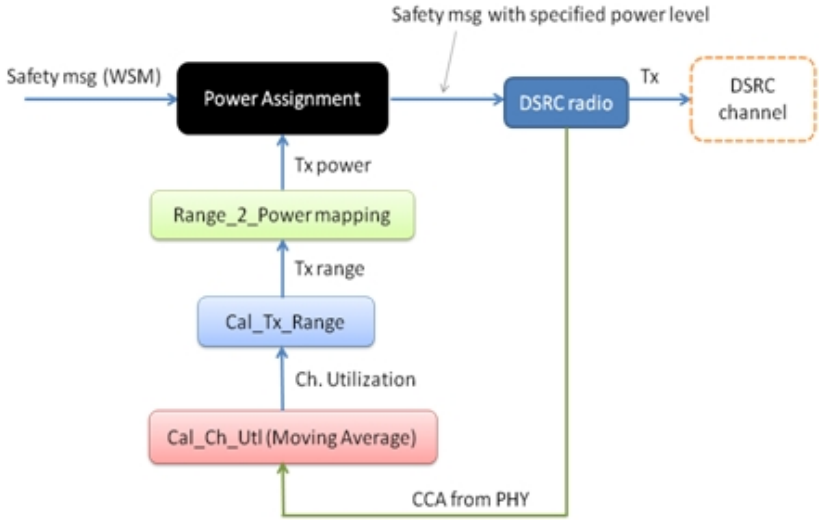

Figure 5.4. Functional blocks of proposed transmission range (power assignment) control

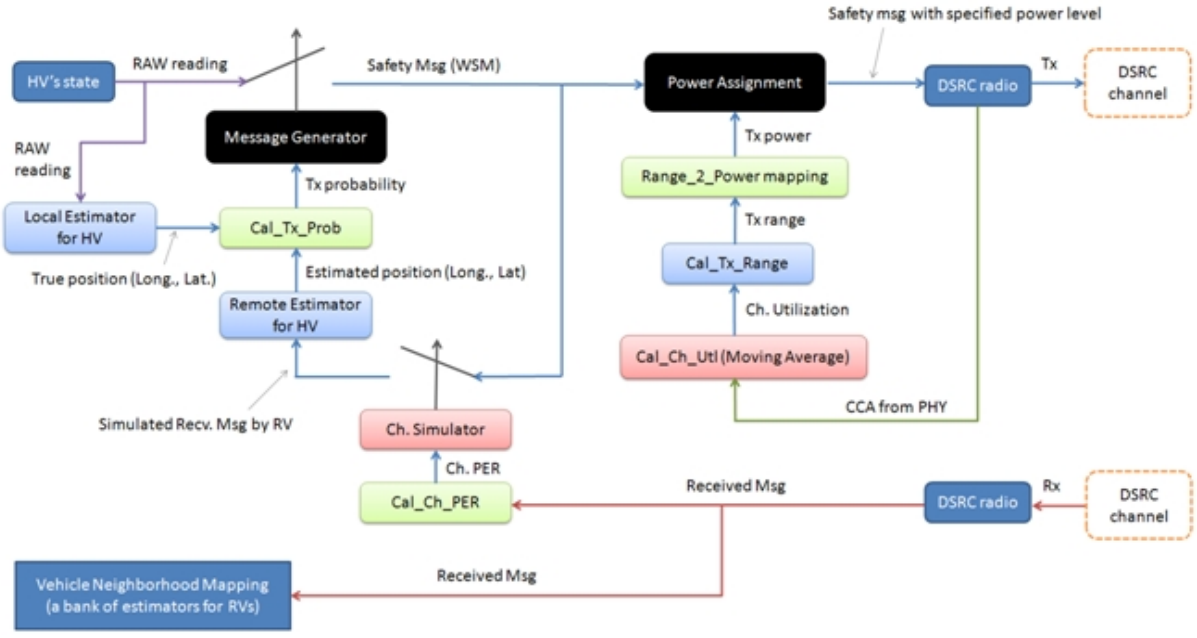

Figure 5.5. Overall functional blocks of both transmission rate and power control

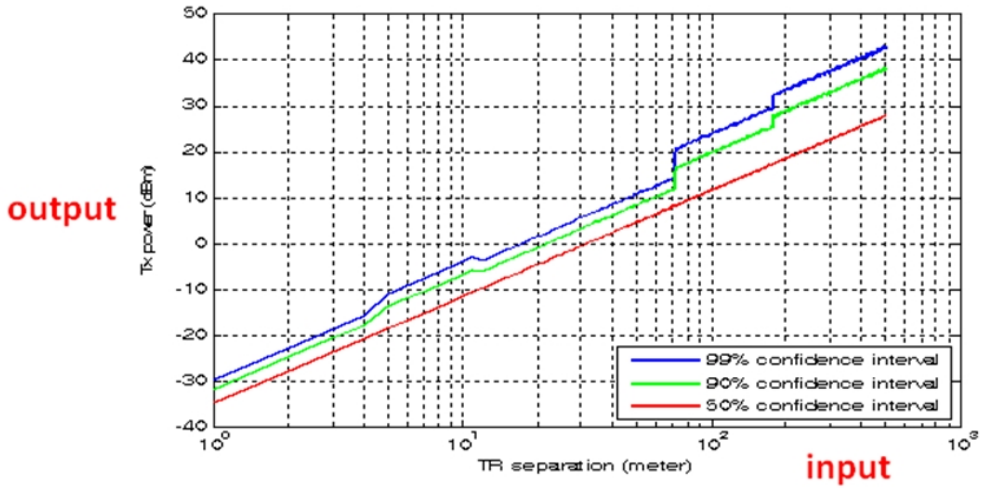

Figure 5.6. Range to Power mapping based on empirical channel model in [54]

transmission probability based on formula:

$$p(t) = \left\{ \begin{array}{l} 1 - \exp(-\alpha \times |\widetilde{e}(t) - T|^k) \text{ if } \widetilde{e}(t) \geq T \\ 0 \text{ otherwise} \end{array} \right\}$$

where T is the error threshold (e.g., T=0.2 meter), α is the error sensitivity that decides how sensitive a HV responds when the suspected tracking error violates the threshold T (e.g., α=10), and k is error exponent (e.g., k=2) for the magnitude of threshold violation.

As explained in Section 4.2, the design rationale of this transmission probability formula is that, when the suspected tracking error $\widetilde{e}(t)$ is below a pre-defined threshold T, a HV does not broadcast any state information at all and leaves the channel to be used by other HVs with larger suspected tracking error. When the suspected tracking error $\widetilde{e}(t)$ violates this threshold, the larger the magnitude of violation results in a higher transmission probability. Since not all HVs have the same suspected tracking error, they will use different levels of transmission probabilities to broadcast self-state information. This design thus alleviates the synchronized collisions when multiple HVs find their suspected tracking errors violating the threshold at the same time. As for the safety message, HV's state information will be put into the *Variable* field in WSM format as indicated in Figure 5.3.

Power Assignment Functional Blocks

6) **Function:** Calculate Channel Utilization (Cal_Ch_Utl). **Member of:** Power Assignment Functional (see Figure 5.4). This functional block calculates the channel utilization metric. The calculation of channel utilization is based on Clear Channel Assessment (CCA) which is an indicator function provided by the IEEE 802.11 protocol stacks [71]. This CCA reports 1 when the channel is sensed busy (i.e., the reception power level is above a threshold) and it reports 0 when the channel is sensed idle (i.e., the reception power level is below a threshold). Our channel utilization metric is essentially a time-average of CCA for a

Table 5.1. Overall Mapping from Channel Utilization to Tx Power

HV's Sensed Channel Utilization	Tx Power to be Used
$> 77.4\%$	10 dBm
74.2% to 77.4%	11 dBm
71.0% to 74.2%	12 dBm
67.8% to 71.0%	13 dBm
64.6% to 67.8%	14 dBm
61.4% to 64.6%	15 dBm
58.2% to 61.4%	16 dBm
55.0% to 58.2%	17 dBm
51.2% to 55.0%	18 dBm
47.2% to 51.4%	19 dBm
$< 47.2\%$	20 dBm

pre-defined interval. More precisely, the calculation of channel utilization is given in below formulas:

$$u(t) = \frac{1}{\sigma} \int_{t-\sigma}^{t} CCA(s)ds$$

where σ is the length of the evaluation interval, $CCA(s)$ is the clear channel assessment provided by 802.11 MAC/PHY layers. We use σ as 1 second in the implementation. This $u(t)$ is then smoothened by an AR-1 model below to further filter out temporal noise or disturbance in this measurement:

$$U(t) = \lambda \times u(t) + (1 - \lambda) \times U(t - \sigma)$$

where λ is the weight factor (e.g., $\lambda = 0.9$), $U(t)$ is the channel utilization metric that will be used by the next functional block to decide the transmission range.

7) **Function:** Calculate Transmission Range (Cal_Tx_Range). **Member of:** Power Assignment Functional (see Figure 5.4). This functional block decides the targeted transmission range based on the channel utilization $U(t)$ from the **Cal_Ch_Utl** functional block. The mapping from $U(t)$ to targeted transmission range $d(t)$ is based on below formula:

$$d(t) = \left\{ \begin{array}{l} d_{max} \text{ if } U(t) \leq U_{max} \\ d_{min} \text{ if } U(t) \geq U_{max} \\ d_{min} + \frac{U_{max} - U(t)}{U_{max} - U_{min}} \times (d_{max} - d_{min}) \text{ otherwise} \end{array} \right\}$$

where d_{max} is the maximum transmission range (e.g., $d_{max} = 250$ meters), d_{min} is the minimum transmission range (e.g., $d_{min} = 50$ meters), U_{min} is the lower threshold below which we consider the channel to be under-utilized (e.g., $U_{min} = 0.4$), U_{max} is the higher threshold above which we consider the channel to be congested (e.g., U_{max}=0.8). The choice of U_{min} and U_{max} and associated analysis can be found in [80,83].

8) **Function:** Range to Power Mapping (Range_2_Power mapping). **Member of:** Power Assignment Functional (see Figure 5.4). This functional block decides transmission power

1	1	1	1	1	4	2	Variable
WSM Version	Security Type	Channel Number	Data Rate	TxPwr_ Level	Provider Service Identifier	WSM Length	WSM Data

Figure 5.7. WSM format and where Tx power level will be specified

level based on targeted transmission range $d(t)$ from the **Cal_Tx_Range** functional block. The mapping used in this functional block is based on the empirical DSRC channel propagation model reported in [54]. This mapping (shown in Figure 5.6) is calculated for a single transmitter to have enough power level to successfully reach a distant receiver with indicated reception probability (by assuming -95 dBm receiver sensitivity).

For example, the 50% reception probability curve roughly maps 50 to 250 meters distance to required transmission power 10 to 20 dBm. We use this mapping in our prototype implementation. Note that, the choice of which reception probability curve does not guarantee the reception of receiver since the channel propagation model in [54] does not consider the effect of interference and channel collisions from multiple transmitting terminals. The overall mapping from sensed channel utilization to required transmission power level (based on 50% reception probability) is listed in Table 5.1.

9) **Function:** Power Assignment. **Member of:** Power Assignment Functional (see Figure 5.4). This functional block assigns transmission power level to the out-going message generated by the **Message Generator** functional block. Based on the derived transmission power from the **Range_2_Power mapping** functional block, this functional block writes the transmission power into the TxPwr_Level field in WSM format, which is highlighted in Figure 5.7. The indicated power level in WSM will then be used by 802.11p PHY layer to transmit this message. After this power assignment, the message will be placed in the queue of 802.11p MAC layer waiting to be broadcast over the air.

5.2 Protocol Evaluations for Outdoor Vehicle Mobility and Scalability

Our work presented in this section is the first to implement and successfully evaluate an adaptive communication design that shows great promise for a large-scale deployment of V2V cooperative safety systems [84]. This paper complements our previous simulation study in [77] by presenting an evaluation of practical and real-world implementation of the proposed V2V transmission control protocol in [77]. Subsection 5.2.1 presents our in-lab evaluation. Subsection 5.2.2 contains results from a simple outdoor test scenario with two radios and vehicle mobility. In Subsection 5.2.3, the results from a test scenario with 15 radios are presented to validate the scalability of proposed V2V transmission control. Subsection 5.2.4 gives a short summary.

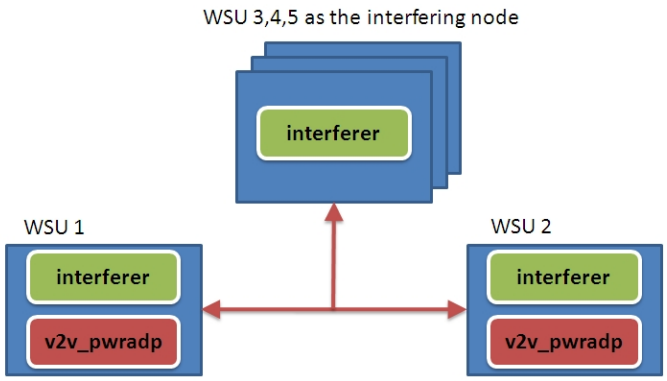

Figure 5.8. Test scenario with 2 dual-radio (#1,#2) and 3 single-radio (#3,#4,#5) WSUs. Each radio runs either *interferer* or our *v2v_pwradp* program.

5.2.1 In-Lab Evaluation for Power Control

The transmission control described in Section 5.1 has been implemented as a testing program on Wireless Safety Units (WSUs) [81,82]. Since the rate control requires a HV's mobility to trigger the message generation, the in lab evaluation's focus is on power control while the rate control evaluation is described in Subsection 5.2.2 and Subsection 5.2.3.

Several test scenarios were evaluated to verify whether the channel utilization is a stable measure and implemented power control assigns power of out-going WSMs according to our design. In each scenario, there were usually one or more WSUs acting as interferers that sent excessive messages to simulate the presence of other WSUs. Due to space limit, only one example scenario is shown in Figure 5.2.1 where the green box **interferer** represents one program as the interferer and the red box **v2v_pwradp** represents our power control program.

In Figure 5.8, three single-radio WSUs and two dual-radio WSUs were used in this scenario and placed within 1 meter radius so that WSUs can sense each other's transmission. On each single-radio WSU, there was one **interferer** program; on each dual-radio WSU, there were one **interferer** program and one **v2v_pwradp** program running for each radio. The **v2v_pwradp** program adapted power every 1 second with 100 millisecond (ms) message sending interval. The **interferer** program used variable sending interval and 20 dBm transmission power. The PHY data rate was 6 Mbps for all radios and the message size was 300 Bytes. Figure 5.9 shows the channel utilization and Figure 5.10 shows the adapted transmission power. Note that, in this scenario, there are five WSUs (7 radios) contending for channel access and the resulting channel utilization during experiments still remains stable. Figure 5.11 shows the time-averaged transmission power used by **v2v_pwradp** and corresponding time-averaged channel utilization from all test scenarios.

In all our test scenarios, the transmission power used by **v2v_pwradp** program matches with our intended power mapping in Table 5.1.

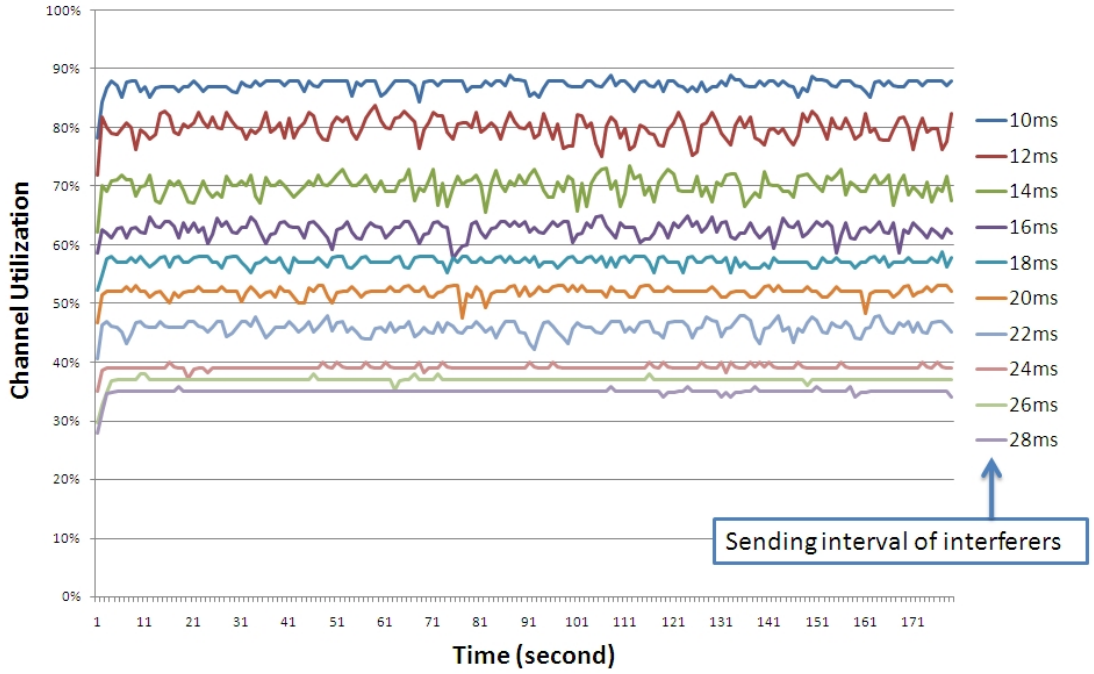

Figure 5.9. Channel utilization vs. time in the test scenario of Figure 5.8.

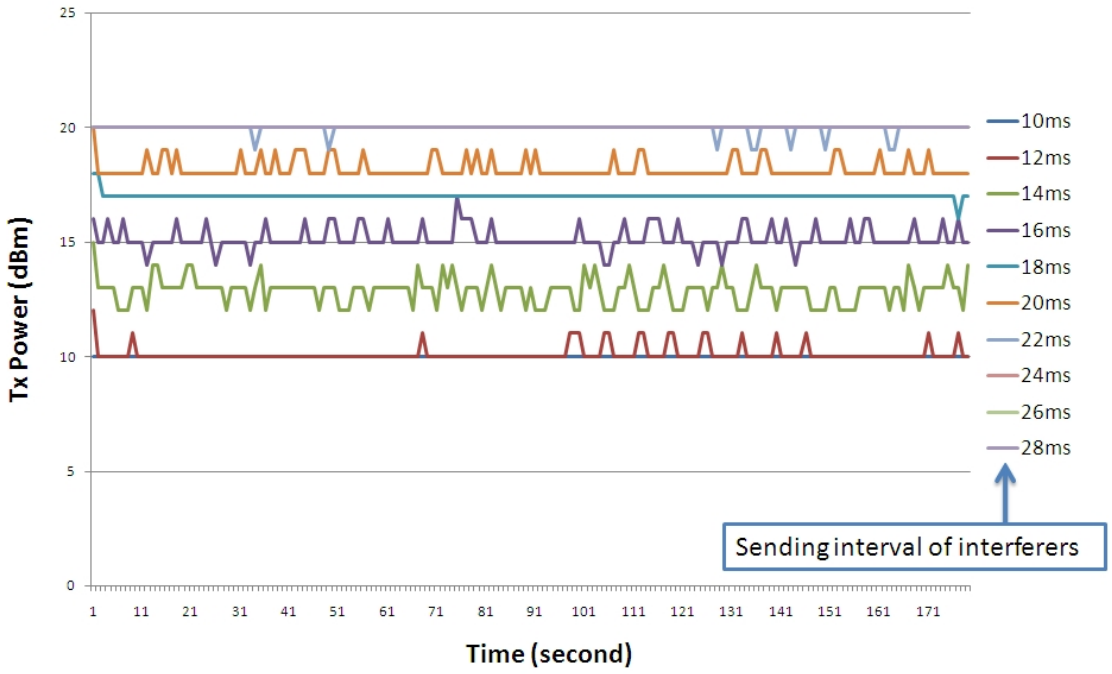

Figure 5.10. Adaptive transmission power vs. time corresponding to Figure 5.9.

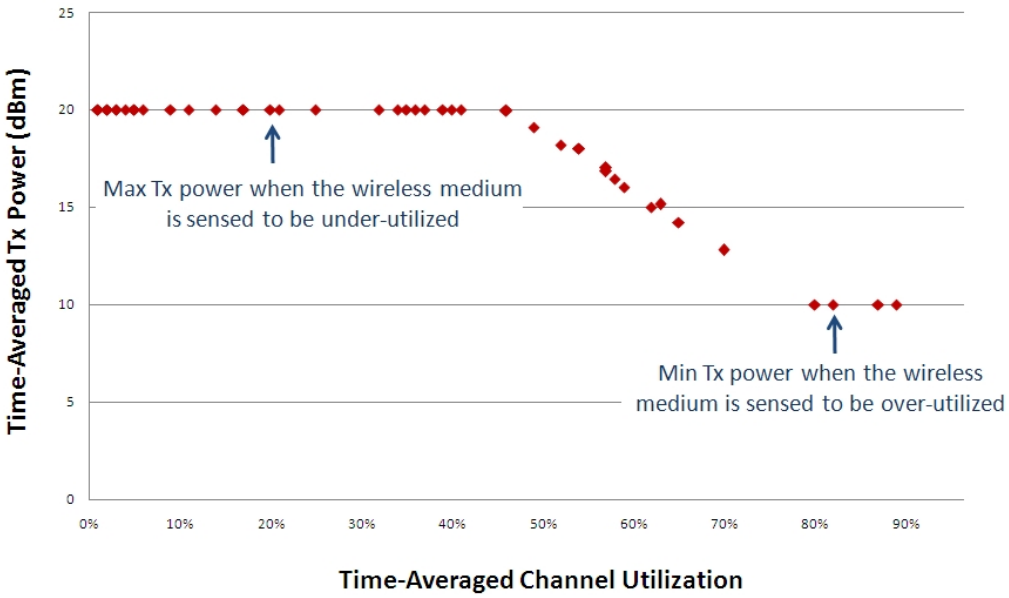

Figure 5.11. Channel utilization vs. power from different in-lab test scenarios.

5.2.2 Outdoor Mobility Tests and Results

The V2V transmission control protocol described in Section 5.1 has been implemented and integrated with General Motors (GM) V2V safety applications [79], which serve as the main testing platform in this subsection and Subsection 5.2.3 to understand how proposed V2V transmission control impacts these safety applications and how accurate the real-time tracking is. One additional protection was added to our rate control: when the latest transmission from a HV is more than 0.5 second ago, a message will be scheduled for transmission. Our scalability evaluation will be presented in Subsection 5.2.3. In this subsection, proposed transmission control is mainly evaluated with 2 radios and vehicle mobility. These outdoor mobility tests were conducted within the GM Technical Center and the test route is shown in Figure 5.12.

Each test run had two vehicles acting as the Leader and the Follower. Each vehicle had a single-radio WSU. These two vehicles tracked each other continuously during the test run. The safety message size was around 400 Bytes and the PHY rate was 6 Mbps for both radios [79]. Each vehicle recorded its own GPS position and each of the communicating RV GPS positions, every 100 millisecond (ms). The RV's *coasted* GPS position is then linearly interpolated to match with the exact time epochs of the HV's GPS time recordings. Every 100 milli-second, the actual tracking error is calculated as the Euclidean distance of the true GPS position of HV and the interpolated and coasting GPS position by the RV.

Two test runs were conducted. In the first test run, both the Leader and Follower vehicles used our proposed transmission control. In the second test run, both the Leader and Follower vehicles used the currently proposed 10 Hz beaconing of safety messages with 20 dBm transmission power. Two communication strategies are also compared.

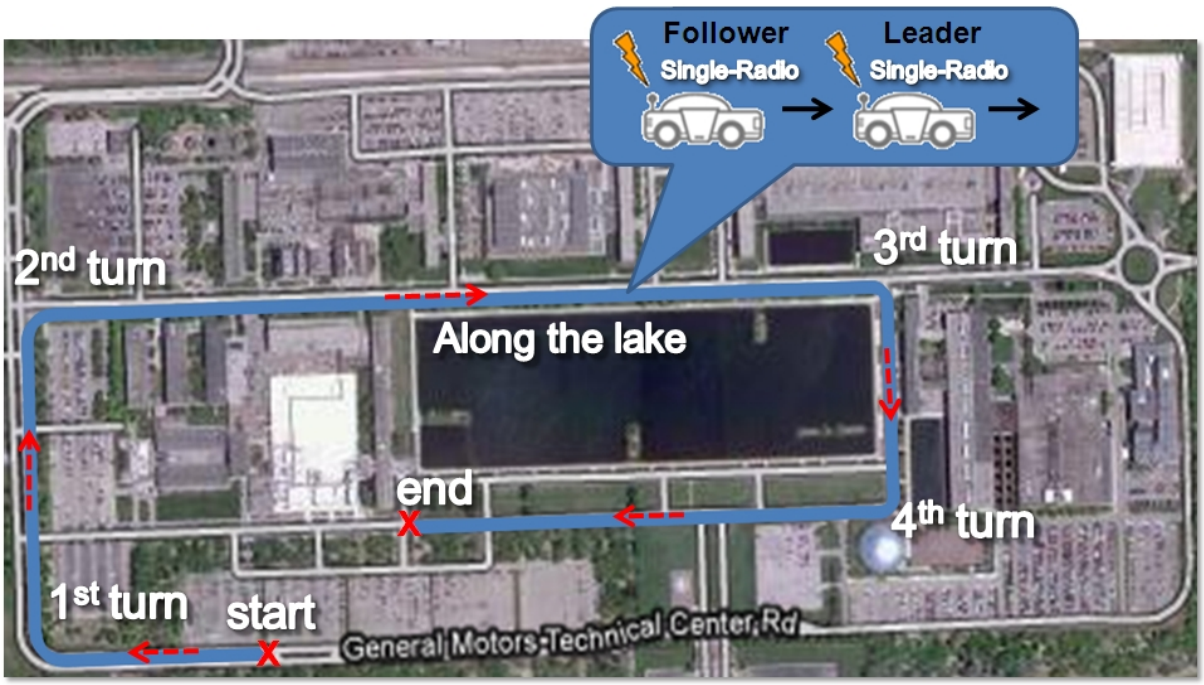

Figure 5.12. Outdoor mobility test route within the GM Technical Center. These four corners of the route can be clearly identified in the mobility profiles Figure 5.13-5.14 and our test results in Figure 5.15-5.24.

A typical vehicle heading profile for the test run is shown in Figure 5.13 and a typical vehicle speed profile is shown in Figure 5.14. Those four turns in Figure 5.12 can be easily identified in Figure 5.13 when there is a 90 degree change of heading and a significant speed slow-down and then speed-up in Figure 5.14. Note that 360 degrees means 0 degree and thus there is no discrepancy happened at the 5^{th} and 14^{th} second in Figure 5.13. In Figure 5.14, the speed slow-down and then speed-up at the 174^{th} second is due to an pedestrian crossing.

Besides the tracking accuracy which is used as the main performance metric in our previous simulation study [11,20], the application level **Target Classification** (TC) of the GM V2V safety applications is also reported. This TC is a HV's lane level identification of a RV's position with respect to that HV's own position [79]. The more accurate this TC is, the better a HV can identify its relative position to that RV and the better safety applications can function accordingly.

Test Results for Proposed Transmission Control

We only show results for the Leader to track the Follower due to the space limit. First, the suspected tracking error by the Follower is shown in Figure 5.15. Note that this suspected tracking error is a HV's guess of the tracking error on the RV toward itself. This suspected error is higher when the HV made a turn since the heading/speed of a HV changed dramatically during a turn. When a HV made more unpredictable maneuvers (to the RV)

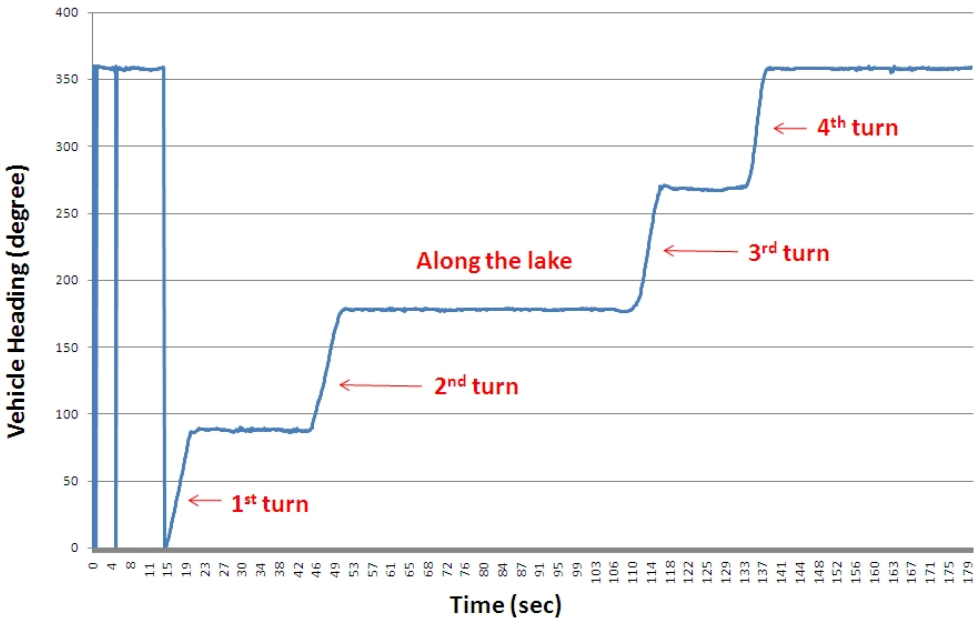

Figure 5.13. A typical vehicle heading profile in the mobility test route.

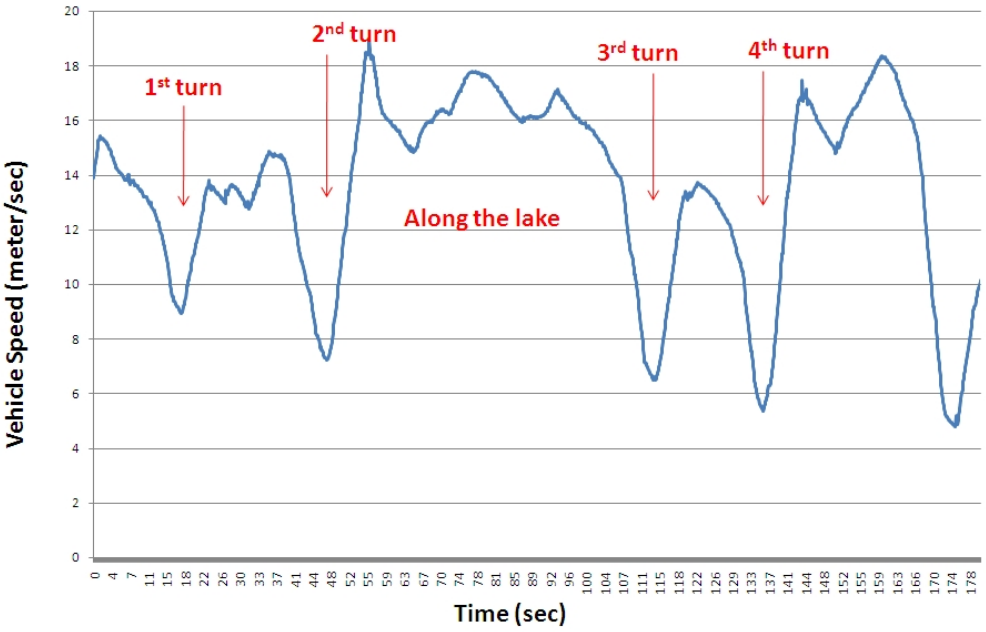

Figure 5.14. A typical vehicle speed profile in the mobility test route.

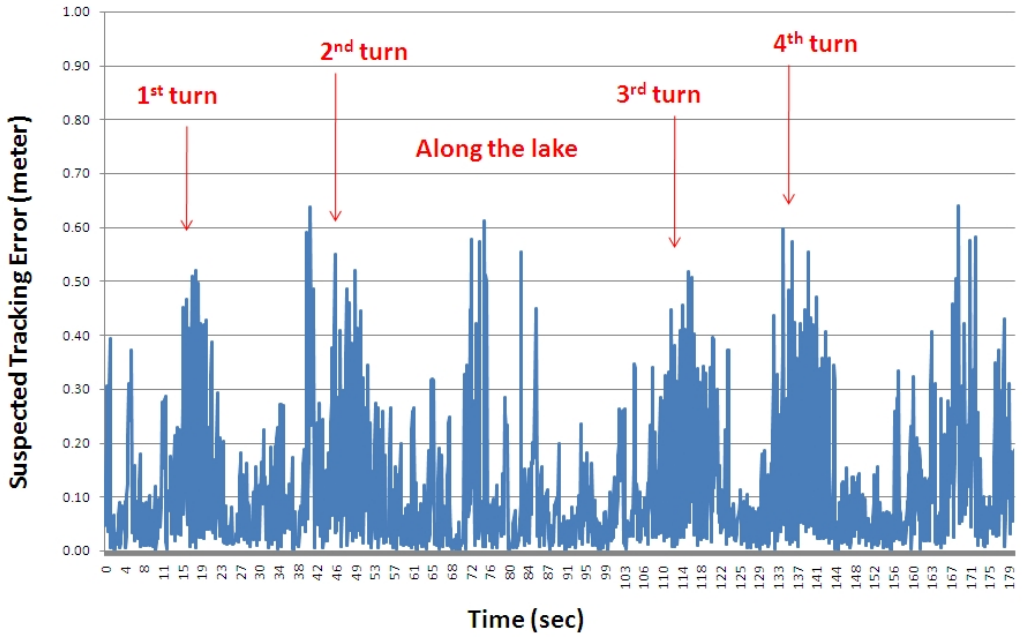

Figure 5.15. Suspected tracking error sensed by the Follower.

and created larger suspected tracking errors, more safety messages were broadcast in Figure 5.16. Based on our on-demand rate control described in Section 5.1, a higher transmission probability will be used by a HV when its suspected tracking error is larger.

The distribution of the time between transmission is in Figure 5.17 while the distribution of the time between messages arrival at the Leader is in Figure 5.18. Most messages were successfully received except for a small portion of them being erased (see the 900-ms bin in Figure 5.18). Figure 5.19 shows the 5-second windowed PER. Figure 5.20 shows the inter-vehicle distance and there is a period when two vehicles were separated by more than 70 meters (at the 73$^{\text{th}}$ second) and it matches with the higher PER period in Figure 5.19. Due to reduced number of transmitted messages from both vehicles, the channel utilization in Figure 5.21 is mostly below 1%.

The actual tracking error on the Leader is shown in Figure 5.22, which has a similar trend as that of the suspected error by the Follower in Figure 5.15. Although the suspected tracking error does not match exactly with the true tracking error, it gives the HV a rough estimate of how large the tracking error is on the RV. This justifies the use of suspected tracking error for a HV to adapt its transmission rate. This on-demand style rate control on two vehicles collaboratively reduces the total amount of messages over the air and mitigates channel congestion. The Lat offset of two vehicles perceived by the Leader is shown in Figure 5.23. Finally, the TC correctness in Figure 5.24 is almost 100% which is similar to the performance of the 10 Hz periodic communication (see Table 5.2).

These results confirm that proposed V2V transmission control works according to our intended design, especially the rate control part. Finally, the results for the Follower to track

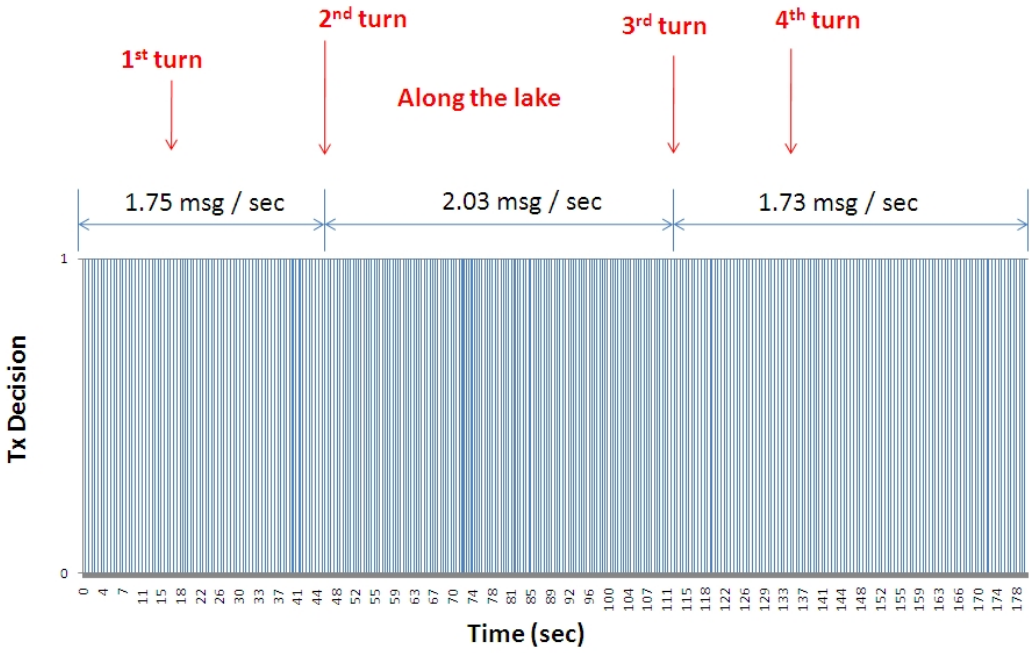

Figure 5.16. Message transmission decision made by the Follower.

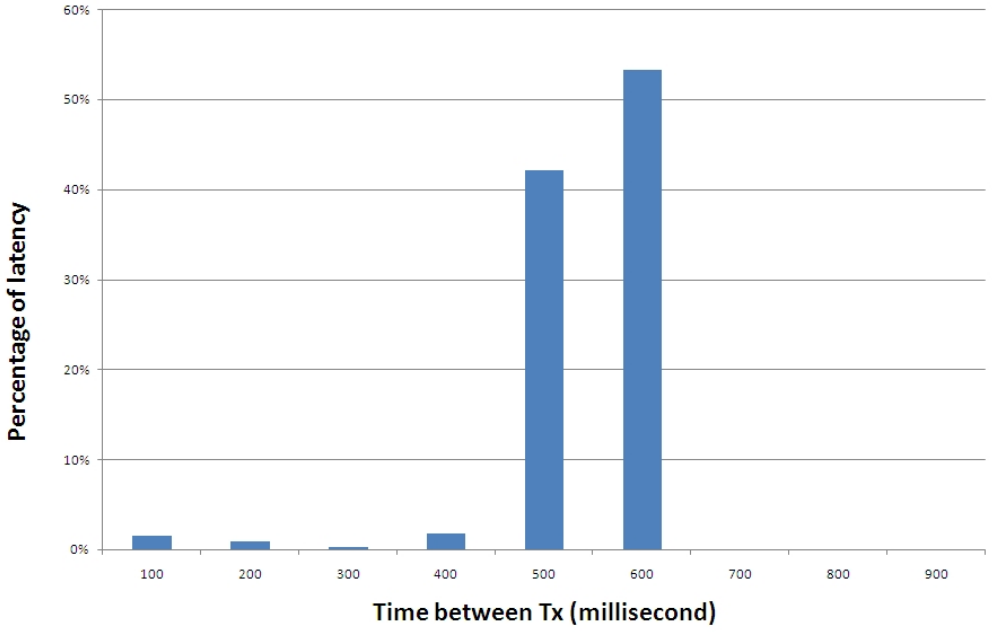

Figure 5.17. Distribution of time between transmission by the Follower.

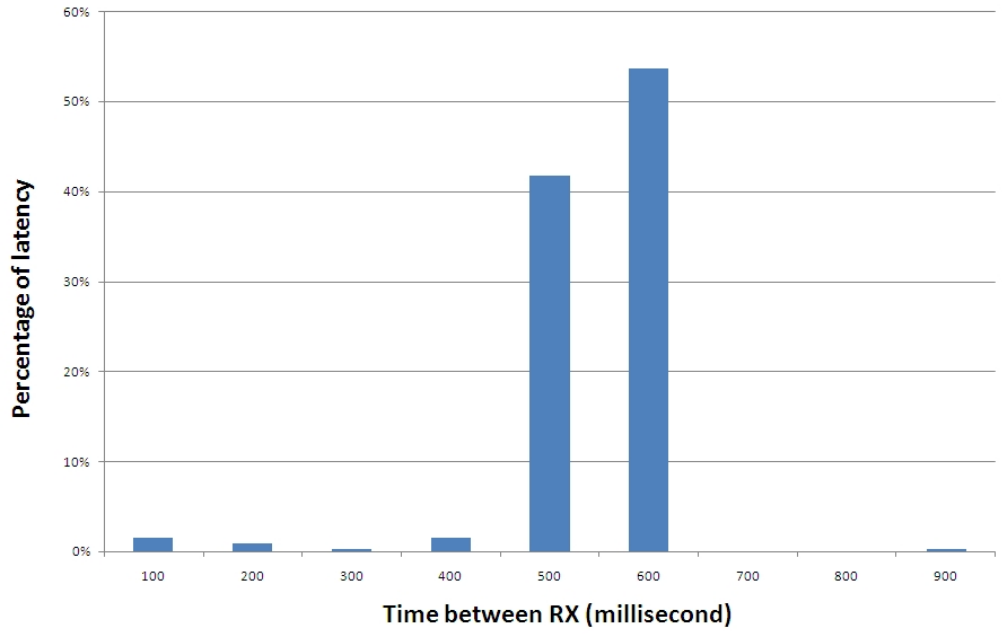

Figure 5.18. Distribution of time between message arrivals at the Leader.

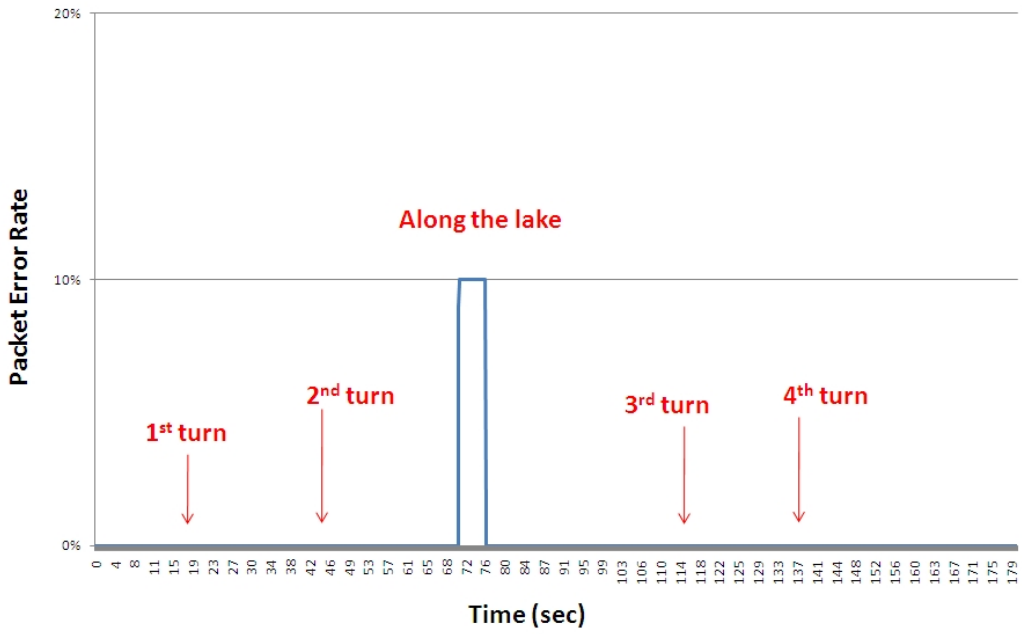

Figure 5.19. 5-Second windowed PER sensed by the Follower.

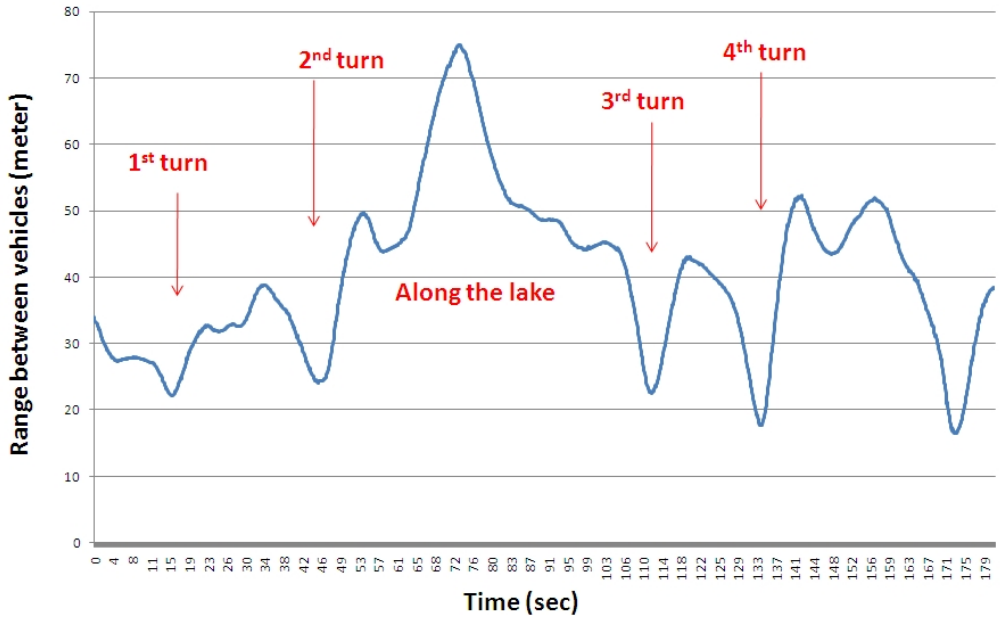

Figure 5.20. Inter-vehicle distance sensed by the Leader.

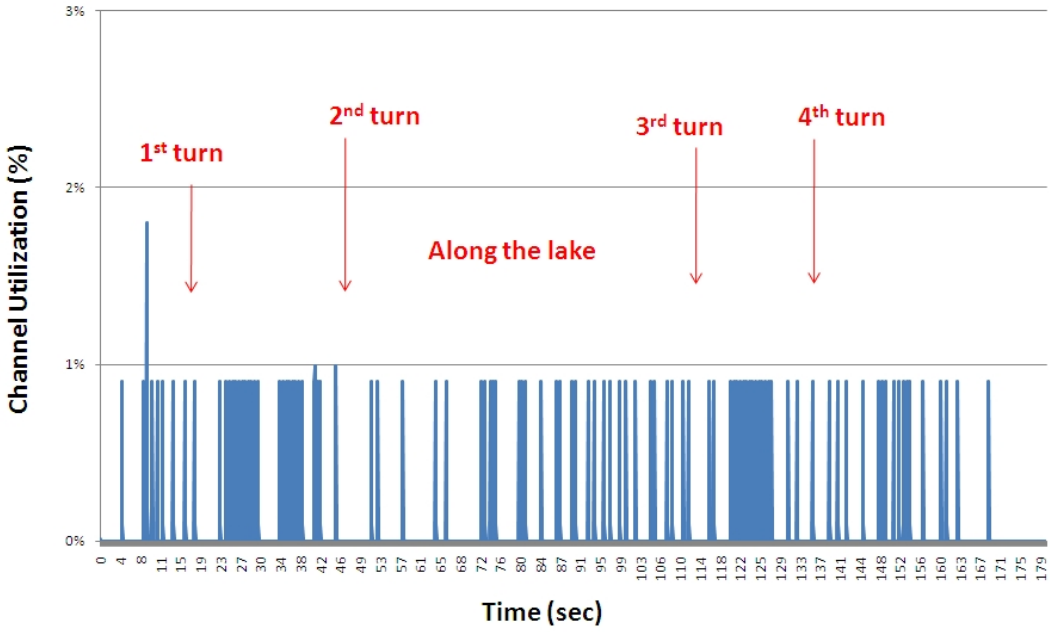

Figure 5.21. Channel utilization sensed by the Follower.

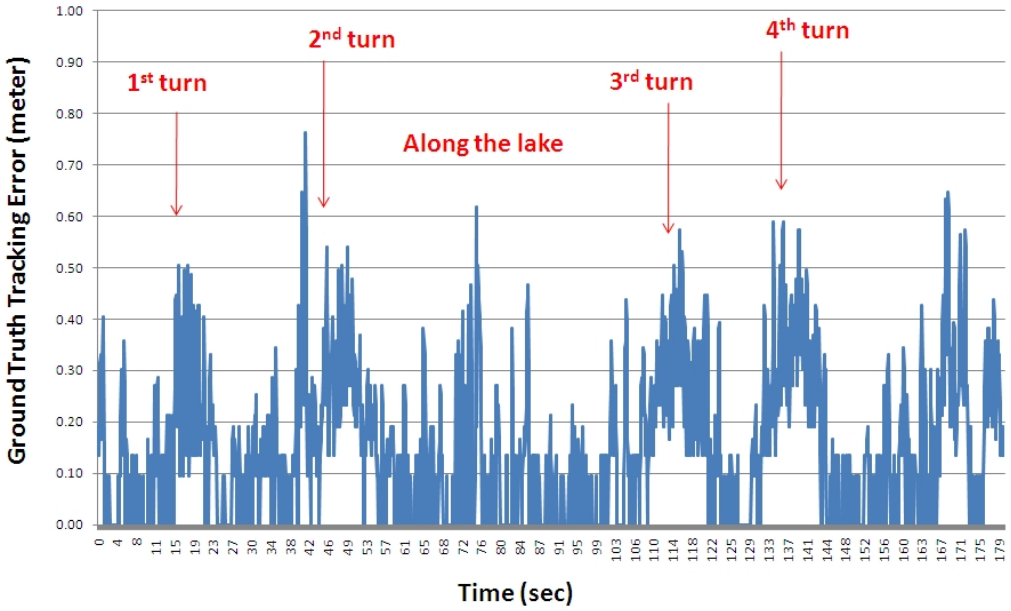

Figure 5.22. Actual Tracking Error of the Leader toward the Follower.

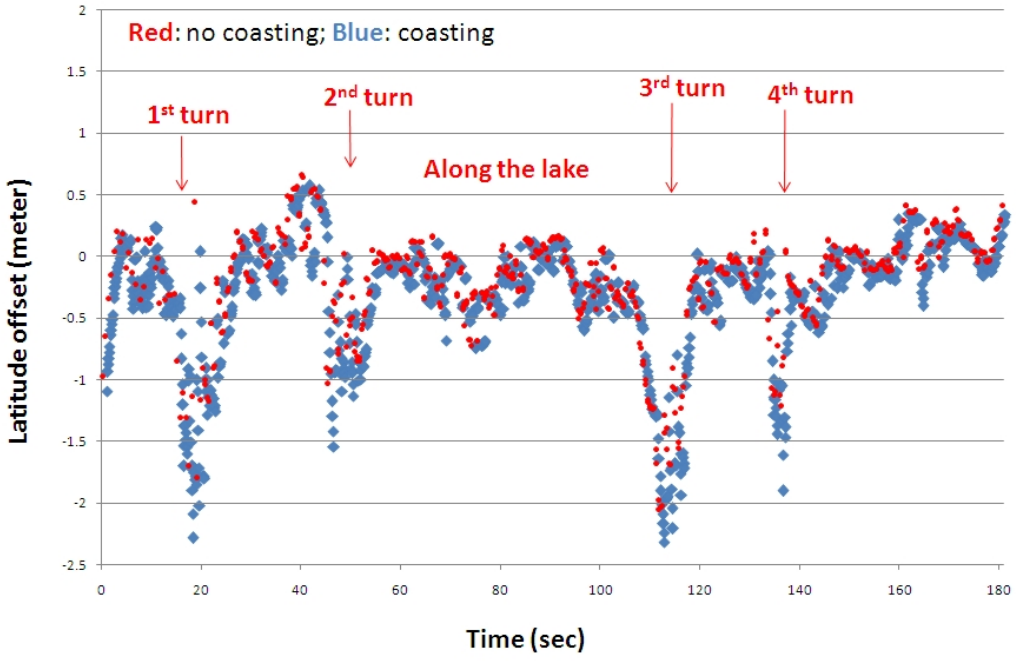

Figure 5.23. Lat offset between two vehicles sensed by the Leader.

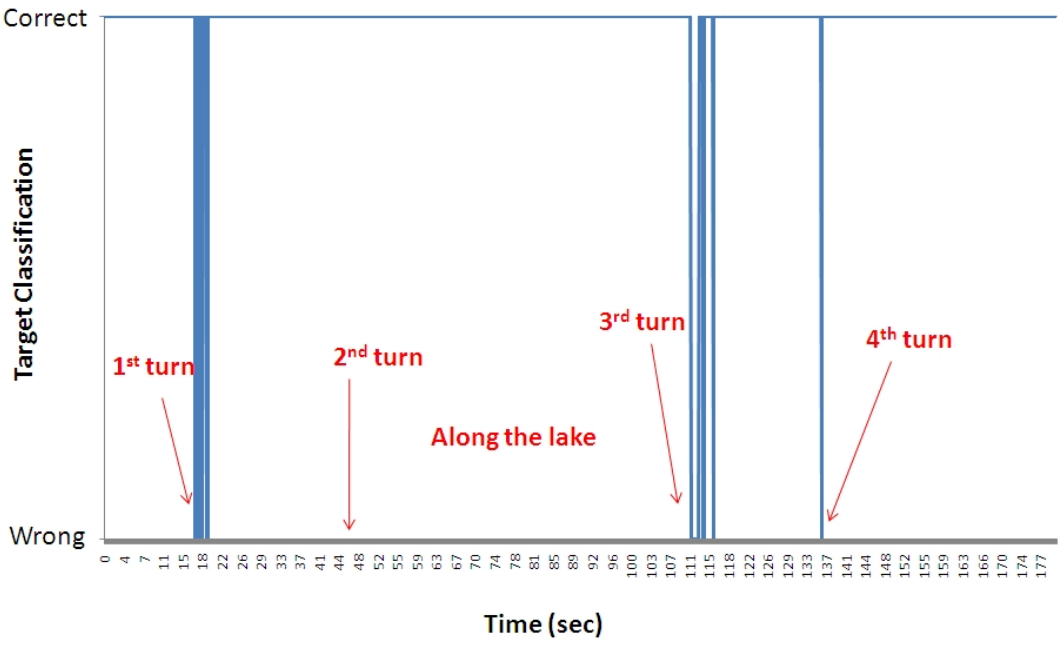

Figure 5.24. TC correctness of the Leader toward the Follower.

the Leader are similar to the case that the Leader tracked the Follower (see Table 5.2 and 5.3), which shows that the tracking performance is symmetrical for both vehicles.

Comparison of Two Communication Strategies

Two communication strategies for V2V safety messages are compared side by side in Table 5.2 and Table 5.3. Table 5.2 summarizes the results for the Leader being tracked by the Follower. First, the 10 Hz communication design always used 10 messages per second and 20 dBm transmission power. Our proposed design used around 2 messages per second and 20 dBm transmission power (since the channel utilization is below 1%). The tracking accuracy is compared based on 95% cut-off error [77,78], which means that, 95% of the time during the test run, the actual tracking error is below this number. For the 10 Hz communication design, its 95% cut-off error is 0.09 meter while that of our transmission control is 0.43 meter. The lane level identification (i.e., TC) for 10 Hz communication design was 99.4% correct while that of our transmission control was 99.1% correct. It means that our design can achieve similar performance in the safety application level as that of 10 Hz communication design with an 80% reduction of communication rate.

Table 5.3 summarizes similar results for the Leader being tracked by the Follower. Comparing the statistics in Table 5.2 and Table 5.3, both communication designs have symmetrical tracking performance for the Leader and the Follower. Note that this test scenario only has two radios and thus it is only used to check whether proposed transmission control works according to our intended design. In such a simple scenario, both communication designs

Table 5.2. Outdoor Mobility Test: Follower Tracked Leader

Parameters	10 Hz Comm. Design	Proposed Tx Control
Tx Message Rate	10 msg/sec	1.87 msg/sec
Tx Power	20 dBm	20 dBm
Channel Utilization	$< 2\%$	$< 1\%$
PER	$< 2\%$	$< 10\%$
95% Cut-Off Error	0.09 meter	0.43 meter
TC Correctness	99.4%	99.1%

Table 5.3. Outdoor Mobility Test: Leader Tracked Follower

Parameters	10 Hz Comm. Design	Proposed Tx Control
Tx Message Rate	10 msg/sec	1.85 msg/sec
Tx Power	20 dBm	20 dBm
Channel Utilization	$< 2\%$	$< 1\%$
PER	$< 2\%$	$< 10\%$
95% Cut-Off Error	0.11 meter	0.45 meter
TC Correctness	99.3%	98.2%

can achieve decent tracking and thus results in Table 5.2 and Table 5.3 do not indicate the scalability of 10 Hz communication design.

5.2.3 Outdoor Scalability Tests and Results

In this subsection, proposed transmission control were evaluated with 15 radios and our design is shown to outperform the currently proposed 10 Hz beaconing with 20 dBm transmission power. These scalability tests were conducted within a parking lot in the GM Technical Center. This small parking lot has a square size of roughly 100 meters by 80 meters and the test route is illustrated in Figure 5.25.

There were four stationary WSUs in the parking lot: three WSUs with dual radios and one WSU with single radio. Each test run had two vehicles acting as the Leader and the Follower. Each vehicle had two dual-radio WSUs; that is, there were 4 radios on each vehicle. Each dual-radio WSU ran two copies of tested communication protocol so that a dual-radio WSU acted like two single-radio WSUs. These two vehicles tracked each other continuously while they were circling around this parking lot for 5 minutes. During these test runs, the message size was around 400 Bytes and the PHY rate was 6 Mbps for all radios [79]. For each 100 ms, the actual tracking error is calculated as that in Subsection 5.2.2.

This test route in Figure 5.25 was more challenging than the test route in Subsection 5.2.2 (see Figure 5.12) in following the two aspects: 1) there were more radios trying to share the wireless channel and thus potentially creating more channel collisions and a higher PER, and 2) there were more turns since vehicles were circling around this small parking lot. From the evaluation in Subsection 5.2.2 (e.g., see Figure 5.13, Figure 5.14, Figure 5.22),

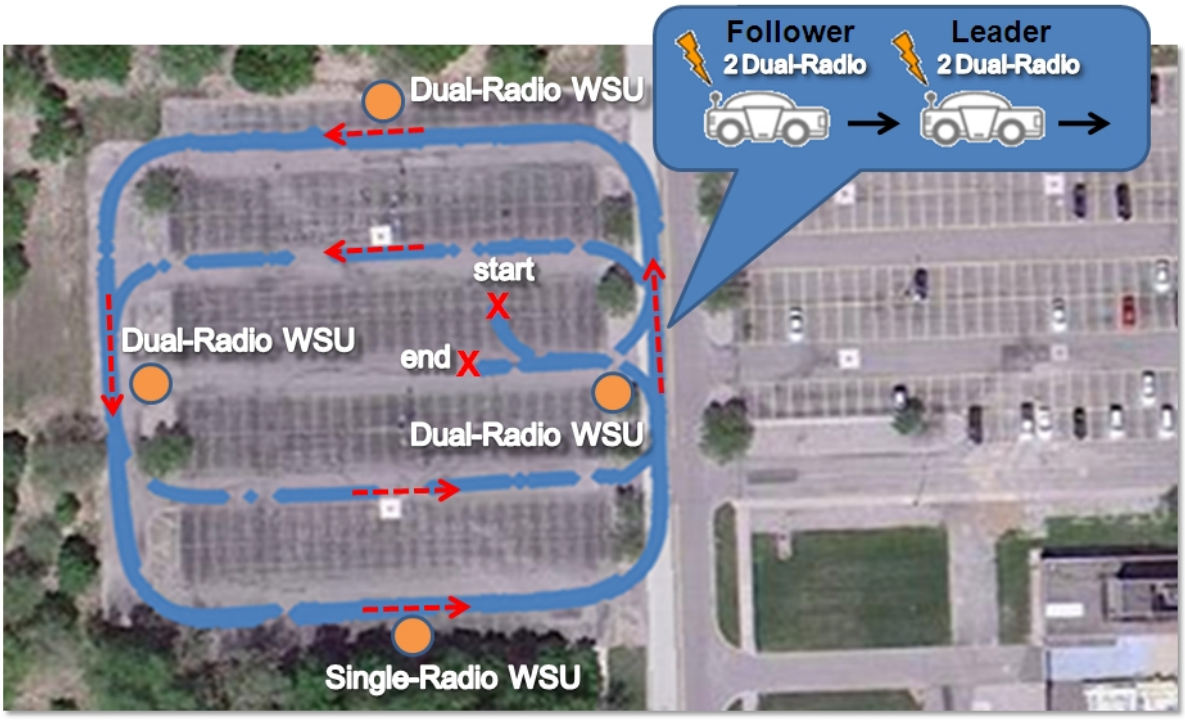

Figure 5.25. Outdoor scalability test route in a parking lot of the GM Technical Center. This test route featured more wireless radios (thus more collisions and interference) than the test route in Figure 5.12.

one can observe that a HV changes its speed and heading quickly during a turn and thus it is harder for a RV to track this HV properly if there are messages lost during a turn.

Two test runs were conducted. In the first run, all 15 radios used our proposed transmission control. In the second run, all 15 radios used 100-ms periodic beaconing of safety messages with 20 dBm transmission power. The second run serves as the baseline scenario. Both the Leader and the Follower vehicles tracked each other continuously during these test runs. Two communication strategies are compared side by side in Table 5.4 and Table 5.5.

Table 5.4 summarizes the results for the Leader being tracked by the Follower. First, the 10 Hz communication always used 10 messages per second and 20 dBm transmission power. Our proposed design used around 2 messages per second and 20 dBm transmission power (since the channel utilization is around 1% to 3%). For the 10 Hz communication design, its 95% cut-off error was 2.41 meter while that of our design was 0.36 meter. The lane level identification (i.e., TC) for 10 Hz communication design was 87.4% correct while that of our design was 99.7% correct, which means proposed transmission control can achieve much better tracking performance than that of 10 Hz communication design.

Table 5.5 summarizes the results for the Follower being tracked by the Leader. Comparing the statistics in Table5.4 and Table 5.5, both communication designs have roughly symmetrical tracking performance for the Leader and the Follower. However, the tracking accuracy and lane level identification of 10 Hz communication design were very poor

Table 5.4. Outdoor Scalability Test: Follower Tracked Leader

Parameters	10 Hz Comm. Design	Proposed Tx Control
Tx Message Rate	10 msg/sec	1.83 msg/sec
Tx Power	20 dBm	20 dBm
Channel Utilization	8% to 10%	1% to 3%
PER	10% to 30%	$< 5\%$
95% Cut-Off Error	2.41 meters	0.36 meter
TC Correctness	87.4%	99.7%

Table 5.5. Outdoor Scalability Test: Leader Tracked Follower

Parameters	10 Hz Comm. Design	Proposed Tx Control
Tx Message Rate	10 msg/sec	1.82 msg/sec
Tx Power	20 dBm	20 dBm
Channel Utilization	8% to 10%	1% to 3%
PER	10% to 30%	$< 5\%$
95% Cut-Off Error	3.39 meters	0.32 meter
TC Correctness	70.2%	100%

compared with those of our transmission control protocol. Upon closer inspection of the tracking error of the 10 Hz communication, large tracking errors usually happened when the HV made a turn but the RV did not get the message from that HV (due to consecutive channel collisions) and assumed that HV was still going straight ahead.

The main reason behind this huge performance difference in Table 5.4 and Table 5.5 is that the 10 Hz communication design produced too many messages by all 15 radios and thus resulted in a higher channel PER. Our transmission control uses an on-demand rate control: a HV uses a higher transmission probability to send out messages if it suspects that RVs have large tracking error toward its own position. Otherwise, a HV tends to stay quiet and lets other vehicles use the channel. This *statistical multiplexing* allows all vehicles to reduce the total message amount and improves the overall efficiency of information exchange. The results in Table 5.4 and Table 5.5 also indicate the scalability of our proposed transmission control over the 10 Hz communication design for a large-scale deployment of V2V cooperative safety systems.

5.2.4 Short Summary

Although previous implementations of V2V safety communications that use 10 Hz periodic broadcast of safety messages with 20 dBm transmission power have been used in small-scale V2V safety application demonstrations, numerous studies have shown that such a naive policy will not be scalable for a large-scale deployment. This paper focuses on the implementation and testing of our proposed transmission control protocol which adapts the

message rate and transmission power based on a closed-loop control concept that accounts for channel unreliability and congestion.

The evaluations presented show that our design works well in practice and is a promising solution to address the scalability of V2V safety communications. Note that proposed design is meant to provide a scalable communication control for the frequently exchanged basic safety messages (BSMs). For event-driven messages of different priorities, they can still be broadcast with different pairs of specified transmission rate and power. Our future work includes large-scale trials of proposed transmission control and its parameter optimization. Proposed design can also be enriched with additional rules, e.g., incorporating traffic engineering intuitions to make it more intelligent and robust in different traffic scenarios.

5.3 Updated Performance Metrics and Simulation Results

In this section, we present our updated performance metrics and identified challenging traffic scenarios in Subsection 5.3.1, and updated simulation results for these challenging scenarios in Subsection 5.3.2 and Subsection 5.3.3. The performance of our proposed design is again compared with the currently proposed 100-millisecond, 20-dBm beaconing. Subsection 5.3.4 gives a short summary.

5.3.1 Updated Performance Metrics and Identified Key Traffic Scenarios

Our new or improved performance metrics are the following two:

- The 95% percentile tracking error: We already have this performance metric processed for each distance bin (e.g., every 30 meters, layered around a host vehicle HV) [66,77]. Our proposed description to this metric is to record only the error for RVs that a HV is tracking. If a RV has not been heard by a HV for more than a defined time-out interval (e.g., 5 seconds), this remote vehicle will not be tracked bv this HV and be considered in this performance metric. An illustration of this performance metric is shown in Figure 4.2.
- The percentage of tracked RVs by a HV over all RVs in each distance. This gives a statistical sense of the likelihood for a RV to be tracked by a HV in each distance bin (e.g., every 30 meters, layered around a host vehicle HV).

The reason why we need a second performance measure is to capture when (time to collision of HV) or how far away (distance to collision of HV) a new RV is first tracked by the HV. This is important for safety considerations since it decides if a HV has enough time to respond to potential hazardous situations due to this new RV. After a RV has

been tracked, the tracking accuracy will be captured by the first performance metric: 95% percentile error. For this purpose, there are three candidates (c1), (c2), (c3) considered for this second performance metric:

(c1) Percentage of tracked RVs over all RVs for each distance radius bin from a HV;

(c2) Distance from a HV (mean or 95% percentile) at which a new RV can be tracked by a HV;

(c3) Time-to-collision to a HV (mean or 95% percentile) at which a new RV will be tracked by a HV.

The equivalent sense can be established among those candidate metrics. Converting from (c2) to (c3) can easily done by introducing either the mean flow speed or the free flow speed (to get the worst case time-to-collision). Converting from (c1) to (c2) is easy as shown below. However, converting from (c2) or (c3) to (c1) is in general not possible since one number (either time or distance) that has been used to summarize the statistics. Conversion from candidate metric (c1) to (c2) can go through below steps:

1. Assumed tracked % of RVs at the x-th distance bin (i.e., metric (c1)): $\lambda_x, x = 1, 2, 3...$ where x is the bin index.
2. Probability of tracking a new RV in a certain distance bin, Pr(a new RV first tracked at bin x): $p_x = \lambda_x \prod_{y>x} \lambda_y$.
3. Mean distance to track a new RV (with $\bar{d}_x$ as the mean radius of the x-th bin): $m \equiv E[d] = \sum_x \bar{d}_x p_x$.
4. Variance (Standard Deviation) of the distance to track a new RV: $\sigma^2 \equiv Var[d] = \sum_x \bar{d}_x^2 p_x - (\sum_x \bar{d}_x p_x)^2$.
5. Assuming Gaussian distribution, the 95% percentile of the distance to track a new RV (i.e., metric (c2)): $m - 1.645 \times \sigma$.

Examples of above calculation can be found in Subsection 5.3.2 and Subsection 5.3.3. Based on candidate metric (c2), (c1) can be converted to (c3) too. Therefore, as we demonstrate above, the candidate metric (c1) contains more information in the sense that candidate metrics (c2) and (c3) can be calculated based on it. Therefore, we recommend (c1) as the 2nd performance metric. However, we will still calculate candidate metrics (c2) and (c3) based on (c1) in Subsection 5.3.2 and Subsection 5.3.3.

There are two key traffic scenarios that are identified as challenging in our previous simulation work [63,64,77]. We describe them below with reasons why they are challenging:

- Typical medium speed flow highway: Medium speed flow (around 30 mph flow) is the most challenging case observed in our highway simulations. The 95% tracking error performance of proposed design for different traffic flow is summarized in Figure 5.26. The medium speed flow traffic scenario has enough vehicle density and enough higher vehicle dynamics to generate more messages transmission and results in higher channel

	mean speed	mean inter-car spacing	vehicle flow	95% tracking error
Low speed flow	14 mph	5.2 meter	960 veh/hr/lane	**1.19 meter**
Medium speed flow	30 mph	11.2 meter	1900 veh/hr/lane	**1.38 meter**
High speed flow	56 mph	20 meter	2220 veh/hr/lane	**1.27 meter**

Figure 5.26. Comparison of our proposed design's 95% cut-off tracking error for RVs within 150-meter radius in different simulated 8-lane, bi-directional traffic flows.

congestion. Compared with medium speed flow traffic, the low speed flow (around 14 mph) has a lot of vehicles but they all move very slowly and thus can be easily tracked in real-time. High speed flow (around 56 mph or above) has few vehicles and thus the channel does not enter congestion, which make real-time tracking easier than the medium speed flow case.

- Signalized intersection: Intersection case poses a challenge to real-time tracking due to the bursty transmission of all vehicles (e.g., sudden stop or move) coordinated by traffic light cycles [63,64]. These bursty messages might get collided over the air and do not reach intended neighboring vehicles. Besides, vehicles at intersection can make 90 degree turns (i.e., dramatic change of speed and heading during a turn) compared with the highway scenario where most of the vehicles are moving in the straight direction without dramatic turns.

These two traffic scenarios will be simulated and discussed based on proposed performance metrics in Subsection 5.3.2 and Subsection 5.3.3 respectively.

5.3.2 Medium Speed Flow Highway Scenario: Updated Simulation Results

We conducted network simulations by OPNET [75] on the most challenging highway traffic scenario identified: a 1-Km bidirectional highway with 8 lanes of identical traffic flows (4 lanes in each direction). The trajectory is generated by SHIFT highway simulator [74]. The traffic flows have an average speed of 30 mph. We run proposed algorithm in this traffic scenario and then evaluate two proposed performance metrics. To avoid boundary effect, we only process the statistics for vehicles between 200 meters to 800 meters on this 1-Km highway.

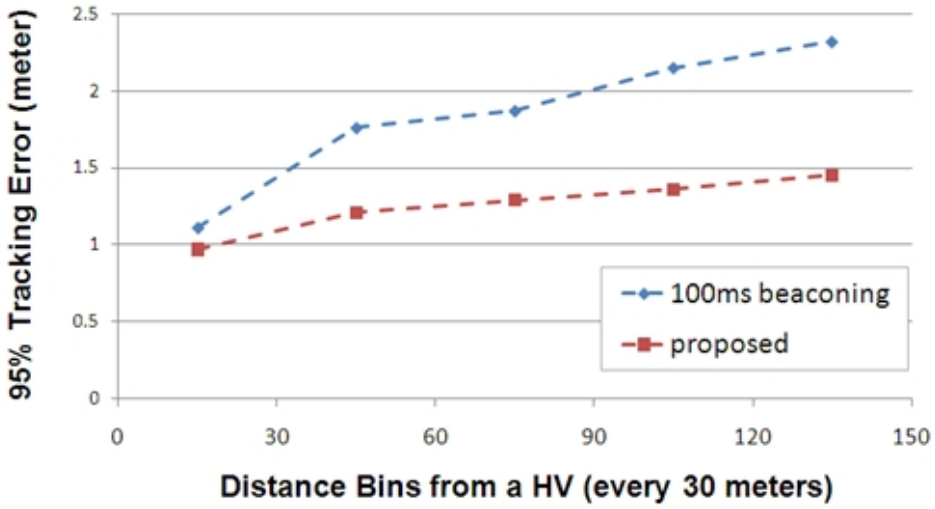

Figure 5.27. Simulation results for performance metric 1: 95% percentile of tracking error in each distance bin (i.e., every 30 meters radius).

Additional Guard Message

The vehicle data broadcast protocol has been enhanced with guard messages for the simulations in Subsection 5.3.4 and Subsection 5.3.5. A guard message will be transmitted when the latest *full-power* (e.g., 20 dBm) message is transmitted more than a defined *guard interval* (e.g., 1 second) ago. A message is considered *full-power* when its transmission power is more 90% of the device maximum power. This design is to ensure that the state information of a host vehicle can still reach farther remote vehicles every defined guard interval.

During our simulation experiments, when this guard message interval is less than 1 second, e.g., 0.5 second, it significantly increases the channel load. The main reason is because, for our proposed design, on average two messages are transmitted in highway scenarios. Therefore, when this guard message interval is 0.5 second or less, it equivalently imposes that almost all the safety messages would be transmitted by maximum power (and thus there is no power control at all). Therefore, in this subsection and Subsection 5.3.3, we use 1 second as the guard message interval in simulations.

Performance Comparison

The first performance metric is the 95% percentile of the real-time tracking error and it is shown in Figure 5.27. This number is reported for each distance bin (every 30 meters in radius). For example, this 95% percentile indicates that, 95% of the time during simulation, the tracking error of a host vehicle for its neighboring vehicles within 0 to 30meter radius is around 1 meter for the proposed design. As it is shown for different distance bins, our

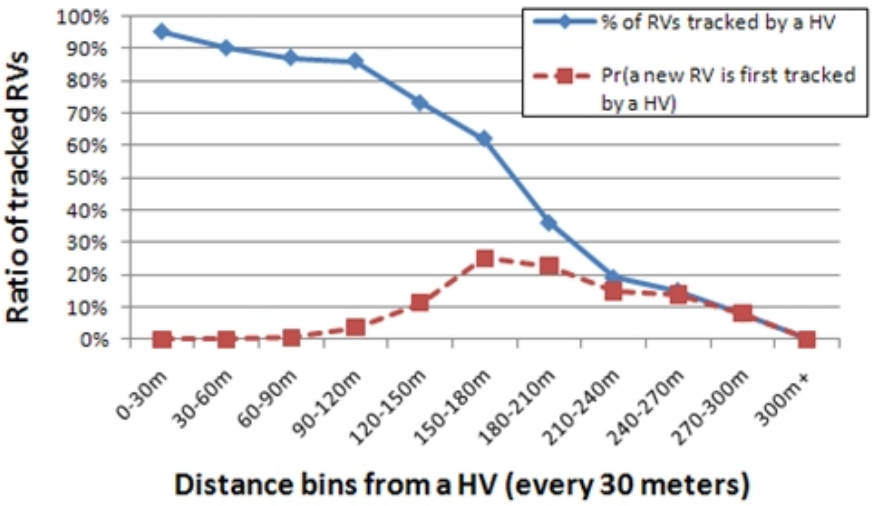

Figure 5.28. Simulation results for performance metric #2 for proposed design: Percentage of tracked RVs in each distance bin (i.e., every 30 meters radius).

proposed design can achieve better tracking accuracy than the 100-ms (millisecond), 20-dBm beaconing.

Second performance metric for proposed design is plotted as the blue curve in Figure 5.28. It shows the ratio of tracked RVs by a HV over all RVs in that distance bin (every 30 meters). The red curve is the calculated probability for a HV to track a new RV for the first time at the indicated distance bin. Based on it, additional information can be calculated as below:

1) **Distance for a new RV to be tracked by a HV by using proposed design**:

- Mean: 196.71 meters,
- Standard Deviation: 47.82 meters,
- 95% percentile bin: 120-150 meters (based on calculated probability),
- 95% percentile: 118.04 meters (assuming Gaussian distribution).

2) **Worst case time-to-collision to a HV by using proposed design** (based on above distance and free flow speed 60 mph):

- Mean: 7.34 seconds,
- 95% percentile: 4.40 seconds.

Note that 95% percentile for the distance means that statistically a HV can detect a new RV at this distance (or this distance bin) with 95% of the probability. In general, the longer

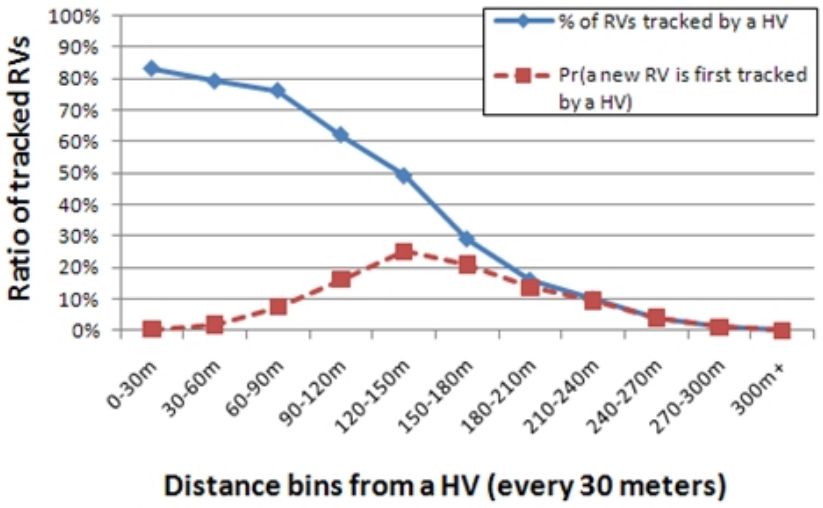

Figure 5.29. Simulation results for performance metric #2 for 100-ms beaconing: Percentage of tracked RVs in each distance bin (i.e., every 30 meters radius).

distance or the longer time-to-collision means a better design since it gives the HV a longer perception range and thus a longer response time to possible safety hazard.

Second performance metric for 100-ms beaconing is plotted as the blue curve in Figure 5.29. It shows the ratio of tracked RVs by a HV over all RVs in that distance bin (every 30 meters). The red curve is the calculated probability for a HV to track a new RV for the first time at the indicated distance bin. Based on it, additional information can be calculated as below:

1) **Distance for a new RV to be tracked by a HV by using 100-ms beaconing**:

- Mean: 152.62 meters,
- Standard Deviation: 50.77 meters,
- 95% percentile bin: 60-90 meters (based on calculated probability),
- 95% percentile: 69.11 meters (assuming Gaussian distribution).

2) **Worst case time-to-collision to a HV by using 100-ms beaconing** (based on above distance and free flow speed 60 mph):

- Mean: 5.69 seconds,
- 95% percentile: 2.58 seconds.

In both performance metrics, our proposed design shows superior performance over the 100-ms beaconing in this highway scenario. Our design provides a better tracking accuracy and a longer time or distance before a HV detects a new RV approaching.

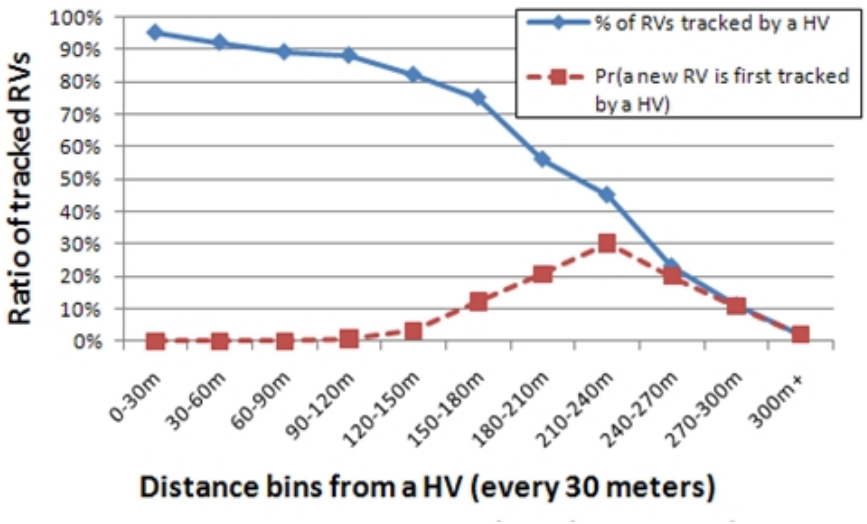

Figure 5.30. Simulation results for performance metric #2 for proposed design: Percentage of tracked RVs in each distance bin (i.e., every 30 meters radius).

5.3.3 Signalized Intersection Scenario: Updated Simulation Results

We conducted OPNET simulations [37] on the intersection traffic scenario identified: an intersection with four branches, 8 lanes in each direction, traffic speed limit 40 mph. The trajectory is generated by an intersection simulator, VITS [33] from Ohio State University. This intersection is coordinated by a traffic light with a 30-second light cycle. All the vehicles are queued when the traffic light is red while traffic in another direction is flowing. The maximum vehicle speed is 40 mph and vehicles are allowed to make turns at the intersection. The guard message mentioned in Subsection 5.3.2 is also used in simulations.

Performance Comparison

The first performance is the 95% percentile of tracking error for a HV tracked by RVs within 60-meter radius of the intersection when this HV is within 60-meter radius of the intersection. For the 100-ms, 20-dBm beaconing, this performance metric is 1.52 meter. For our proposed design, this performance metric is 0.86 meter, which is again better than the tracking accuracy of the 100-ms beaconing. Our proposed design generates on average 3.61 messages per second, which is a little higher than the message rate generated in the highway scenario (around 2 messages per second).

Second performance metric for proposed design is plotted as the blue curve in Figure 5.30. It shows the ratio of tracked RVs by a HV over all RVs in that distance bin (every 30 meters). The red curve is the calculated probability for a HV to track a new RV for the first time at the indicated distance bin. Based on it, additional information can be calculated as below:

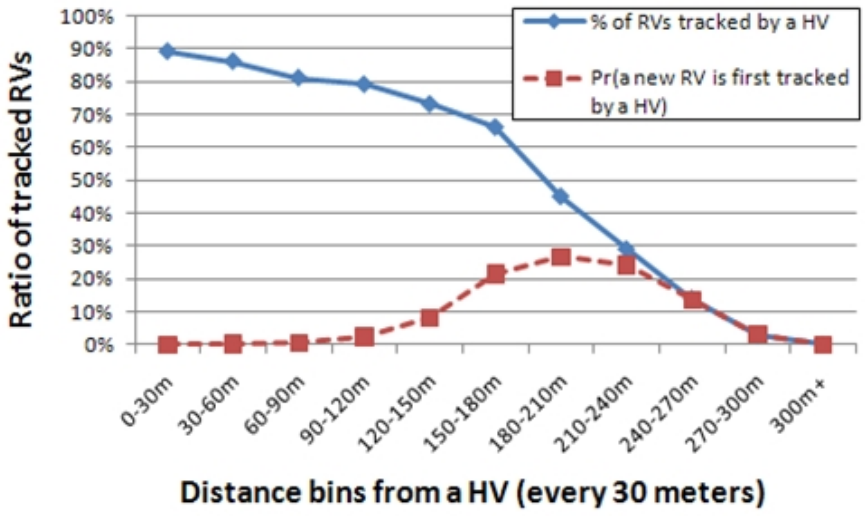

Figure 5.31. Simulation results for performance metric #2 for 100-ms beaconing: Percentage of tracked RVs in each distance bin (i.e., every 30 meters radius).

1) **Distance for a new RV to be tracked by a HV by using proposed design**:

- Mean: 221.56 meters,
- Standard Deviation: 40.96 meters,
- 95% percentile bin: 150-180 meters (based on calculated probability),
- 95% percentile: 154.18 meters (assuming Gaussian distribution).

2) **Worst case time-to-collision to a HV by using proposed design** (based on above distance and free flow speed 60 mph):

- Mean: 8.26 seconds,
- 95% percentile: 5.75 seconds.

Second performance metric for 100-ms beaconing is plotted as the blue curve in Figure 5.31. It shows the ratio of tracked RVs by a HV over all RVs in that distance bin (every 30 meters). The red curve is the calculated probability for a HV to track a new RV for the first time at the indicated distance bin. Based on it, additional information can be calculated as below:

1) **Distance for a new RV to be tracked by a HV by using 100-ms beaconing**:

- Mean: 198.88 meters,
- Standard Deviation: 41.38 meters,

- 95% percentile bin: 120-150 meters (based on calculated probability),
- 95% percentile: 130.81 meters (assuming Gaussian distribution).

2) **Worst case time-to-collision to a HV by using 100-ms beaconing** (based on above distance and free flow speed 60 mph):

- Mean: 7.42 seconds,
- 95% percentile: 4.88 seconds.

In both performance metrics, our proposed design shows superior performance over the 100-ms beaconing in this intersection scenario. Overall, our design provides a better tracking accuracy and a longer time or distance before a HV detects a new RV approaching.

5.3.4 Short Summary

In this subsection, we present our updated performance metrics, identified challenging traffic scenarios, and updated simulation results for these challenging scenarios. The reason why we need a second performance measure is to capture when (time to collision of HV) or how far away (distance to collision of HV) a new RV is first tracked by the HV. This is important for safety considerations since it decides if a HV has enough time to respond to potential hazardous situations due to this new RV. After a RV has been tracked, the tracking accuracy will be captured by the first performance metric: 95% percentile error. Two challenging traffic scenarios are identified and simulated. The performance of our proposed design is again compared with the 100-ms, 20-dBm beaconing. Overall, our design provides a better tracking accuracy and a longer time or distance before a host vehicle detects a new remote vehicle approaching.

Chapter 6

Concluding Remarks

The main contribution of this dissertation is to address the question of how to allow multiple dynamical systems to track each other in real-time over a shared and potentially unreliable channel. This dissertation covers a wide spectrum of results: from theories, engineering designs, computer simulations, to prototype implementation and real-world evaluations. Our theoretical work is presented in Chapter 2. Our engineering design and analysis for multiple dynamical systems to track each other over a shared channel is presented in Chapter 3. An error-collision-dependent message rate transmission control for V2V safety communications is proposed for achieving robust tracking performance in different traffic scenarios. In Chapter 4, the error-dependent message rate control from Chapter 3 is extended with a transmission power control. We also state our design approach and theoretical understanding to vehicular safety communications for real-time tracking. Simulation verification is presented show the effectiveness of the proposed transmission rate/power control. In Chapter 5, the prototype implementation, evaluations, and enhancements to the design are presented.

In Chapter 2, we first analyze the real-time tracking MMSE of a scalar linear continuous-time source over a scalar AGWN channel *without* channel feedback. With the Gaussian distributed source innovation, the optimality of the linear innovation encoder and associated optimal tracking performance are shown for the one-to-one channel case. We then extend the one-to-one channel formulation to the case of tracking multiple sources over a shared AWGN channel and study a simple case of tracking two identical linear sources. As a corollary, we show that it is impossible to achieve finite asymptotic MSE for real-time tracking an unstable process *without* feedback. With another quqeing formulation, we have derived a condition for stable real-time tracking of an unstable, scalar, LTI dynamical system. In particular, a G/G/1-∞ queue is assumed to model a broad class of unreliable networks. Derived stability condition is a bound on the entropy rate of the unstable process, which is a function of the moment to be stabilized, encoder efficiency, quantization accuracy, and network parameters. Finally, we apply this bound for stable real-time tracking over a multiple access channel using different access protocols.

In Chapter 3, model-based real-time tracking over the multi-access network is first studied with non-adaptive channel access policies. A mathematical framework is proposed and the estimation MSE of three non-adaptive channel access schemes is analyzed. Asymp-

totic behavior and stability condition are also derived. Our analysis suggests that, while designing real-time tracking systems, the channel access scheme should be chosen based on the amplification factor $|a|$ of the LTI dynamic process. If $|a| \geq 1$, the deterministic design (round-robin scheduling) can achieve strictly lower estimation MSE. Otherwise, for $0 < |a| < 1$, three methods have roughly the same range of MSE asymptotically. We then explore the *Error-Dependent* communication control for real-time tracking in a multiple access channel and the tracking MSE of error-dependent communication policy is analyzed. Its performance is compared with non-adaptive policies. A transmission message generation control algorithm is proposed for each vehicle to disseminate its own state information. The proposed algorithm has an on-demand nature and adapts the V2V message rate for each vehicle in a decentralized fashion. Performance evaluations, both in preliminary Matlab and in large-scale traffic/network simulations, confirm that the proposed algorithm achieves better tracking accuracy than the currently proposed 100-millisecond beaconing solution and is more robust against channel congestion and various traffic conditions.

In Chapter 4, we propose to first control the message generation rate based on vehicle dynamics and sensed tracking errors for safety considerations. Given a message rate, for network considerations, we propose to control the transmission range to maximize the information broadcast throughput for the given channel utilization. Therefore, our design responds to channel congestion by maintaining the same information intensity to the nearest neighboring vehicles and temporarily stopping communication to farther vehicles by reducing transmission range. Our proposed joint rate/power control helps each vehicle decide when it should broadcast a safety message (i.e., when to talk) and how to allocate the transmission power for each safety message (i.e., how load it should talk). To verify the robustness of the proposed design, we simulate its tracking performance in different traffic scenarios. Simulation results confirm that the proposed design is robust and can considerably reduce the tracking error compared to that of the currently proposed solution (i.e., 100-millisecond beaconing or 500-millisecond beaconing with 20 dBm transmission power).

In Chapter 5, the implementation of our proposed transmission control protocol is described as message generation and power assignment functional blocks. The real-world evaluations in General Motors Technical Center show that our design works well in practice and is a promising solution to address the scalability of V2V safety communications. In addition, we present our updated performance metrics, identified challenging highway and intersection scenarios, and updated simulation results for these challenging scenarios. The performance of our proposed design is again compared with the 100-millisecond beaconing with 20-dBm power. Overall, our design provides a better tracking accuracy and a longer time or distance before a host vehicle detects a new remote vehicle approaching. Our design has been adopted by General Motors R&D and under consideration for the standard defining how vehicles should communicate with each other for active safety applications.

Bibliography

[1] C. E. Shannon, "A Mathematical Theory of Communication," *Bell System Technical Journal*, vol.27, July 1948.

[2] J. C. Walrand, P. Varaiya, "Optimal causal coding-decoding problems," *IEEE Trans. Info. Theory*, vol.29, no.6, Nov. 1983.

[3] S. Tatikonda, A. Sahai, S. K. Mitter, "Stochastic linear control over a communication channel," *IEEE Trans. on Automat. Contr.*, vol.49, no.9, Sept. 2004.

[4] A. Sahai, Anytime Information Theory, Ph.D. dissertation, Dept. EECS, MIT, Cambridge, MA, Feb. 2001.

[5] P. Seiler, R. Sengupta, "An H_∞ approach to networked control," *IEEE Trans. on Automat. Contr.*, vol.50, no.3, March 2005.

[6] B. Sinopoli, L. Schenato, M. Franceschetti, K. Poolla, M. I. Jordan, S. S. Sastry, "Kalman Filtering with Intermittent Observations," *IEEE Trans. Automat. Contr.*, vol.49, no.9, Sept. 2004.

[7] Y. Xu, J. Hespanha, "Estimation under uncontrolled and controlled communication in Networked Control Systems," *Proc. of the IEEE Conf. Decision and Contr.*, Dec. 2005.

[8] V. Gupta, Distributed Estimation and Control in Networked Systems, Ph.D. dissertation, California Institute of Technology, CA, June 2006.

[9] D. Teneketzis, "On the Structure of Optimal Real-Time Encoders and Decoders in Noisy Communication," *IEEE Trans. Info. Theory*, vol.52, no.9, Sept. 2006.

[10] A. Zygmund, Trigonometric series, 2nd Edition, Cambridge University Press, 1988.

[11] J. M. C. Clark, "Conditions for one-to-one correspondence between an observation process and its innovation," *Center for Computing and Automation, Imperial College, London, Tech. Rep. 1*, 1969.

[12] P. A. Frost, T. Kailath, "An Innovations Approach to Least-Squares Estimation - Part III: Nonlinear Estimation in White Gaussian Noise," *IEEE Trans. Automat. Contr.*, vol.16, no.3, June 1971.

[13] T. J. Goblick, "Theoretical Limitation on Transmission of Data from Analog Sources," *IEEE Trans. Info. Theory*, vol.11, no.4, Oct. 1965.

[14] M. Gastpar, B. Rimoldi, M. Vetterli, "To Code, or Not to Code: Lossy Source-Channel Communication Revisited," *IEEE Trans. Info. Theory*, vol.49, no.5, May 2003.

[15] T. S. Rappaport, Wireless Communications: Principles and Practice, 2nd Edition, Prentice-Hall, 2002.

[16] N. Ikeda, S. Watanabe, Stochastic Differential Equations and Diffusion Processes, North-Holland Publishing Company, 1981.

[17] J. T. Lo, "On optimal nonlinear estimation-Part I: continuous observation," *Proc. 8th Allerton Conf. on Cir. and Sys. Theory*, 1970.

[18] A. Papoulis, S. U. Phillai, Probability, Random Variables and Stochastic Processes, McGrawHill, 2002.

[19] R. Durrett, Probability: Theory and Examples, Brooks/Cole, 2002.

[20] T. Duncan, P. Varaiya, "On the solutions of a stochastic contorl systems," *SIAM J. Control*, vol.9, no.3, Aug. 1971.

[21] R. S. Lipster, Lecture Notes #10 for the course "Stochastic Process": http://www.eng.tau.ac.il/∼liptser/lectures/lect_new10.pdf.

[22] J. Galambos, Advanced Probability Theory, CRC Press, 1988.

[23] D. Bertsekas, R. Gallager, Data Networks, Prentice Hall, 1992.

[24] C. Striebel, "Sufficient Statistics in the Optimal Control of Stochastic Systems," *J. of Math. Analysis and App.*, vol.12, pp. 576-592, 1965.

[25] A. Lapidoth, S. Tinguely, "Sending a Bivariate Gaussian Source over a Gaussian MAC," *IEEE Trans. Info. Theory*, vol.56, no.6, June 2010.

[26] P. A. Floor, *et. al.* "On Transmission of Two Correlated Gaussian Memoryles Sourcese over a Gaussian MAC using Delay-Free Mappings," submitted to *IEEE Transactions on Communications*, 2011.

[27] T. Cover, J. Thomas, Elements of Information Theory, Telecommunications, New York: Wiley, 1991.

[28] J. F. C. Kingman, "The Heavy Traffic Approximation in the Theory of Queues," *Proc. Sympos. Congestion Theory. Chapel Hill: University of North Carolina Press*, 1965.

[29] J. F. C. Kingman, "Inequalities in the Theory of Queues," *Jour. Roy. Statist. Soc.*, Ser. B. 32, 1970.

[30] L. Kleinrock, Queueing Systems: Volume II - Computer Applications, Wiley Interscience, 1976.

[31] G. Raina, D. Wischik, "Buffer sizes for large multiplexers: TCP queueing theory and instability analysis," *EuroNGI conference on Next Generation Internet Networks*, 2005.

[32] X. Lu, J. K. Hedrick, M. Drew, "ACC/CACC-control design, stability and robust performance," *Proc. of Amer. Contr. Conf.*, 2002.

[33] S. Yuksel, T. Basar, "Quantization for LTI systems with noiseless channels," *Proc. of IEEE Conf. Control Appl.*, Jun. 2003.

[34] Y. Xu, J. Hespanha, "Optimal Communication Logics for Networked Control Systems," *Proc. of IEEE Conf. Decision and Contr.*, 2004.

[35] X. Liu, A. Goldsmith, "Kalman filtering with partial observation losses," *Proc. of IEEE Conf. Decision and Contr.*, 2004.

[36] Z. Jin, V. Gupta, R. M. Murray, "State Estimation over Packet Dropping Networks using Multiple Description Coding," *Automatica*, vol.42, no.9, Sept. 2006.

[37] V. Gupta, A. Dana, J. Hespanha, R. Murray, "Data Transmission over Networks for Estimation," *Proc. of Int. Symp. on the Math Theory of Networks and Syst.*, 2006.

[38] A. Mahajan, D. Teneketzis, "On Jointly Optimal Encoding, Decoding and Memory Update for Noisy Real-Time Communication Systems," submitted to *IEEE Trans. Info. Theory*, Jan. 2006.

[39] R. Sengupta, S. Rezaei, S. E. Shladover, J. A. Misener, S. Dickey, H. Krishnan, "Cooperative Collision Warning Systems: Concept Definition and Experimental Implementation," *Jour. of Intell. Transport. Systems*, vol.11, no.3, pp. 143-155, 2007.

[40] S. Rezaei, R. Sengupta, H. Krishnan, X. Guan, "Reducing the Communication Required by DSRC-based Vehicle Safety Systems," *Proc. of 4th ACM VANET*, 2007.

[41] C. L. Huang, R. Sengupta, "Analysis of Channel Access Schemes for Model-based Estimation over Multi-access Networks," *Proc. of IEEE MSC*, 2008.

[42] N. Elia, S. Mitter, "Stabilization of linear systems with limited information," *IEEE Trans. on Automat. Contr.*, vol.46, no.9, 2001.

[43] W. S. Wong, R. W. Brockett, "Systems with finite communication bandwidth constraints. II: Stabilization with limited information feedback," *IEEE Trans. on Automat. Contr.*, vol.44, no.5, 1999.

[44] J.K. Yook, *et. al.*, "Trading computation for bandwidth: Reducing communication in distributed control systems using state estimators," *IEEE Trans. Contr. Syst. Technol*, vol.10, no.4, July 2002.

[45] G.N. Nair, R.J. Evans, "Exponential stabilisability of finite dimensional linear systems with limited data rates," *Automatica*, vol.39, no.4, Apr. 2003.

[46] Y. Xu, J. Hespanha, "Communication Logics for Networked Control Systems," *Proc. of the Amer. Contr. Conf.*, June 2004.

[47] D.R. Cox, "Some statistical methods connected with series of events," *Jour. Royal Stat. Society*, vol.17, no.2, 1955.

[48] C. Chang, A. Sahai, "Sequential Random Coding Error Exponents for Multiple Access Channel," *IEEE WirelessCom 05 Symposium on Information Theory*, Feb. 2005.

[49] J. Hespanha, *et. al.*, "A Survey of Recent Results in Networked Control Systems," *Proc. of IEEE, Special Issue on Networked Control Systems*, Jan. 2007.

[50] ITS Joint Program Office, US DOT, "VII Architecture and Functional Requirements Version 1.1," July, 2005.

[51] Smart-AHS, http://path.berkeley.edu/SMART-AHS/.

[52] BErkeley AeRobot (BEAR), http://robotics.eecs.berkeley.edu/bear/.

[53] P. Gupta, P. R. Kumar, "The capacity of wireless networks," *IEEE Trans. Info. Theory*, vol.46, no.2, Mar. 2000.

[54] L. Cheng, B. E. Henty, D. D. Stancil, F. Bai, P. Mudalige "Mobile Vehicle-to-Vehicle Narrow-Band Channel Measurement and Characterization of the 5.9 GHz Dedicated Short Range Communication Frequency Band," *IEEE JSAC*, vol.25, no.8, Oct. 2007.

[55] F. Bai, H. Krishnan, V. Sadekar, G. Holland, T. ElBatt, "Towards Characterizing and Classifying Communication-based Automotive Applications from a Wireless Networking Perspective," *Proc. of the 1st IEEE Workshop on Automotive Networking and Applications*, Dec. 2006.

[56] A. Chakravarthy, K. Song, E. Feron, "Preventing Automotive Pileup Crashes in Mixed-Communication Environments," *IEEE Trans. ITS*, vol.10, no.2, Jun. 2009.

[57] M. Saito, J. Tsukamoto, T. Umedu, T. Higashino, "Design and Evaluation of Inter-vehicle Dissemination Protocol for Propagation of Preceding Traffic Information," *IEEE Trans. ITS*, vol.8, no.3, Sept. 2007.

[58] J. J. Blum, A. Eskandrian, " A Reliable Link-Layer Protocol for Robust and Scalable Intervehicle Communications," *IEEE Trans. ITS*, vol.8, no.1, Mar. 2007.

[59] H. Tan, J. Huang, "DGPS-Based Vehicle-to-Vehicle Cooperative Collision Warning: Engineering Feasibility Viewpoints," *IEEE Trans. ITS*, vol.7, no.4, Dec. 2006.

[60] M. Torrent-Moreno, J. Mittag, P. Santi, H. Hartenstein, "Vehicle-to-Vehicle Communication: Fair Transmit Power Control for Safety-Critical Information," *IEEE Trans. Vehicular Technology*, vol.58, no.7, 2009.

[61] M. Artimy, "Local Density Estimation and Dynamic Transmission-Range Assignment in Vehicular Ad Hoc Networks," *IEEE Trans. ITS*, vol.8, no.3, Sept. 2007.

[62] C. Robinson, L. Caminiti, D. Caveney, K. Laberteaux, "Efficient Coordination and Transmission of Data for Vehicular Safety Applications," *Proc. of the 3rd ACM VANET*, Sept. 2006.

[63] S. Rezaei, R. Sengupta, H. Krishnan, X. Guan, R. Bhatia, "Tracking the Position of Neighboring Vehicles Using Wireless Communications," *Elsevier Journal Transportation Research Part C: Emerging Technologies, Special Issue on Vehicular Communication Networks*, June, 2010.

[64] S. Rezaei, "Cooperative Vehicle Safety," Ph.D. dissertation, U.C. Berkeley, Aug. 2008.

[65] C. L. Huang, R. Sengupta, "Decentralized Error-Dependent Transmission Control for Estimation over a Multi-Access Network," *Proc. of the 4th WICON*, Nov. 2008.

[66] C. L. Huang, Y. P. Fallah, R. Sengupta, H. Krishnan, "Information Dissemination Control for Cooperative Active Safety Applications in Vehicular Ad-Hoc Networks," *Proc. of Globecom 2009*.

[67] S. Cheng, C. Fang, C. Chen, S. Chen, "Critical Motion Detection of Nearby Moving Vehicles in a Vision-Based Driver-Assistance System," *IEEE Trans. ITS*, vol.10, no.1, Mar. 2009.

[68] M. M. Trivedi, T. Gandhi, J. McCall, "Looking-In and Looking-Out of a Vehicle: Computer-Vision-Based Enhanced Vehicle Safety," *IEEE Trans. ITS*, vol.8, no.1, Mar. 2007.

[69] Z. Kim, "Robust Lane Detection and Tracking in Challenging Scenarios," *IEEE Trans. ITS*, vol.9, no.1, Mar. 2008.

[70] T. Dao, K. Leung, C. M. Clark, J. P. Huissoon, "Markov-Based Lane Positioning Using Inter-vehicle Communication," *IEEE Trans. ITS*, vol.8, no.4, Dec. 2007.

[71] IEEE 802.11 WG, Part 11: Wireless LAN Medium Access Control (MAC) and Physical Layer Specifications, Aug. 1999.

[72] Wireless Access in Vehicular Environments (WAVE) in Standard 802.11, Specific Requirements: IEEE 802.11p/D2.01, Mar. 2007.

[73] IEEE 1609 trial standard for Wireless Access in Vehicular Environments (WAVE), Apr. 2007.

[74] California PATH SHIFT, http://path.berkeley.edu/SHIFT/.

[75] OPNET Modeler 14.0, http://www.opnet.com/.

[76] Vehicle Safety Communications Consortium (VSCC), "Vehicle Safety Communications Project, Task 3 Final Report: Identify Intelligent Vehicle Safety Applications Enabled by DSRC," 2005.

[77] C. L. Huang, Y. P. Fallah, R. Sengupta, H. Krishnan, "Adaptive Inter-Vehicle Communication Control for Cooperative Safety Systems," *IEEE Network*, Jan./Feb. 2010.

[78] C. L. Huang, Y. P. Fallah, R. Sengupta, H. Krishnan, "Inter-Vehicle Transmission Rate Control for Cooperative Active Safety System," *IEEE Trans. ITS, Special Issue: Exploiting Wireless Communication Technologies in Vehicular Transportation Networks*, Sept. 2011.

[79] Crash Avoidance Metrics Partnership (CAMP), "Vehicle Safety Communications - Applications Final Report," May 2010.

[80] Y. P. Fallah, C. L. Huang, R. Sengupta, H. Krishnan, "Design of Cooperative Vehicle Safety Systems based on Tight Coupling of Communication, Computing and Physical Vehicle Dynamics," *Proc. of International Conference on Cyber Physical Systems*, Apr. 2010.

[81] DENSO, "Wireless Safety Unit: Developer's Guide," Sept. 2009.

[82] DENSO, "Wireless Safety Unit: User's Guide," Oct. 2009.

[83] Y. P. Fallah, C. L. Huang, R. Sengupta, H. Krishnan, "Analysis of Information Dissemination in Vehicular Ad-Hoc Networks with Application to Cooperative Vehicle Safety Systems," *IEEE Trans. Vehicular Tech.*, Jan. 2011.

[84] C. L. Huang, H. Krishnan, R. Sengupta, Y. P. Fallah, " Implementation and Evaluation of Scalable Vehicle-to-Vehicle Safety Communication Control," *IEEE Communications Magazine*, Nov. 2011.

[85] VITS: Integrated Wireless Intersection Simulator: http://car.eng.ohio-state.edu/v2v